



**ELECTROCHEMICAL DYNAMICS OF CYTOCHROME P450
(2D6) BIOSENSORS FOR SELECTIVE SEROTONIN
RE-UPTAKE INHIBITORS (SSRIs)**

BY

RACHEL FANELWA NGECE

A thesis submitted in fulfilment of the requirements for a degree of

MAGISTER SCIENTIAE

in the Department of Chemistry

UNIVERSITY *of the* WESTERN CAPE

SUPERVISED BY

PROFESSOR EMMANUEL I. IWUOHA

AND

DOCTOR PRISCILLA BAKER

DECLARATION

I hereby declare that the work 'ELECTROCHEMICAL DYNAMICS OF CYTOCHROME P450 (2D6) BIOSENSORS FOR SELECTIVE SEROTONIN RE-UPTAKE INHIBITORS (SSRIs)' which I now submit for the assessment on the programme of study leading towards the award of a masters degree is entirely my work; quotes and phrases obtained from the work of others have been fully acknowledged and referenced.

Signed: _____

Rachel Fanelwa Ngece

ID NO: 830217 0464 087



Date: 14 May 2007

**DEDICATED TO MY PARENTS,
NOMAWAKA NGECE AND
MALAYIPHELI SOJADA**



ACKNOWLEDGEMENTS

To God, Thank You for giving me strength and guidance throughout my life.

I wish to acknowledge everyone who has believed in me and encouraged me during the course of this study.

To my supervisors, Professor Emmanuel Iwuoha and Doctor Priscilla Baker, thank you for the support and encouragement that you have always given me. From you I have learnt to believe more in myself and work hard for what I want in life.

To the academic, technical and administrative staff of the Chemistry Department at the University of the Western Cape, thank you for always providing assistance and motivation. Thank you to all the members of the Sensor Research Laboratory for all the help, love and support you have given me.

My sincere gratitude and thanks to my mother for loving me and always believing that I will make it in life irrespective of any obstacle that may come my way. Enkosi mama wam. To the man I love, Olagoke Ajayi, thank you for putting up with all my nagging when my experiments were not going well. Thank you for always being there for me and always guiding me. Bradley, Thuliswa and Anele Ngece thank you for loving me always. Thank you to the Ngece and Thomson family for all your encouragements.

Thank you to all my friends for your support and encouragement in times of need. Special thanks goes to Nothando Mungwe, Busiswa Dyan, Nangamso Miti, Nandi Malumbazo, Unathi Mgwetyana, Pamela Ntanjana, Sarah Maeola and Xoliswa Siyo-Mswi who have felt my miseries the most from the initial days of my studies at the University of the Western Cape. Thank you for everything ladies.

TABLE OF CONTENTS:

PAGE NO:

Title page	i
Declaration	ii
Dedication	iii
Acknowledgements	iv
Table of contents	v-ix
List of scheme	x
List of figures	xi-xvi
List of tables	xvii
List of abbreviations	xviii-xix
Keywords	xx
Abstract	xxi
CHAPTER ONE	1
<i>1.1 Introduction</i>	2-4
<i>1.2 Rationale and Motivation</i>	5-6
<i>1.3 Aim of the study</i>	7
<i>1.4 References</i>	8-9
CHAPTER TWO	10
<i>2.1 Biosensors</i>	11-12
<i>2.1.1 Receptors</i>	13-14
<i>2.1.2 Transducers</i>	15-16



2.2 Enzymes	17
2.2.1 Mechanism of enzyme action	17-18
2.2.1.1 Lock and Key Theory	18
2.2.1.2 Induced Fit Model	18-19
2.2.2 Factors affecting the rate of enzyme reaction	20
2.2.2.1 Temperature	20
2.2.2.2 Enzyme concentration	20
2.2.2.3 pH	20-21
2.2.2.4 Substrate concentration	21
2.2.3 Classification of Enzymes	22
2.2.4 Enzyme Kinetics	23-25
2.2.4.1 Enzyme Inhibition	25
2.2.4.1.1 Competitive Inhibition	25-26
2.2.4.1.2 Non-competitive Inhibition	26-27
2.2.4.1.3 Mixed effects Inhibition	27
2.2.5 Immobilization of Enzymes	28-29
2.2.5.1 Properties of free enzyme	29-31
2.2.5.2 Enzyme support	31-32
2.2.5.3 Enzyme attachment and support activation	33



2.2.6 Choice of Immobilization Method	34
2.2.6.1 Physical Adsorption	35-36
2.2.6.2 Occlusion	36-37
2.2.6.3 Cross-Linking	37-38
2.2.6.4 Covalent-Binding	38-39
2.2.7 Characteristics of immobilized enzymes	40-41
2.3 Cytochrome P450 (2D6)	42
2.3.1 Occurance of the enzyme	42
2.3.2 Cytochrome P450-2D6 (CYP2D6)	43-44
2.3.3 Kinetics of Catalytic reaction	44-46
2.3.4 Classification of Cytochrome P450	47
2.4 Selective Serotonin Re-uptake Inhibitors	48
2.4.1 Fluoxetine	49-51
2.4.2 Fluvoxamine	52-55
2.4.3 Sertraline	56-58
2.4.4 Paroxetine	59-61
2.4.5 Citalopram	62-65
2.4.6 Zimelidine	66-67
2.5 Polymers	68
2.5.1 Conducting Polymers	68-69
2.5.2 Synthesis of Conducting Polymers	69-70

2.5.2.1 Polypyrrole	70-71
2.5.2.2 Polyindole	71
2.5.2.3 Polycarbazole	72
2.5.2.4 Polyaniline	72-76
2.6 Applications of Conducting Polymers	77-78
2.7 References	79-84
CHAPTER THREE	85
3. Experimental	86
3.1 Reagents	86
3.2 Electrochemical Setup	86
3.3 Methodology	86
3.3.1 Polymerization of 8-anilino-1-naphthalene sulfonic acid on gold electrode.	87
3.3.2 Characterization of Au/PANSA in H ₂ SO ₄ using CV	88
3.3.3 Characterization of Au/PANSA in PBS using CV	88
3.4 Enzyme Immobilization	89
3.4.1 Characterization of Au/PANSA/CYP in PBS using CV and SWV	89
3.5 Electrochemical measurements	90-91



CHAPTER FOUR	92
<i>4. Results and Discussion</i>	92
<i>4.1 Electrosynthesis of PANSA on gold electrode</i>	93-95
<i>4.2 CV characterization of Au/PANSA in 0.5M H₂SO₄</i>	96-98
<i>4.3 CV characterization of Au/PANSA in 0.1M Phosphate buffer (0.1M KCl,pH 7.4)(PBS)</i>	99-101
<i>4.4 CV and SWV characterization of Au/PANSA/CYP in 0.1M Phosphate buffer (0.1M KCl,pH 7.4)(PBS)</i>	102-104
<i>4.5 PANSA-mediated electrocatalytic reduction of substrates and SSRI drugs</i>	105-106
<i>4.5.1 Electrocatalytic reduction of SSRIs using CV</i>	107-115
<i>4.5.2 Electrocatalytic reduction of SSRIs using DPV</i>	116-121
<i>4.5.3 Electrocatalytic reduction of SSRIs using SWV</i>	122-127
<i>4.6 Inhibition of CYP2D6 by Paroxetine</i>	128-132
<i>4.7 Steady State Amperometry</i>	133-135
<i>4.8 Conclusion</i>	136
<i>4.9 Acknowledgements</i>	137
<i>5. References</i>	138-141

LIST OF SCHEMES:

Scheme 2.1: Mechanism of enzyme action

Scheme 2.2: Reaction mechanism of CYP 2D6

Scheme 2.3: Structure of Fluoxetine prior to metabolism

Scheme 2.4: Metabolism of Fluoxetine by isoenzymes

Scheme 2.5: Structure of Fluvoxamine prior to metabolism

Scheme 2.6: Metabolism of Fluvoxamine by isoenzymes

Scheme 2.7: Structure of Sertraline prior to metabolism

Scheme 2.8: Metabolism of Sertraline by isoenzymes

Scheme 2.9: Structure of Paroxetine prior to metabolism

Scheme 2.10: Metabolism of Paroxetine by isoenzymes

Scheme 2.11: Structure of Citalopram prior to metabolism

Scheme 2.12: Metabolism of Citalopram by isoenzymes

Scheme 2.13: Structure of Escitalopram prior to metabolism

Scheme 2.14: Structure of Zimelidine

Scheme 2.15: The different forms of PANI namely; PNB, ES, LEB and EB

Scheme 2.16: Structure of 8-anilino-1-naphthalene sulfonic acid

LIST OF FIGURES:

Figure 2.1: Components of a biosensor

Figure 2.2: Illustration of Michaelis-Menten Kinetics

Figure 2.3: Illustration of Competitive and Non-competitive Inhibition

Figure 4.1: Electrosynthesis of PANSA film on Au electrode in 0.5 H₂SO₄ at a potential window of -300 mV to +1100 and scan rate of 50 mV/s

Figure 4.2: Electrochemical characterization of the PANSA film in 0.5 H₂SO₄ at 5, 40, 80, 150, 250 and 350 mV/s at a potential window of -300 mV to +1100 mV

Figure 4.3: Electrochemical characterization of the PANSA film in 0.5 H₂SO₄ on Au electrode illustrating the main polymerization peaks

Figure 4.4: Electrochemical characterization of the PANSA film in PBS at 5, 40, 80, 150, 200 and 350 mV/s at a potential window of -300 mV to +1100mV

Figure 4.5: Dependency of peak current on potential scan rate for the Au/PANSA electrode

Figure 4.6: Peak currents as a function of square root of scan rate for the Au/PANSA electrode

Figure 4.7: Electrochemical characterization of Au/PANSA/CYP2D6 in PBS at 5, 14, 30, 60, 100 and 150 mV/s at a potential window of -300 mV to +1100 mV using CV

Figure 4.8: Electrochemical characterization of Au/PANSA/CYP2D6 in PBS at 5, 10 and 15 Hz at the potential window of -500 mV to +800mV

Figure 4.9: CV of CYP2D6 biosensor in the presence of varying concentrations of fluoxetine under aerobic conditions in the potential window of +500 mV to -700 mV at a scan rate of 10 mV/s

Figure 4.10: CV of CYP2D6 biosensor in the presence of varying concentrations of sertraline under aerobic conditions in the potential window of +500 mV to -800 mV at a scan rate of 10 mV/s

Figure 4.11: CV of CYP2D6 biosensor in the presence of varying concentrations of clomipramine under aerobic conditions in the potential window of +500mV to -700 mV at a scan rate of 10 mV/s

Figure 4.12: CV of CYP2D6 biosensor in the presence of varying concentrations of fluvoxamine under aerobic conditions in the potential window of +500 mV to -700 mV at a scan rate of 10 mV/s

Figure 4.13: CV of CYP2D6 biosensor in the presence of varying concentrations of debrisoquine sulphate under aerobic conditions in the potential window of +500 mV to -700 mV at a scan rate of 10 mV/s

Figure 4.14 : CV of CYP2D6 biosensor in the presence of varying concentrations of zimelidine under aerobic conditions in the potential window of +500 mV to -800 mV at a scan rate of 10 mV/s

Figure 4.15: Calibration curve of fluoxetine illustrating the linear range of the biosensor with a detection limit of 0.94 μM

Figure 4.16: Calibration curve of zimelidine illustrating the linear range of the biosensor with a detection limit of 0.03 μM

Figure 4.17: Calibration curve of fluvoxamine illustrating the linear range of the biosensor with a detection limit of 0.15 μM

Figure 4.18: DPV of CYP2D6 biosensor in the presence of varying concentrations of zimelidine under aerobic conditions in the potential window of +300 mV to – 500 mV at a scan rate of 10 mV/s

Figure 4.19: DPV of CYP2D6 biosensor in the presence of varying concentrations of clomipramine under aerobic conditions in the potential window of +200 mV to – 600 mV at a scan rate of 10 mV/s

Figure 4.20: DPV of CYP2D6 biosensor in the presence of varying concentrations of debrisoquine sulphate under aerobic conditions in the potential window of +200 mV to – 600 mV at a scan rate of 10 mV/s

Figure 4.21: DPV of CYP2D6 biosensor in the presence of varying concentrations of fluvoxamine under aerobic conditions in the potential to – 600 mV at a scan rate of 10 mV/s

Figure 4.22: DPV of CYP2D6 biosensor in the presence of varying concentrations of sertraline under aerobic conditions in the potential window of -100 mV to –400 mV at a scan rate of 10 mV/s

Figure 4.23: DPV of CYP2D6 biosensor in the presence of varying concentrations of fluoxetine under aerobic conditions in the potential window of -100 mV to –400 mV at a scan rate of 10 mV/s

Figure 4.24: Calibration curve of debrisoquine sulphate illustrating the linear range biosensor with a detection limit of 0.02 μ M

Figure 4.25: SWV of CYP2D6 biosensor in the presence of varying concentrations of fluoxetine under aerobic conditions at a potential window of +100 mV to –600 mV at a frequency of 10 Hz

Figure 4.26: SWV of CYP2D6 biosensor in the presence of varying concentrations of sertraline under aerobic conditions at a potential window of +100 mV to –600 mV at a frequency of 10 Hz

Figure 4.27: SWV of CYP2D6 biosensor in the presence of varying concentrations of fluvoxamine under aerobic conditions at a potential window of +100 mV to –600 mV at a frequency of 10 Hz

Figure 4.28: SWV of CYP2D6 biosensor in the presence of varying concentrations of zimelidine under aerobic conditions at a potential window of 0 mV to –600 mV at a frequency of 10 Hz

Figure 4.29: SWV of CYP2D6 biosensor in the presence of varying concentrations of debrisoquine sulphate under aerobic conditions at a potential window of +100 mV to –600 mV at a frequency of 10 Hz

Figure 4.30: SWV of CYP2D6 biosensor in the presence of varying concentrations of clomipramine under aerobic conditions at a potential window of 0 mV to –500 mV at a frequency of 10 Hz

Figure 4.31: Calibration curve of sertraline illustrating the linear range biosensor with a detection limit of 0.13 μM

Figure 4.32 : Calibration curve of clomipramine illustrating the linear range biosensor with a detection limit of 0.05 μM

Figure 4.33: DPV of CYP2D6 biosensor in the presence of varying concentrations of paroxetine under aerobic conditions in the potential window of +300 mV to -700 mV at a scan rate of 10 mV/s

Figure 4.34: SWV of CYP2D6 biosensor in the presence of varying concentrations of paroxetine under aerobic conditions at a potential window of +100 mV to -600 mV at a frequency of 10 Hz

Figure 4.35: CV of CYP2D6 biosensor in the presence of varying concentrations of paroxetine under aerobic conditions in the potential window of +500 mV to -700 mV at a scan rate of 10 mV/s

Figure 4.36 (a): CV of CYP2D6 biosensor in the presence of varying concentrations of paroxetine and fluvoxamine under aerobic conditions at a potential window of +100 mV to -700 mV at a scan rate of 10 mV/s

Figure 4.36 (b): CV of CYP2D6 biosensor in the presence of varying concentrations of paroxetine and fluvoxamine under aerobic conditions at a potential window of +100 mV to -700 mV at a scan rate of 10 mV/s

Figure 4.37: Calibration curve of paroxetine illustrating the linear range biosensor with a detection limit of $-0.085 \mu\text{M}$

Figure 4.38: Response times of fluvoxamine and fluoxetine

Figure 4.39: Response times of sertraline and debrisoquine sulphate

LIST OF TABLES:

Table 2.1: Bioactive components and transducers used in biosensor construction.

Table 2.2: Tissues used to date and their respective analytes.

Table 2.3: Classification of enzymes and their biochemical properties.

Table 2.4: Examples of enzymes used in biosensors and analytes that have
been analysed.

Table 2.5: CYP enzymes classified by family, subfamily and gene.

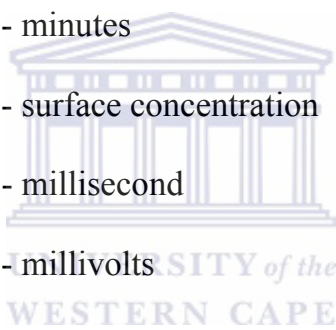
Table 4.1: Compounds and their respective biosensor analyses:



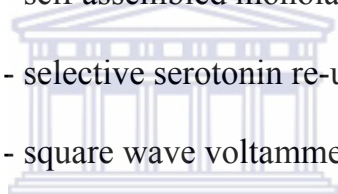
LIST OF ABBREVIATIONS:

Ag/AgCl	- Silver/Silver Chloride
ANSA	- 8-anilino-1-naphthalene sulfonic acid
Au	- gold
$^{\circ}\text{C}$	- degrees celcius
cm^2	- cubic centimetres
cm s^{-1}	- diffusion coefficient
CV	- cyclic voltammetry
CYP 2D6	- cytochrome P450-2D6
<i>De</i>	- diffusion coefficient
DPV	- diffusion coefficient
$E_{p,a}$	- anodic peak potential
$E_{p,c}$	- cathodic peak potential
E_i	- initial potential
E_{λ}	- final potential
ΔE_p	- the change in potential
FAD	- flavin adenine dinucleotide
Fe^{2+}	- iron in 2+ oxidation state
Fe^{3+}	- iron in 3+ oxidation state
FMN	- flavin mononucleotide
H_2O	- water
H_2SO_4	- sulphuric acid
H_2O_2	- hydrogen peroxide

5-HT	- 5-hydroxytryptamine
I_{\max}	- maximum current
$I_{p,a}$	- anodic peak current
$I_{p,c}$	- cathodic peak current
K_{cat}	- enzyme catalytic turnover rate constant
KCl	- potassium chloride
K_m	- Michaelis-Menten constant
M	- molarity
mL	- millilitres
min	- minutes
$\text{mol}\cdot\text{cm}^{-2}$	- surface concentration
msec	- millisecond
mV	- millivolts
mV/s	- millivolts per second
MWNTS	- multiwall carbon nanotubes
N	- nitrogen
NaCl	- sodium chloride
NADH	- reduced nicotinamide adenine dinucleotide phosphate
NADPH	- nicotinamide adenine dinucleotide phosphate
NSA	- naphthalene sulfonic acid
NQS	- 1,2 naphthaquinone-4-sulfonate
O_2	- oxygen



PANI	- polyaniline
PANSA	- poly (8-anilino-1-naphthalene sulfonic acid)
PBS	- 0.1M, pH 7.4 phosphate buffer
PM	- poor metabolizers
Pt	- platinum
r	- linear regression
s	- second
S/R	- cis/trans
S.cm ⁻¹	- conductivity
SAM	- self assembled monolayer
SSRIs	- selective serotonin re-uptake inhibitors
SWV	- square wave voltammetry
TCAs	- tricyclic antidepressants
μA/V	- microamperes per volt
μL	- microlitres
V _{max}	- maximum velocity



WESTERN CAPE

KEYWORDS:

Selective serotonin reuptake inhibitors (SSRIs)

biosensors

biotransformation

cytochrome P450-2D6 (CYP2D6)

poly (anilinonaphthalene sulfonic acid) (PANSA)

electrochemically

biotransformation

cyclic voltammetry (CV),

square wave voltammetry (SWV)

differential voltammetry (DPV)

electroactive

Michaelis-Menten kinetics

ABSTRACT:

Selective serotonin reuptake inhibitors (SSRIs) are a new class of antidepressants used mainly for the treatment of depression and other forms of related disorders. There are a number of side effects associated with these drugs which include loss of weight, sexual dysfunction, nervousness and nausea. A fast and reliable detection method such as biosensing for the determination of the SSRIs metabolic profile is therefore essential for the appropriate dosing of these drugs. Biosensors for the determination of the SSRIs biotransformation were prepared with cytochrome P450-2D6 (CYP2D6) isoenzyme and poly (anilinonaphthalene sulfonic acid) (PANSA) film electrochemically deposited on gold. The biotransformation of the SSRIs was studied by the use of Cyclic voltammetry (CV), Square wave voltammetry (SWV) and Differential voltammetry (DPV) under aerobic conditions. The surface concentration of the adsorbed electroactive film was determined and estimated to be 1.0257×10^{-6} mol cm⁻² and the charge transfer coefficient was estimated to be 3.8225×10^{-2} cm s⁻¹. The biosensor response time, sensitivity, detection limit and dynamic linear range were determined for sertraline, fluoxetine, fluvoxamine, citalopram, zimelidine and paroxetine. Analysis of the Michaelis-Menten region of the sensor response curves for the SSRs gave apparent Michaelis-Menten constants which were higher than the peak plasma concentration (C_{max}) value of 0.55 μM, thereby making the sensor systems suitable for the determination of the respective analytes in serum.

CHAPTER



ONE

UNIVERSITY *of the*
WESTERN CAPE

Background:

1.1 INTRODUCTION:

About 121 million people worldwide have a common mental disorder known as depression. Depression is believed to be as a result of a deficit in the availability of serotonin and noradrenalin (*Pedrazza et al, 2007*). It is assumed that 50% of all suicide attempts in the Western World are due to depression while 25% of severe depressed patients attempt at least one suicide. This illness affects both the economic as well as the social functioning (*Pedrazza et al, 2007*) of the individual patient thus leading to suicidal behaviour. According to research done by the World Health Organization, this disorder will be the second major contributor to disease by the year 2020, calculated for both sexes and for both ages. Between the years 1960 to 1980, this condition was treated with tricyclic antidepressants (TCAs) and monoamine oxidase inhibitors (*Wilke et al, 2005; Heimke et al, 2000; Malfara et al, 2007*).

However it was later discovered that the side effects as well as severe drug-drug interaction of these compounds in conjunction with the development of the study of the central nervous system, has led to the production and development of several new antidepressants (*Wilke et al, 2005; Heimke et al, 2000, Murrin et al, 2007*). Today depression is treated by a new class of antidepressants known as Selective Serotonin Reuptake Inhibitors (SSRIs), of which Fluoxetine is the most commonly known and used (*Heimke et al, 2000*). This group of drugs also includes, Fluvoxamine, Citalpram, Sertraline, Zimelidine and Paroxetine. Studies have shown that depression is linked to a lack of stimulation of the recipient neuron at a synapse. Therefore, SSRIs function in a manner whereby they block the re-uptake of serotonin from the synaptic junctions in the brain, enhancing central serotonergic function. This way serotonin would have enough time and the chance to be recognized again and again by receptors of the recipient cell,

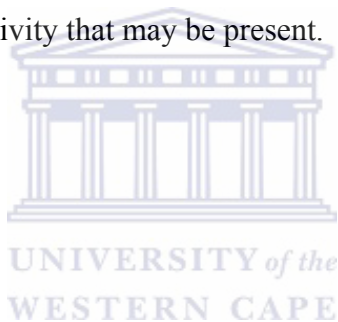
which are then stimulated. Since SSRIs have a high selectivity for serotonin reuptake, they therefore do not cause the unwanted blockage of peripheral and central adrenergic, cholinergic and histaminergic receptors that is characteristic of TCAs and monoamine oxidase inhibitors (*Bistrolas et al, 2005; Heimke et al, 2000; Schreiber et al, 2006*).

SSRIs became popular instantly and this was attributed to the advantages over the TCAs and monoamine oxidase inhibitors in terms of safety, tolerability and ease of dosing. Since their introduction in the mid-eighties, over 35 million patients have been treated with SSRIs. Later it was discovered that certain limitations, associated with a failure in response in many of the severely affected patients resulted in many of them to end treatment. The ending is mainly due to the side effects such as gastrointestinal complaints; nervousness and agitation, sexual dysfunction and weight gain mainly to long-term users. These factors outlined a problem with the dosing of these drugs among diagnosed patients.

The aim of this work is the development of a bio-analytical device, which is suitable for the appropriate dosing of clinically, diagnosed patients by the measurement of SSRIs. This device is known as a biosensor which when constructed is tailored to match the individual demands of the specified analyte (*D 'Orazio et al, 2003*). A review of the current literature suggests that an isoform of the heme-thiolate cytochrome P450 proteins is indicated in the metabolism of these drugs. CYP2D6, isoform also known as debrisoquine hydroxylase is thought to be responsible for the biotransformation of fluoxetine to nor-fluoxetine and it is therefore believed that it will behave in the same manner with the other SSRIs. On the other hand this enzyme is inhibited by high

concentrations of fluoxetine and is therefore incapable of normal functions (*Hermeryck et al, 2003*).

Currently high performance liquid chromatography and gas chromatography methods are used for quantifying the levels of fluoxetine and its metabolites in blood and plasma. Although these methods are well established and accurate they require substantial sample preparation, which then led to the construction of biosensors as they have reduced sample preparation time and allow for point of care analyses. In this project I will investigate the electrochemical interaction between CYP2D6 and fluoxetine as well as other SSRIs mediated by poly (8-anilino-1-naphthalene sulphonic acid). I will also investigate the role of inhibitors of CYP2D6 bioactivity that may be present.



1.2 RATIONALE AND MOTIVATION:

The study being proposed is a synergy of electrochemical and molecular electronic principles in the development of novel micro- or nano-structured or nano-meter scale electrochemical sensor devices for biomedical, environmental and biomolecular analysis. The material of interest in this study is the polymer PANSA synthesized from a derivative of naphthalene sulphonic acid, aniline naphthalene sulfonic acid (ANSA). The specific application of the proposed sensor system for the elucidation of the metabolism of SSRI drugs is being proposed. The advent of SSRI drugs increased the pharmacological options for the treatment of depression by enhancing serotonergic transmission and inducing down-regulation of postsynaptic receptors. These third generation antidepressants provide effective antidepressant activity without the sedating, anticholinergic, or cardiotoxic reactions observed with tricyclic antidepressants (*Gram et al, 1994; Hermeryck et al, 2003; Pedrazza et al, 2007*). Fluoxetine, an SSRI drug is presently the most prescribed antidepressant mainly due to its proven efficacy, ease of administration, generally benign side-effect profile (involving mainly the gastrointestinal system) and remarkable safety in over-dose (*Schreiber et al, 2006; Malfara et al, 2007*). However, the fate of fluoxetine after administration still remains controversial (*Wedlund et al, 2004*). Norfluoxetine the metabolite of fluoxetine, is also as potent as the parent compound. It has an elimination half-life of about 330 hours, so that pharmacologically active compounds remain present in the body for up to 7 days following a fluoxetine dose (*Hermeryck et al, 2003*).

In this study I will combine the bioelectronics and bioelectrochemistry of redox enzyme isoforms with the electron mediating ability and conductivity of electroactive nanopolymers for electrochemical study and modelling of SSRIs metabolism. The

feasibility of the study is borne out by the fact that recent studies (*Wedlund et al*, 2004; *Koyama et al*, 1997; *Vickers et al*, 2001; *Degtyarenko et al*, 1995; *Iwuoha et al*, 1997) suggest that cytochrome P450-2D6 may be the major enzyme catalysing the N-demethylation of fluoxetine to R- and S-norfluoxetine. Incidentally, human CYP2D6 is evolutionarily of the Type II P450 (microsomal) class (*Shumyantseva et al*, 2005) which normally consists of an NADPH: P450 reductase (FAD- and FMN-containing flavoprotein) and the P450 enzyme. The design of the resultant device is to eliminate the need for CYP2D6 physiological or artificial co-factors in the biocatalysis of SSRIs metabolism, by elegantly combining the use of genetically engineered CYP2D6 and cathodic polarization of the enzyme immobilized in the nanopolymer as the source of the requisite electrons.

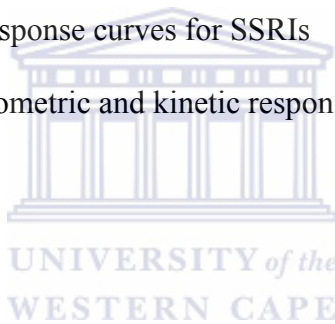
Clinically it is important to determine the CYP2D6 profile of patients before administering fluoxetine or other SSRIs drugs metabolised by CYP2D6. The SSRIs drugs metabolising status of patients would be evaluated by the use of sensor systems that would consist of poly (8-anilino-1- naphthalene sulphonic acid) PANSA modified electrodes and samples of SSRIs.

1.3 AIM OF THE STUDY:

The project will investigate the electrochemical interactions between CYP2D6 and SSRIs. This interaction will be mediated by PANSA on a gold electrode. The result of this will then establish an electrochemical method for studying the biotransformation of SSRIs by amperometric transduction.

The objectives of the study are:

- 1) To prepare biorecognition electrodes containing CYP2D6 isoforms in poly (8-anilino-1-naphthalenesulphonic acid).
- 2) To demonstrate electrochemical responses and reactivities of the sensors.
- 3) To generate Dose response curves for SSRIs
- 4) To model the amperometric and kinetic responses of the nanosensor systems



1.4 REFERENCES:

Bistrolas N, Wollenberger U, Jung C, Scheller F. W: 'Cytochrome P450 biosensor A review:' *Biosensors and Bioelectronics*, 2005, 20: 2409

Degtyarenko K.N: 'Structural domains of P450-containing monooxygenase systems' *Protein Engineering*, 1995, 8: 737-747

Gram L.F: 'Drug Therapy: Fluoxetine' *New English Journal of Medicine*, 1994, 331:1352-1361

Hermeryck A, Belpaire F.M: 'Selective Serotonin Reuptake Inhibitors and Cytochrome P-450 Mediated Drug-Drug Interactions: An Update' *Current Drug Metabolism*, 2003, 3: 13-17

Iwuoha E. I, Saenz de Villaverde D, Carcia N.P, Smyth M. R: 'Reactivities of organic phase biosensors. 2. The amperometric behaviour of horseradish peroxidase immobilised on a platinum electrode modified with an electrosynthetic polyaniline film' *Biosensors and Bioelectronics*, 1997, 12: 747-761

Koyama E. , Chima K., Tani M. , Ishaizaki T. : 'Reappraisal of Human CYP Isoforms Involved in Imipramine N-Demethylation and 2-Hydroxylation: A Study Using Microsomes Obtained from Putative Extensive and Poor Metabolizers of Mephenytoin and Eleven Recombinant Human CYPs¹, *Journal of Pharmacology and experimental Therapeutics*, 1997, 281:1199-1210

Malfara W.R, Bertucci C, Quiroz M.E.C: 'Reliable HPLC Method for Therapeutic Drug Monitoring of Frequently Prescribed Tricyclic and Nontricyclic Antidepressants' *Journal of Pharmaceutical and Biomedical Analysis*, 2007, Newly accepted manuscript

Murrin L.C, Sanders J.D, Bylund D.B: 'Comparison of the maturation of the adrenergic and serotonergic neurotransmitter systems in the brain: Implications for differential drug effects on juveniles and adults' *Biochemical Pharmacology*, 2007. 73: 1225

Pedrazza E.L, Senger M.R, Pedrazza L: 'Sertraline and clomipramine inhibit nucleotide catabolism in rat brain synaptosomes' *Toxicology in Vitro*, 2007, 21: 671

Schreiber S, Pick C.G: 'From selective to highly selective SSRIs: A comparison of the antinociceptive properties of fluoxetine, fluvoxamine, citalopram and escitalopram' *European Neuropsychopharmacology*, 2006: 16: 464-465

Shumyantseva V.V, Bulko T.V, Archakov A.I: 'Electrochemical reduction of Cytochrome P450 as an approach to the construction of biosensors and bioreactors' *Journal of Inorganic Biochemistry*, 2005, 99: 1057

Vickers E., Zollinger M., Dannecker R., Tynes R: 'In Vitro Metabolism of Tegaserod in Human Liver and Intestine: Assessment of Drug Interactions' *Drug metabolism and Disposition*, 2001, 20:1269-1276

Wedlund P. J, de Leon J: 'Cytochrome P450 2D6 and antidepressant toxicity and Response: What is the evidence?' *Clinical Pharmacology and Therapeutics*, 2004, 75:373-374

Wilke M.R., Moudens K. E, Van Peteghem C.H: 'Development of a solid phase extraction for 13 new new generation antidepressants and their active metabolites for gas chromatography-mass spectrometric analysis' *Journal of Chromatography A*, 2005, 1090:19-20

CHAPTER



TWO

UNIVERSITY *of the*
WESTERN CAPE

Literature Review:

2.1 BIOSENSORS:

Biosensors are increasingly becoming practical and useful, if not essential tools in medicine, food quality control, environmental monitoring and research. In their design they can be tailored to match individual analytical demand for almost any target molecule or compound that interacts specifically with a biological system. Biosensors are devices that are used to detect analytes as a result of their interaction with a bioactive substance, which is usually attached to an electrode. Generally, these devices are composed of a bioactive substance as well as a physical transducer (Brennan *et al*, 1996; D 'Orazio *et al*, 2003) as illustrated in Figure 2.1.

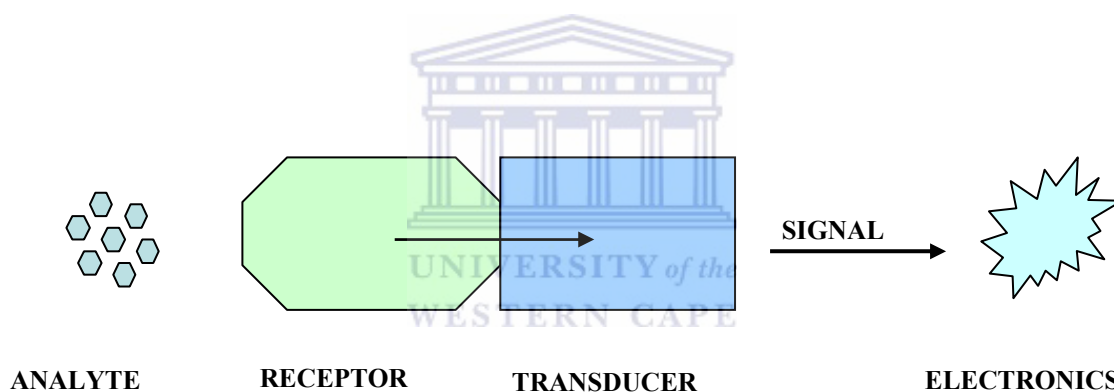


Fig 2.1: Components of a biosensor

The bioactive substance is immobilized in close proximity to a transducer that relays the interaction of the analyte and the bioactive substance into a measurable response which is most often an electronic signal (Brennan *et al*, 1996; D 'Orazio *et al*, 2003). The bioactive substance also known as a chemically selective layer or sometimes as a receptor is responsible for the determination of the sensitivity of the sensor. Each receptor has its own specific detector, which is able to produce a particular expected signal. Table 2.1

(Conn *et al*, 1987) illustrates the most commonly used receptors and detectors in biosensor construction.

Table 2.1: Bioactive components and transducers used in biosensor design

BIOACTIVE COMPONENT	TRANSDUCER
Organisms	Potentiometric
Tissues slices	Amperometric
Whole microbial Cells	Conductometric
Organelles	Impedimetric
Membranes	Optical
Enzymes	Calorimetric
Enzyme components	Acoustic
Receptors	Mechanical
Antibodies	Molecular electronic
Nucleic acid	
Organic molecules	

Biosensors can be divided into three generations depending on their level of integration. The first generation comprises of a biocatalyst that is either bound or entrapped in a membrane. The second generation of biosensors involves the adsorption of the biological components to the transducer surface thereby eliminating semi-permeable membranes. In the third generation, there is a direct binding of the biocatalyst to an electronic device that transduces and then amplifies the signal. Conducting polymer based biosensors are placed in this category (Chaubey *et al*, 2002). A successful biosensor possesses some beneficial features such as; the bioactive substance should be highly specific for the purpose of the analyses. The reaction, which takes place, should be independent of physical parameters such as stirring, pH and temperature as this would allow minimal

pre-treatment of samples prior to analysis. The obtained response after analysis should be accurate, precise, reproducible and linear over the useful analytical range. The response should also be free from electrical noise. Most importantly, the complete biosensor should be cheap, small, portable and capable of being operated by semi-skilled operators (*Ryan-Byrne et al, 1997*). Some potential applications of biosensors are in clinical diagnosis, agricultural and horticultural analysis, pollution, water and microbial contamination analysis.

2.1.1 Receptors:

In biosensors, receptors are compounds or materials that give biosensors their selectivity characteristics. In most cases these receptors undergo reactions with their respective analytes which is denoted by an end signal. Various receptors have been employed in sensor construction. In this section we shall give an indication of a few commonly used receptors.

Plant tissues as well as some sections of mammals have been employed in the construction of biosensors resulting in sensor systems with greater selectivity's when compared to those constructed with bacterial cells. This is due to the fact that plants and animals are not metabolically versatile. Each type of tissue slice functions the best when the appropriate analyte is present. Different types of tissues and their corresponding analytes are shown in Table 2.2 obtained from (*D'Orazio et al, 2003*). Whole microbial cells are also widely utilized in the study of biosensors and are often used when the desired enzyme is either unstable or difficult to purify. A slight disadvantage associated with these biosensors is that they have a slow response time and they require a need for frequent calibration. Whole cell biosensors have been constructed to analyse ammonia,

antibiotics, enzyme activities, sugars, peptides, vitamins, nitrates, alcohols, biological oxygen demand and organic acids.

Enzymes are the most widely used biological components and research has shown that most enzymes have been successfully used in the construction of biosensor. These components are unique since they are a combination of selectivity and sensitivity and they allow for a wide selection of transducers to be used (Conn *et al*, 1987). The signals of enzyme sensors are strongly influenced towards their application by inhibition, temperature and pH dependence (D’Orazio *et al*, 2003). Our work involves the construction of a biosensor with the aid of the enzyme cytochrome P450 2D6 immobilized onto a polymer film.

Table 2.2: Tissues used to date and their respective analytes

TISSUE	ANALYTE
Mouse intestinal mucosa	Adenosine
Cucumber leaf	Cysteine
Banana pulp	Dopamine
Yellow squash	Glutamate
Bovine liver	H₂O₂
Corn kernel	Pyruvate
Sugar beet	Tyrosine
Jack bean meal	

2.1.2 Transducers:

The role of a transducer in biosensor construction is to relay the interaction of the biological active compound and the analyte into a measurable response which in most cases is an electronic signal (*Brennan et al, 1996*). A suitable transducing system can be adapted in sensor construction depending on the nature of the biochemical interaction of the bioactive substance with the species of interest.

Physical transducers vary from thermal, piezometric, spectroscopic, surface wave technology and electrochemical. Electrochemical transduction is the most common where amperometric and potentiometric transduction are the commonly utilized types in sensor studies. These methods are unique in such a manner that during the bio-interaction process, electrons are either consumed or generated producing an electrical signal, which is then detected by an electrochemical detector. An amperometric biosensor is driven by an external constant potential, during which an electrochemical reaction takes place, and the resultant current is measured (*Malhotra et al, 2006; Chaubey et al, 2002; Tess et al, 1999*). Potentiometric biosensors are based on ion-selective or gas sensing electrodes where a movement of ions into a membrane at a zero current allows for the monitoring of the cell potential (*Malhotra et al, 2006; Chaubey et al, 2002*). A Piezometric sensor is another type which is based on the movement of materials into or out of a surface layer where the change in mass is monitored (*Rojas-Malgarejo et al, 2003; D 'Orazio et al, 2003*). Another type is thermometric biosensors which are based on the measurement of changes in temperature of the enzymatic reaction by the simple measurement of variation in resistance (*Conn et al, 1987*).

Biosensors that employ enzymes as their receptors require that the enzyme be immobilized onto a membrane and onto an appropriate electrode. Depending on the type of electrode to be used, example glassy carbon, diamond, pyrolytic graphite, there are either two or only one membrane separating the enzyme and the medium.



2.2 ENZYMES:

Enzymes are protein catalysts, which are responsible for speeding up the rates of chemical reactions without being used up in the chemical processes. They lower the activation energy needed to convert a substrate into a product by temporarily binding to the substrate. The activation energy of a reaction is the energy required to form the transition state, so it is lowered when the enzyme stabilizes the transition state. The macromolecular components of almost all enzymes are composed of protein except for a class of Ribonucleic Acid modifying catalyst known as Ribozymes (*Conn et al*, 1987).

Ribozymes are molecules of ribonucleic acid, which are responsible for catalysing reactions on the phosphodiester bond of other Ribonucleic acids. There are about 40,000 different enzymes in human cells, in which each of them controls a specific reaction. The rates of reactions are increased by a factor between 10^6 to 10^{12} times which therefore allows the chemical reactions, which make life possible to take place at normal temperature (*Conn et al*, 1987).

2.2.1 Mechanism of enzyme action:

The basic mechanism by which enzymes speed up the rate of chemical reactions begins with the binding of the substrate or substrates to the active site of an enzyme to form an enzyme-substrate complex as illustrated in Scheme 2.1.



Scheme 2.1 Mechanism of enzyme action

The active site of an enzyme (E) is the specific region of the enzyme where the substrate (S) attaches, therefore it is said to have a geometric shape that is complementary to the geometric shape of the substrate. This enzyme-substrate (ES) interaction causes changes in the distribution of electrons in the chemical bonds of the substrate thereby stimulating the reactions that lead to the formation of products (P). Once the products are produced, the enzyme is released and regenerated for another reaction. The mechanism of enzyme action can be further explained using the Lock and Key Theory and the Induced Fit Model (*McMurry et al*, 1998).

2.2.1.1 Lock and Key Theory:

This theory is based on the concept that a substrate molecule fits into the active site of an enzyme like a key fitting into a lock. This means that only those specifically sized substrates will be able to fit into a particular shaped enzyme. When this interaction occurs, the shape of the enzyme changes slightly, changing the substrate and the active site, making it more likely to change into the product. If however the substrate does not fit correctly to the active site then no reaction occurs (*McMurry et al*, 1998).

2.2.1.2 Induced Fit Theory:

The induced fit model is as a result of the assumption that the substrate plays a role in determining the final shape of the enzyme. The model also suggests that the initial enzyme-substrate interaction results in conformational changes in the enzyme, which causes the binding to strengthen. Transition-state complexes and reaction products are generated after binding by one or more mechanisms of catalysis.

There are four mechanisms of catalysis namely:

- (a) Catalysis by Bond Strain is a catalysis where strained substrate bonds are produced as a result of the induced structural rearrangement which takes place when the enzyme and substrate bind.
- (b) Catalysis by Proximity and Orientation is when the reactive group in an enzyme-substrate interaction are orientated and brought into close proximity with one another.
- (c) Catalysis Involving Proton Donors and Acceptors.
- (d) Covalent Catalysis occurs when the substrate is orientated to an active site on the enzyme such a manner that a covalent intermediate is generated between the enzyme and the substrate (*Conn et al, 1987*).

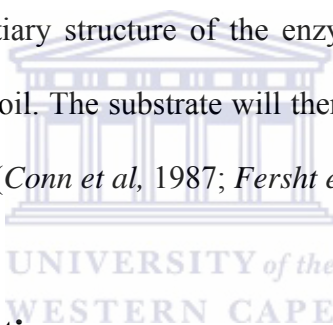


2.2.2 FACTORS AFFECTING THE RATE OF ENZYME

REACTION:

2.2.2.1 Temperature:

Enzymes function at an optimum temperature and each enzyme functions best at its own particular temperature. As the temperature rises the rate increases due to the fact that the enzyme and the substrate molecules both have more kinetic energy and hence will collide more often and will have sufficient energy to overcome the activation energy. The increase in rate with temperature can be quantified as a Q₁₀, which is the relative increase for a 10⁰C rise in temperature. Beyond the optimum temperature, the enzymes become denatured and ineffective. The thermal energy breaks the hydrogen bonds holding the secondary and tertiary structure of the enzymes, so that the enzyme loses shape and becomes a random coil. The substrate will then be unable to bind to it and the reaction is no longer catalyzed (*Conn et al, 1987; Fersht et al, 1984*).



2.2.2.2 Enzyme concentration:

When the concentration of the enzyme is increased, the rate of the reaction increases linearly due to the unavailability of enzyme molecules to catalyze the reaction. At very high enzyme concentration, the rate stops increasing as a result of the substrate concentration being rate-limiting (*Conn et al, 1987; Fersht et al, 1984*).

2.2.2.3 pH:

Enzymes have an optimum pH at which they function the best and for most enzymes this pH is from 7-8, which is the physiological pH of most cells. A few enzymes can work at extreme pH, such as protease enzymes in the stomach of animals which have an optimum pH of 1. The charge of the amino acids at the active site is affected by pH and therefore

the properties of the active site change causing the substrate to no longer bind to the enzyme (*Conn et al, 1987; Fersht et al, 1984*).

2.2.2.4 Substrate concentration:

As the concentration of the substrate increases, the rate also increases because more substrate molecules collide with the enzyme molecules, so more reactions will take place. At higher substrate concentrations the enzyme molecules become more saturated with the substrate, resulting in fewer free enzyme molecules. Therefore addition of more substrate towards the reaction with the enzyme does not make much difference. The rate of an enzyme-catalyzed reaction shows a curved dependence on substrate concentration, although it will increase the rate of the enzyme-substrate collisions. At infinite substrate concentration, the maximum rate is called V_{\max} and the substrate concentration that gives half of V_{\max} is called K_m . Therefore an effective enzyme has a high V_{\max} and a low K_m (*Conn et al, 1987; Fersht et al, 1984*).

2.2.3 CLASSIFICATION OF ENZYMES:

Enzymes are classified on the basis of their composition. Those enzymes, which are composed of protein only, are known as simple enzymes as apposed to complex enzymes, which are composed of protein and a small organic molecule. Complex enzymes are also known as haloenzymes in which the protein component is known as the apoenzyme and the non-protein component is known as the coenzyme or a prosthetic group. Those enzymes that require a metal in their composition are known as metalloenzymes provided that after binding they still retain their metal atom under all reaction conditions (*Conn et al, 1987*). Enzymes can be classified as shown in Table 2.3:

Table 2. 3: Classification of enzymes and their biochemical properties

CLASSIFICATION	BIOCHEMICAL PROPERTIES
OXIDOREDUCTASES	Remove or add Hydrogen by acting on chemical groupings
TRANSFERASES	They transfer functional groups between donor and acceptor molecules.
HYDROLASES	They hydrolyse bonds by adding water across it
LYASES	Add ammonia, water or carbon across double bonds, or remove those elements to produce double bonds.
ISOMERASES	Carry out many kinds of isomerisation, L and D isomerisation and mutase reactions.

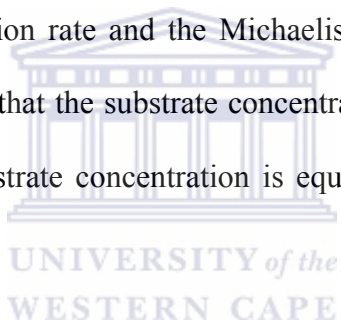
2.2.4 ENZYME KINETICS:

Enzyme kinetics is the study of the rate at which enzymes work. It is studied as a function of the substrate concentration available to the enzyme. The kinetics of simple reactions was first characterized by the biochemists Michaelis and Menten.

The Michaelis-Menten Equation is as follows:

$$\frac{V_i = V_{\max} [S]}{\{K_m + [S]\}}$$

This equation describes the relationship between the rate of a particular enzyme-catalysed reaction [V_i], the concentration of the substrate [S] and the two constants, V_{\max} and K_m , which are the maximum reaction rate and the Michaelis-Menten constant respectively. The above equation illustrates that the substrate concentration that produces exactly half of the maximum rate, the substrate concentration is equal to K_m . The equation can be rearranged as follows:



$$K_m = [S] \{[V_{\max} / V_i] - 1\}$$

Therefore since the substrate concentration is half that required to enhance the maximum rate of reaction, the observed rate, V_i , will be equal to V_{\max} divided by two. At this substrate concentration V_{\max} / V_i will be equal to two, with the result that $[S](1) = K_m$. A graphical representation of reaction rate (V_i) versus concentration [S] produces a hyperbolic rate plot as shown in Figure 2.2 (*Fersht et al*, 1984).

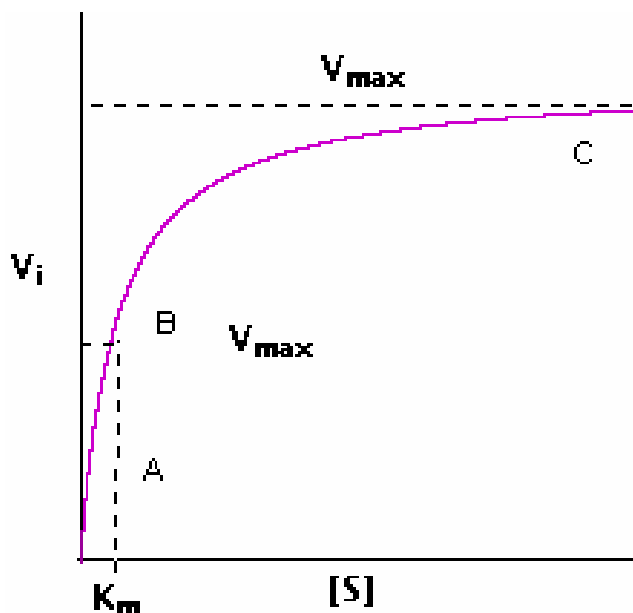


Fig 2.2: Illustration of Michaelis-Menten Kinetics

The plot has key features denoted as points A, B, and C. It has been found that at high substrate concentration, the rate of reaction denoted by C is almost equal to V_{max} with the difference being in nearby substrate concentrations, being almost negligible. If the plot is extrapolated to infinitely high substrate concentration, the extrapolated rate is equal to V_{max} . On the other hand, the rate of reaction becomes independent of the concentration of the substrate, and the rate is said to be zero order. The substrate concentration has a very small difference in reaction velocity around point C, meaning that at these concentrations, almost all of the enzyme molecules are bound to the substrate and the rate is not dependent on the substrate.

Point A and B are the lower substrate concentrations and here the velocities are lower which indicates that at any moment, a portion of the enzyme molecules are bound to the substrate. In fact, at the substrate concentration denoted by point B, exactly half of the enzyme molecules are in the enzyme-substrate complex at any instant and the rate is exactly one half of V_{max} . At substrate concentrations, near point A the rate appears to be

directly proportional to substrate concentration, and the reaction rate is said to be first order. In our study, V_{\max} as well as K_m have been calculated based on this kinetics study (Fersht *et al*, 1984).

2.2.4.1 Enzyme Inhibition:

Enzyme inhibitors are compounds that have the ability to reduce the rate of enzyme-catalyzed reaction, by interacting with the enzyme, cofactor or the substrate. Upon inhibition, the enzyme is unable to bind the substrate and the catalytic ability of the enzyme is reduced hence K_m is affected. K_{cat} , which is the amount of substrates converted to form products at a unit time, as well as the catalytic efficiency of the enzymatic reaction is also affected. There are two types of inhibitors namely; reversible and irreversible.

Irreversible inhibitors are unable to be physically separated from the enzyme and it had been observed that their degree of inhibition tends to increase with time. On the other hand, reversible inhibitors can be separated physically from the enzyme restoring the enzymatic activity it had prior to inhibition. Therefore a reversible inhibition process occurring for a single-intermediate enzymatic reaction can be described as competitive, uncompetitive, non-competitive, mixed effects and allosteric inhibition (Conn *et al*, 1987; Fersht *et al*, 1984).

2.2.4.1.1 Competitive Inhibition:

Competitive inhibitors have a similar structure to the normal substrate molecule and they compete with the substrate for the active site of the enzyme, causing the reaction to be slower. The enzyme-bound inhibitor can either inactivate the enzyme's ability to function

or it can be bind to an unfavourable position for the catalytic reaction to take place with potential substrate molecules. During a catalytic reaction, at a particular enzyme and substrate concentration, if the substrate concentration is lower than that of the inhibitor, then the inhibitor will favourably compete with the substrate for the enzyme binding site and the degree of inhibition is high. When the substrate concentration is high, this effect is reversed. These inhibitors increase K_m for the enzyme but have no effect on V_{max} , so the rate can approach a normal rate if the substrate concentration is increased high enough (Conn *et al*, 1987; Fersht *et al*, 1984).

$$\frac{V}{K_m(1 + 1/K_i) + [S]} = \frac{V_{max} [S]}{K_m + [S]}$$

2.2.4.1.2 Non-competitive Inhibition:

Non-competitive inhibitors are quite different in structure to the substrate molecule and therefore do not fit into the active site of enzymes. Inhibition occurs at other parts of the enzyme changing the shape of the entire enzyme including the active site in such a manner that the substrates can no longer bind. The inhibitors decrease V_{max} but have no effect on K_m . The following equation clearly illustrates these findings.

$$V = \frac{(V_{max} [S])(K_m + [S])}{1 + 1/K_i}$$

In this case the degree of inhibition is dependant on the concentration of the inhibitor as well as its affinity for the enzyme or the enzyme-substrate complex. These interactions are displayed in a Lineweaver-Burk Plots as illustrated in Figure 2.3.

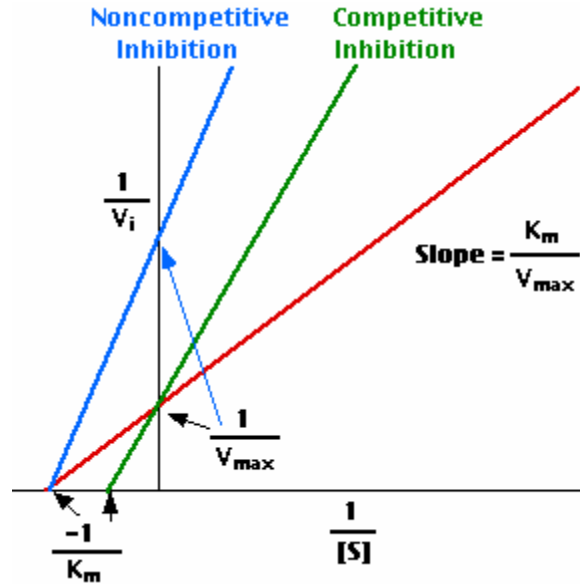


Fig.2.3: Illustration of Competitive and Non-competitive Inhibition

2.2.1.3 Mixed effects inhibition:

This method is used to describe inhibition systems which obey Michaelis-Menten kinetics. These systems do not show any characteristics that are any way similar to competitive and non-competitive inhibition. In this case both K_m and K_{cat} are affected (Fersht et al, 1984).

2.2.5 IMMOBILIZATION OF ENZYMES:

The phrase immobilization implies the physical attachment of an enzyme to a solid support over which a substrate is passed and converted to products. These enzymes are confined with retention of their catalytic activity and permit the re-use of the costly biological molecule thereby allowing a significant simplification of the analytical apparatus. Enzymes are by far the most commonly used biological components in biosensor construction. The localization of enzymes can be achieved through a variety of methods, which fall into four main categories (*Worsfold et al*, 1995) classified as follows:

- (a) Covalent binding of the enzyme to a derivatised, water insoluble matrix
- (b) Intermolecular cross-linking of enzyme molecules using multifunctional reagents
- (c) Adsorption of the enzymes onto a water-insoluble matrix
- (d) Entrapment of the enzyme inside a water-insoluble polymer lattice or semi-permeable membrane.

Immobilized enzymes have become increasingly popular in the past decade due to their reusability; hence their cost saving, greater efficiency and the ability to control their catalytic activity such as predictability of decay rates, potentially longer half-lives and more efficient multi-step reactions. There are three distinct forms in which immobilized enzymes can be presented:

- (a) As solid-phase immobilized enzyme reactors (packed bed and open tubular).
These are mainly used in continuous flow techniques such as flow injection analysis and post-column derivatization in liquid chromatography.
- (b) When immobilized enzyme membranes are incorporated into sensors such as potentiometric enzyme electrodes and optical sensors.

- (c) Solid-phase immobilized enzyme films are used in disposable, dry reagent kits with photometric detection.

There are aspects of the immobilization procedure, which have to be well understood before the procedure can be successfully carried out. These aspects are not dependent on the physical form of the immobilized enzymes, whether it may be solid-phase reactor or membrane phase film.

They are namely

- (a) The properties of the free enzyme
- (b) The type of support used
- (c) The methods of support activation and enzyme attachment (*Worsfold et al, 1995*).

2.2.5.1 Properties of free enzymes:

In nature, each enzyme irrespective of its origin or its metabolism has its own unique systematic name which gives the description of the type of catalysis carried out by the enzyme. Each enzyme possesses a four-number code, which describes other aspects of the enzyme. The classification scheme for enzymes was developed in 1961 by the International Commission on Enzymes but is was originally established in 1956 by the International Union of Biochemistry in consultation with IUPAC; however this scheme is regularly updated. The first number in the code gives an indication of the type of reaction that is being catalysed by the enzyme, the following two numbers indicates the subclass and the sub-subclass of the reaction and finally the fourth number identifies the enzyme. In addition to this, each enzyme has a rival name, which is commonly used. An example of this is the enzyme lipase as it is commonly known but also has the systematic name of

glycerol ester hydrolase with an associated code number of 3.2.1.1 (*Worsfold et al, 1995*).

Table 2.4 gives a few commonly used enzymes and their respective analytes.

Table 2.4: Examples of enzymes used in biosensors and analytes
That have been analysed.

ENZYMES	ANALYTE
β-Glucosidase	Amygdalin
Asparaginase	Asparagine
Cholesterol oxidase	Chloesterol
Chymotrypsin	Esters
Glucose oxidase	Glucose
Catalase	H₂O₂
Lipase	Lipids
Penicillinase	Penicillin G
Trypsin	Peptides
Amylase	Starch
Invertase	Sucrose
Urease	Urea
Uricase	Uric acid

Comparison of enzymes is an important factor since the source of the enzyme is usually of great interest; however a few steps have to be taken in order to achieve this effectively. First and foremost is the specification of the properties of the original enzyme prior to

immobilization in which the working names including the systematic name along with the associated code number have to be well stated. The following information which is also of importance is; the source of the enzyme, its physical form such as being lyophilized, its purity which is usually given in a percentage, its method of purification, its catalytic activity and the details of other constituents have to be clearly stated as well. Therefore, if one has four different enzymes then a precise and direct comparison of the enzymes can be made based on the information stated on the respective enzyme containers. Another important enzyme parameter is catalytic activity since it has a direct bearing on sensitivity.

The most widely used unit of activity is the International Unit (I.U.) which states that one I.U. is the amount of enzyme activity that catalyzes the transformation of one micromole of substrate per minute at 25⁰C under optimal experimental conditions. The most recommended unit however, is the katal, which can be defined as the amount of enzyme activity that catalyses the transformation of one mole of substrate per second at 25⁰C under optimal experimental conditions (*Worsfold et al*, 1995).

2.2.5.2 Enzyme Support:

It is very difficult to predict in advance which support is the most suitable for a particular enzyme due to the fact that the support has a somewhat important and a critical effect on the stability and hence the efficiency of the immobilization of the enzymes. The support material must meet certain criteria for it to be efficient for immobilization and this includes its capability of being soluble in water, its increased capacity to bind a particular enzyme, its mechanical stability and finally if it is chemically inert or not. The term inert

solely refers to the degree of non-specific adsorption of the pH, pressure and the stability of temperature including hydrophilicity as well as charge transfer. The binding capacity of an enzyme is determined by the availability of surface area, which includes both the internal pore size as well as the external bead sizes of the tubular diameter. In addition to these, the extents of ease at which the support can be activated together with the resultant density of the enzyme's binding sites are also taken into consideration. The activity of the immobilized enzyme is very important as it governs the enzymes reaction, therefore due to this, the local diffusion properties of the system as well as the bulk mass transfer should be closely monitored (*Worsfold et al, 1995*).

Presently there is no universally recommended support material. Various materials have been used to compromise for each particular enzyme and experimental system. However the type of support materials can be classified into one of three categories, namely:

- (a) Supports which are hydrophilic biopolymers based on natural polysaccharides such as agarose, dextran and cellulose.
- (b) Those, which are lipophilic synthetic organic polymers such as polyacrylamide, polystyrene and nylon.
- (c) Those support which are inorganic materials such as controlled pore glass and iron oxide.

The chemical structure of the support must be clearly shown as defined and if there are any quantitative physical and chemical data relevant to the three factors stated above should be provided (*Worsfold et al, 1995*).

2.2.5.3 Enzyme attachment and Support Activation:

An activated support is defined as a material possessing an enzyme reactive functional group, which is covalently attached to a supposedly inert surface. Consideration of the stability of the resultant bond now existing between the enzyme and the support, the local environment of the enzyme as well as the potential loss of activity upon immobilization, are highly important. There are a number of procedures, which aid in the activation of support materials and each differs according to the type of support. Support activation for polysaccharides is through derivatization of available hydroxyl functions using reagents such as cyanogens bromide, epoxides triazine derivatives such as cyanuric chloride, sodium periodate or benzoquinone. It has been noted that polyacrylamide and its derivatives can be activated by their reactions with diamines while on the other hand, inorganic supports are commonly silanized and activated by reacting with glutaraldehyde. Other support activation mechanisms are diazotization or reaction with carbodiimides, thionyl chloride, N-hydroxysuccinimide or transition metal salts such as titanium chloride. The activated support is now suitable for covalently linking the enzymes and in most cases this is through direct reactions with available amino functions such as lysine residues as well as through thiols and phenol functions. Entrapment techniques for enzyme immobilization have been popular for quite some time but in the past few decades, covalent binding of enzymes to a suitable activated support has been by far the most common approach and hence the most useful technique. Later we will discuss the reason for the popularity of covalent binding as well as the other immobilization techniques (*Worsfold et al, 1995*).

2.2.6 CHOICE OF IMMOBILIZATION METHOD:

Prior to the immobilization of an enzyme it is of extreme importance to choose the appropriate immobilization method, which is aimed at reactive groups outside the active catalytic and binding site of that enzyme. Knowledge of the active sites of a particular enzyme should be known in order to enable a choice from various methods that would avoid reaction with the essential groups therein. On the other hand, these active sites of the enzyme can be protected during the attachment process provided the protective groups can be removed without the loss of enzyme activity.

The surface on which the enzyme is to be immobilized has several vital roles to play which include the retaining of tertiary structure in the enzyme by hydrogen bonding or the formation of electron transition complexes. Increasing the thermal state by the retention of the tertiary structure in the immobilized state of the enzyme is also important, therefore it is a requirement to examine and intensively follow new discoveries in the chemical nature of soluble thermostable enzymes. The immobilized enzyme together with the microenvironment of that particular enzyme possess an anionic or a cationic nature of the surface that has the ability to make a change in the optimum pH of the enzyme up to two pH units. In most cases it is together with a broadening of the pH region in which the enzyme can work effectively. The methods, which are associated with immobilization of enzymes, fall into four main categories as described in the following sections.

2.2.6.1 Physical Adsorption:

Physical adsorption of an enzyme onto a solid support is the simplest method for immobilising enzymes. This method involves a non-specific physical interaction between the enzyme in use and the surface of the support as a result of mixing a concentrated enzyme solution with the solid. The binding is mainly by hydrogen bonds, multiple salt linkages and the Van der Waal's forces, causing this method to be less disruptive towards the enzyme as compared to chemical means of attachment. The major advantage of adsorption is that there are no reagents required and only a minimal number of activation steps are required. The weak bond involvement between the enzyme and the support is sometimes a problem mainly caused by changes in temperature, pH, ionic strength or the presence of a substrate, thereby resulting in the desorption of the enzyme. Non-specific adsorption of other enzymes or substances is also another disadvantage, since as the immobilized enzyme is used, its properties are altered. If the substance adsorbed is the substrate for the enzyme, then the rate usually decreases but this depends on the surface mobility of the enzyme and the substrate. Adsorbed enzymes have been temporarily stabilized and this has been achieved by cross-linking the enzyme in a chemical reaction subsequent to its physical adsorption.

This type of immobilization technique has been used for the immobilization of horseradish peroxidase (HRP) on totally cinnamoylated derivatives of D-glucose and D-Manitol in the form of glassy beads. The immobilization of this enzyme on these supports involved an intense hydrophobic interaction between the cinnamoyl groups of the support and the enzyme. The polymerisation and cross-linking of the derivatives was achieved by irradiation in the ultraviolet region, where these compounds showed maximum sensitivity. It was discovered that the immobilized enzyme was more resistant

to inactivation by hydrogen peroxide and also to heat at neutral pH. Several aspects, which included HRP concentration, support concentration, immobilization time and pH, were studied in order to find the best immobilization conditions (*Rojas-Malgarejo et al, 2003*).

Physical adsorption was also used to immobilize polyelectrolyte-stabilized enzymes into activated macroporous and conductive carbon material for the construction of stable biosensors. Polyelectrolytes used in this case were polyethylenimine and diethylaminoethyl-dextran. Polyethylenimine is responsible for the stabilization of the secondary structures of various enzymes thus preventing denaturation. It also prevents the oxidation of enzymes sulphide groups prohibiting its inactivation and stability. The enzymes used in this work were lactate oxidase, tyrosinase, fructose dehydrogenase, pyranose oxidase and pyruvate oxidase, which were stabilized to carbon paste before being immobilized on the carbon material, which served as the immobilization matrix as well as the electrochemical transducer (*Dimakis et al, 2002*).

2.2.6.2 Occlusion:

This method of enzyme immobilization involves the confinement of enzymes within lattices of polymerised gels allowing the free diffusion of low molecular weight substrates and reaction products. A hydrophilic matrix is polymerised in an aqueous solution of the enzyme and is later broken up to the desired particle size. There is no bond formation existing between the enzyme and the polymer matrix, therefore there is no enzyme disruption making occlusion also an applicable method. A disadvantage of this method is that only low molecular weight substrates diffuse to the enzyme thus making

this method suitable for enzymes such as trypsin, ribonuclease, dextranase, etc which act on macromolecular substrates. Upon polymerisation, free radicals are generated which also cause problems by affecting the activity of the entrapped enzyme. It is always advised that the entrapped enzyme should be cross-linked with glutaraldehyde in order to prevent leakage of the enzyme as a result of the broad distribution in pore size of the synthetic gels especially of the polyacrylamide type. Finally, occlusion of the enzyme can be achieved by using ultra filtration membranes of well-defined pore sizes.

This technique was used to immobilize D-fructose-5-dehydrogenase onto a platinum electrode to produce a biosensor, which was used for the fructose detection. The immobilization was done in polypyrrole film where sodium ferricyanide was used as the mediator for the system (*Garcia et al*, 1998).

Occlusion was also used in a study, which involved the immobilization of the enzyme ascorbate oxidase in a graphite/epoxy electrode in a poly (ethylene-co-vinyl acetate) matrix. After subsequent preparation, enzyme immobilization was achieved with the aid of glutaraldehyde (*Fernandes et al*, 1999).

2.2.6.3 Cross-Linking:

Generally, the immobilization of enzymes using this technique is achieved by intermolecular cross-linking of the enzyme either to another enzyme or to the functional groups of an insoluble support. Cross-linking an enzyme to itself is extremely expensive and insufficient due to the fact that some of the enzymatic material will act mainly as the support, resulting in a relatively low enzymatic activity. This method is best utilized in

relation with one of the other mentioned methods. It is advantageous in a way because it prevents leakages from polyacrylamide gels but most importantly, it is used as a means of stabilizing adsorbed enzymes.

This method was used for the immobilization of the enzyme tyrosinase (Tyr) in the presence of the mediator NQS for the determination of dichlorvos organophosphate pesticides. The activity of Tyr is based on the ability to reduce the quinone form of the mediator NQS to the reactive o-diol form substrate of Tyr (H_2NQS) at the working electrode, thus allowing modulation of the catalytic activity of the enzyme and measurement of the inhibition produced by the pesticides (Vidal *et al*, 2006).

In another study, an amperometric biosensor for the determination of hydrogen peroxide was developed based on cross-linking horseradish peroxidase with the aid of glutaraldehyde with MWNTs/chitosan composite film coated on a glassy carbon nanotube/chitosan composite film coated on a glassy carbon electrode (Quian *et al*, 2001)

2.2.6.4 Covalent Binding:

The formation of covalent bonds between the enzyme and the solid support is the most intensely studied of the immobilization techniques. The type of reaction by which a particular enzyme should be immobilized is chosen with regards to the fact that the binding reaction should be performed under conditions that would not cause the loss of enzymatic activity, and that the enzyme active site must be unaffected by the utilized reagents. The functional groups of enzymes, which are suitable for covalent binding under mild conditions, include:

- (i) The alpha amino groups of the chain and the epsilon amino groups of lysine and arginine
- (ii) The alpha carboxyl group of the chain and the beta and gamma carboxyl groups of aspartic and glutamic acids
- (iii) The phenol ring of tyrosine
- (iv) The thiol group of cysteine.

There are only a small number of reactions which have been designed to couple with functional groups on the enzyme other than the amino and phenolic residues. Similar to cross-linking, covalent-binding provides stability as well as insolubilized enzyme derivatives that do not leach the enzyme into the surrounding solution.

Covalent binding was the method used in a project whereby two biosensors were prepared for oxalate determination using two enzymes respectively, namely oxalate oxidase and horse radish peroxidase which were incorporated into carbon paste modified electrode with silica gel coated with titanium oxide containing toluidine blue (*Perez et al*, 2001).

2.2.7 CHARACTERISTICS OF IMMOBILIZED ENZYMES:

Factors such as activity and stability have a significant effect on immobilized enzymes and therefore, it is important that the percentage or the amount of immobilized enzyme together with the enzyme activity remaining after immobilization should be stated along with the experimental conditions which are well suited for the determination. The activity of the enzymes is the most important information for the comparison of immobilization techniques and is often not available. It is vital that one knows the amount of enzyme immobilized onto a support and this is usually achieved by measuring the amount of enzyme remaining in the supernatant after immobilization and then subtracting this from the amount which was originally present. There is a fraction of difficulty in the determination of absolute activity of the enzyme on the support material after immobilization; therefore the apparent activity is measured which involves the mass transfer as well as diffusional restrictions in the experimental method being used (Worsfold *et al*, 1995).

The stability of the immobilized enzyme with respect to time, temperature, storage conditions and at times experimental variables are critical performance indicators that should be noted. There are various methods in which this can be addressed however the recommended and most popular is the storage of the enzyme under normal operating conditions also known as the ambient temperature in the appropriate buffer solution. After a fixed time period the activity of the enzyme is monitored following the same procedure as that for the determination of the enzyme activity after immobilization. Each enzyme has its own lifetime and maximum analyses strength. To account for the efficiency of a particular enzyme, the effect of introducing synthetic standards, reference material, as well as the introduction of samples at predefined intervals and frequencies

should be determined prior. Consideration should also be placed on what the effect would be on the enzyme during the immobilization step by paying special attention to aspects such as pH, temperature, ionic strength and the incorporation of impurities during the procedure. The optimum pH, oxidation and reduction working range and the apparent Michaelis constant for the appropriate substrate of an immobilized enzyme, could all be affected by immobilization and the experimental conditions therefore; prior knowledge of the details of the experiment should be noted (*Worsfold et al, 1995*).



2.3 CYTOCHROME P450 (2D6):

The sensing enzyme used in this study is Cytochrome P450 (2D6). In this section, the structure, biochemistry and the reaction kinetics of this enzyme will be discussed.

2.3.1 Occurance of the enzyme:

Iron Porphyrin enzymes also known, as cytochromes were first investigated by Warburg and at the time they were referred to as cell pigments. It was discovered that carbon monoxide had the inhibitory factor on respiration cells in the dark, however upon illumination, respiration was resumed. Since it was known that iron-carbon monoxide complexes were photo-dissociated, Warburg then suggested that in respiration a compound of iron was involved. The photo effect was examined more closely and it was discovered that a specific wavelength was involved which was a characteristic absorption wavelength of iron hema-chromogen containing porphyrins. Warburg then came to the conclusion that the respiratory pigments were similar to these compounds (*Key et al*, 1966).

MacMunn later continued the study on these compounds but it was Keilen who revisited his work who discovered that at specific wavelengths a pigment was absorbed in several cells, which were then given the name cytochrome. Therefore, all the cells, which were examined and contained this pigment, could be readily observed on reduction due to a change in light absorption. CYP 2D6 was discovered fifty years ago among multiple pigments of 450nm (*Key et al*, 1966). However, approximately ten years ago, the first gene to code for a specific CYP enzyme was isolated. A number of these genes were isolated which were used to produce the enzymes in their most purified forms hence; their amino acid sequences could be determined (*Hermeryck et al*, 2002).

2.3.2 Cytochrome P450-2D6 (CYP2D6):

CYP 2D6-P450 (CYP2D6) forms part of a multigene family of heme enzymes which have the ability to catalyse the NADPH – dependant monooxygenase as well as other reactions of different exobiotic and endobiotic lipophilic substrates. These enzymes are capable of metabolizing over 1,000,000 chemicals and undergo mono-oxygenation reactions which are very useful as they are responsible for the hydroxylation of a number of compounds including steroids, fatty acids, drugs, food additives, fungi, bacteria, (*Harris et al*, 2001; *Subehan et al*, 2006) alkanes and polyaromatic and polychlorinated hydrocarbons. Among the biotransformation reactions of CYP2D6 included are N-, O-, or S-, demethylation, dealkylation, S- oxidation, Epoxidation, Aliphatic oxidation, Reductive Dehalogenation and Sulfoxide formation (*Shumyanteva et al*, 2005; *Bistolos et al*, 2005). In man most of the CYP2D6 is found in the liver which is the main organ involved in processes of drug and toxin removal. A remarkable amount of this enzyme is also found in the small intestine but usually CYP2D6 sits around the microsomal part of the cytoplasm in the endoplasmic reticulum, as well as in mitochondria (*Iwuoha et al*, 1998). The enzymes isolated from mitochondria are known as Steroidogenic CYP2D6 enzymes, which are situated in single, cell organisms and are phylogenetically older. They usually consist of an iron-sulphur protein, NADPH and NADH-dependant reductase (on FAD-type flavoprotein) and P450 enzyme. Steroidogenic enzymes are responsible for steroid synthesis as well as other substances which are required for maintaining the cell wall integrity. Another form of these enzymes is Xenobiotic CYP2D6 enzymes, which has evolved from Steroidogenic CYP2D6 enzymes over one billion years ago. The term Xenobiotic is based on the fact that these enzymes have the ability to metabolise foreign biological substances. They are located in the smooth endoplasmic reticulum of cells,

while some studies indicate that they have evolved during the period of plant-animal differentiation. These enzymes are known to be constituted by NADPH: P450 reductase (FAD-and FMN- containing flavoprotein) and P450 enzyme (*Iwuoha et al, 2003, Lewis et al, 2002*).

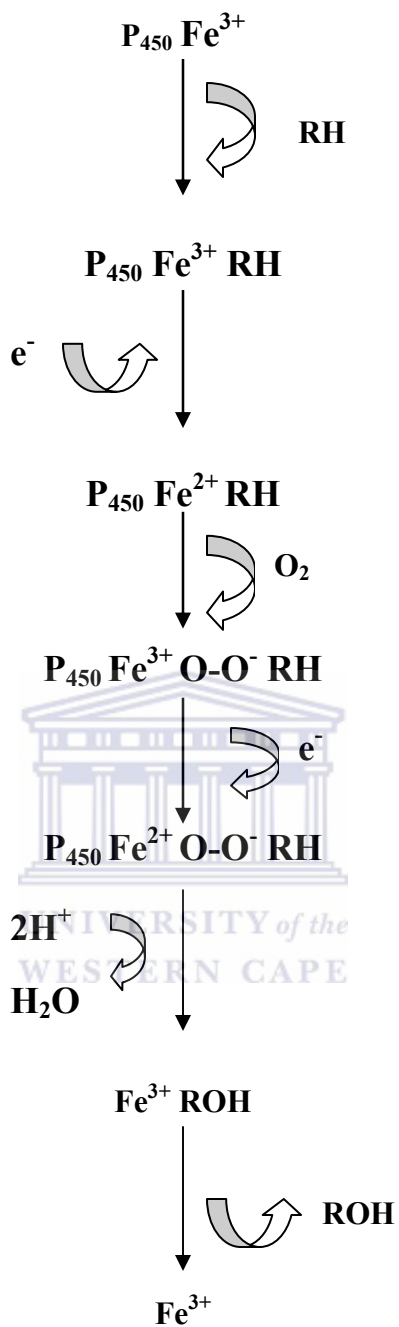
2.3.3 Kinetics of Catalytic Reaction:

The active site of CYP 2D6 is the iron-protoporphyrin IX that consists of an axial thiolate of a cysteine residue as the fifth ligand. The metal iron exists in two oxidation states namely; Fe²⁺ and Fe³⁺. Almost all iron complexes are octahedral and practically all are paramagnetic which is due to the unpaired electrons in the 3d orbital. As mentioned before, heme (Fe²⁺) enzymes exhibit characteristic visible absorption spectra due to the presence of protoporphyrin IX. However, their spectra differ according to the identities of the lower axial ligands donated by the protein and the oxidation state of the iron, as well as the identities of the upper axial ligands donated by the substrates (*Harris et al, 2001*).

At the initial stage of the catalytic cycle of CYP2D6, the active site, which is the iron-protophyrin, has an axial thiolate of a cysteine residue as the fifth ligand. The enzyme at this point is in the hexa-coordinated low spin ferric form (Fe³⁺) possessing water as the sixth ligand. CYP2D6 is now said to be resting since it is in the ferric form (*Shumyanteva et al, 2005*). Substrate hydroxylation with the aid of the CYP2D6 mono-oxygenase results in the insertion of an oxygen atom into the substrate denoted by RH. The second oxygen atom is then reduced to water while ROH is formed as a result of the consumption of two reducing equivalents (*Lewis et al, 2002*). This can be summarized as follows:



The source of electrons in this type of system is from flavoproteins, ferredoxin like proteins, NADPH (*Lewis et al, 2002*), the mediator or an electrode. The mechanism for substrate hydroxylation by CYP, which is generally accepted, involves the following steps although there are still several details that still remain unsolved. When the substrate binds to the hexa-coordinated low-spin ferric enzyme, water is excluded from the active site, thereby resulting in a change in the 5-coordinate low spin state. This causes a decrease in polarity which is accompanied by a positive shift (*Bistolos et al, 2005*) or lowering of the redox potential by 110 mV to 130 mV which makes the first electron transfer step thermodynamically favourable, from its redox partner NADH or NADPH (*Shumyanteva et al, 2005*). The transfer of the first electron from one of the redox partners reduces the ferric iron to the ferrous enzyme and this process is called reduction. This form of the enzyme can now bind molecular oxygen resulting in a ferrous-dioxygen ($\text{Fe}^{\text{II}} - \text{O}_2$) complex. A second electron transfer takes place along with a proton gain forming an iron-hydroperoxo ($\text{Fe}^{\text{III}}\text{-OOH}$) intermediate (*Bistolos et al, 2005*). The O_2^{2-} reacts with two protons from the surrounding solvent, thus breaking the O-O bond to release a water molecule and a highly active iron-oxoferryl intermediate. One hydrogen atom is abstracted from the substrate by the intermediate to produce a one electron reduced ferryl species ($\text{Fe}^{\text{IV}}\text{-OH}$) and a substrate radical. On the other hand, the ferryl species reacts with the C – H bond of the substrate in a concerted reaction without the radical intermediate formation. The final step of the process is the formation of the enzyme product complex and the release of the product denoted ROH. The low-spin state of the enzyme is then regenerated (*Bistolos et al, 2005*). The reaction mechanism of this enzyme is illustrated in the following scheme:



Scheme 2.2: Reaction mechanism of CYP450 (2D6)

2.3.4 Classification of Cytochrome P450 enzymes:

Different enzymes have certain similarities such as amino acid sequence homology, which then resulted in the development of a classification system for enzymes. The basis of this classification is based on the principle that, the more similar the structure of the enzymes, the more closely are they both phylogenetically and functionally. The CYP enzymes are grouped into families that are represented by the first number; example in P450 (2D6) the first number is represented by 2. The idea behind this grouping is based on the fact that all the enzymes in the same family have at least 40% amino acid sequence homology. These families are then further grouped into subfamilies where at least 55% of the amino acid sequences are homologous among the enzymes. There are at least 74 CYP families with only 17 of these described in man. The subfamilies are denoted by an alphabetical letter which in P450 (2D6) is D. The last number which in P 450 (2D6) is 6 represents the gene that codes for the enzyme. There are about 30 of these described in man. The following is a table showing all of the human CYP enzymes grouped into families and subfamilies.

Table 2.5: CYP Enzymes as classified by family, subfamily and gene

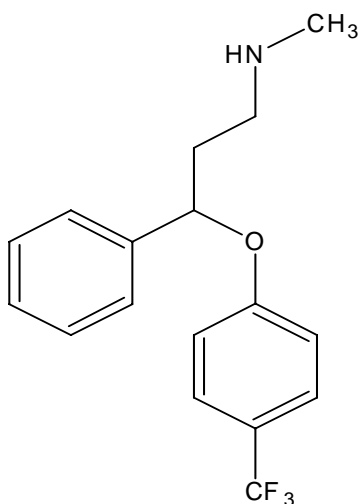
1A1	2A 6	3A3/4	4A9	7	11A1	17	19	21A2	27
1A2	2A7	3A5	4B1		11B1				
	2B 6	3A7	4F2		11B2				
	2C 8		4F3						
	2C 9								
	2C18								
	2C19								
	2D 6								
	2E 1								
	2F1								

2.4 SELECTIVE SEROTONIN RE-UPTAKE INHIBITORS

(SSRIs):

Depression is a recurrent illness, in which the neurotransmitter, serotonin is affected. This condition affects both the economic as well as the social functioning of the individual patient thus leading to suicidal behaviour (*Pedrazza et al, 2007*). Tricyclic antidepressants have been used for the treatment of this condition between the years 1960 to 1980; however the increased side effects associated with these drugs have led to diagnosed patients to end treatment (*Malgara et al, 2007*). The need for new drugs with minimal side effects then resulted in the development of selective serotonin re-uptake inhibitors (SSRIs). These drugs function by enhancing serotonergic transmission and inducing down-regulation of postsynaptic receptors (*Murrin et al, 2007*). The most commonly prescribed SSRIs used for the treatment of depression are fluoxetine, fluvoxamine, paroxetine, sertraline and citalopram. All these drugs have a similar effect in terms of antidepressant treatment as well as a similar side-effect pattern. The only difference among these drugs is in their metabolism, chemical structure and pharmacokinetic properties (*Hermeryck et al, 2002*).

2.4.1 Fluoxetine:

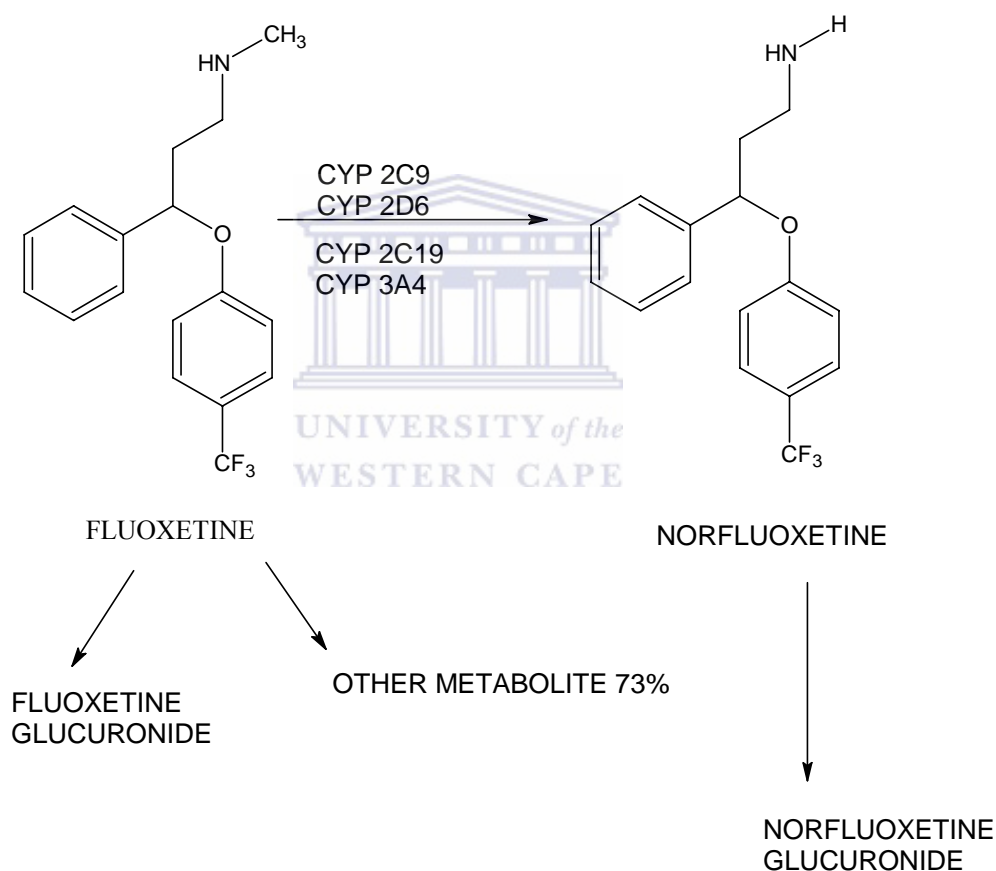


Scheme 2.3: Structure of fluoxetine prior to metabolism

Fluoxetine (scheme 2.3) is a bicyclic derivative of phenyl-proplamine [D,L-N-methyl-3-phenyl-3-(α,α,α -trifluoro-*p*-toxyloxy)-polyamine hydrochloride] whose metabolism is responsible for *N*-demethylation to norfluoxetine (Kovacevic *et al* , 2006; Vlase *et al*, 2005). Fluoxetine is used in the treatment of obsessive-compulsive disorder, panic disorder, premenstrual dysphoric disorder and bulimia. A low level of serotonin is currently seen as one of the neurochemical symptoms of depression; therefore this drug is designed to elevate the level of the presynaptic cell. Fluoxetine is said to be selective because it has a weak effect on the other monoamine transporters, thus it has a little influence on the level of the other neurotransmitters (Heimke *et al*, 2000).

In most countries, this drug was the first SSRI that became available for clinical use. It is a racemic mixture of two enantiomers, in which the S-enantiomer is approximately 1, 5 times more potent than the R-enantiomer. It undergoes extensive metabolic conversion resulting in the active metabolite norfluoxetine as well as multiple other metabolites. The

pharmacological difference among the enantiomers is even more evident for the metabolite norfluoxetine. The S-enantiomer is found to have approximately 20 times higher reuptake blocking potency than the R-enantiomer. This drug is absorbed orally and it is almost completely absorbed in the human system. After oral administration, fluoxetine is mainly excreted in urine, with less than 10% excreted unchanged or as fluoxetine N-glucuronide. The metabolism of this drug is illustrated in scheme 2.4.

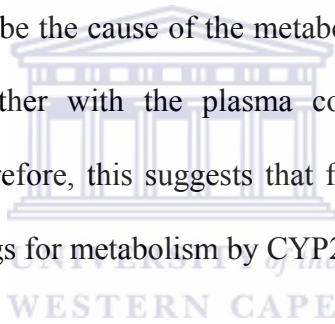


Scheme 2.4: Metabolism of fluoxetine by isoenzymes

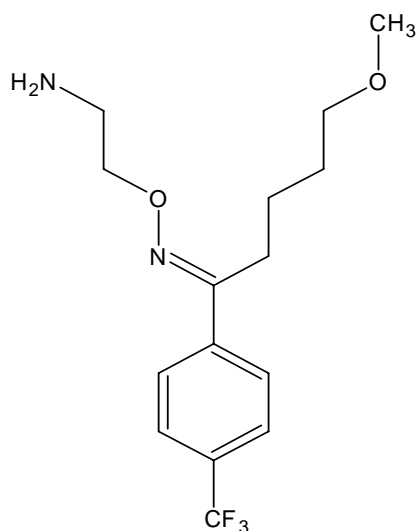
A number of studies have investigated the metabolism (scheme 2.4) of Fluoxetine and have found the CYP isoenzymes to be responsible for the metabolism. From *in vitro*

studies, it has been suggested that CYP2C9 plays vital role in the N-demethylation of Fluoxetine. CYP2C19 and CYP3A4 have been also found to play a similar role while that of CYP2D6 was found to be negligible. On the other hand, the clearance of R- and S-fluoxetine as well as S- norfluoxetine, have been shown to be strongly dependant on CYP2D6 (*Heimke et al, 2000*).

The most prominent feature of all SSRI's is their potential and ability for pharmacokinetic drug interaction with other classes of drugs. This type of interaction was first reported for fluoxetine and relevant clinical interactions have been observed for TCAs as well as neuroleptics. The inhibitory effects of fluoxetine and norfluoxetine on the isoenzyme CYP2D6 could be the cause of the metabolism of these interactions, with the extent of inhibition together with the plasma concentration of fluoxetine and norfluoxetine respectively. Therefore, this suggests that fluoxetine and norfluoxetine are able to compete with other drugs for metabolism by CYP2D6 (*Heimke et al, 2000*).



2.4.2 Fluvoxamine:



Scheme 2.5: Structure of fluvoxamine prior to metabolism

Fluvoxamine (scheme 2.5) became popular in 1999 after it was discovered that one of two teenage shooters who was involved in the Columbine High School massacre, was on this medication for the treatment of depression. At this point, the public as well as other economic sectors was pointing fingers at fluvoxamine and its manufacturer, Solvay Pharmaceutical, due to the fact that its clinical traits indicated that the drug had the ability and propensity to enhance mania in only 4% of the youth who took it.

Fluvoxamine is also a selective serotonin reuptake inhibitor that is used primarily to treat depression, anxiety and Obsessive Compulsive Disorder. This drug functions by blocking the reuptake of serotonin at the serotonin reuptake pump of the neuronal membrane, thereby enhancing the actions of serotonin on 5 HT_{1A} autoreceptors. Its effects are similar to other SSRIs but it acts differently on the neurochemistry of the body. The difference is most beneficial to patients who experience usual or limiting side effects from other antidepressants. As compared to other SSRI's, fluvoxamine has been found to cause a fewer side effects, especially in terms of loss of sex drive. Examples are the

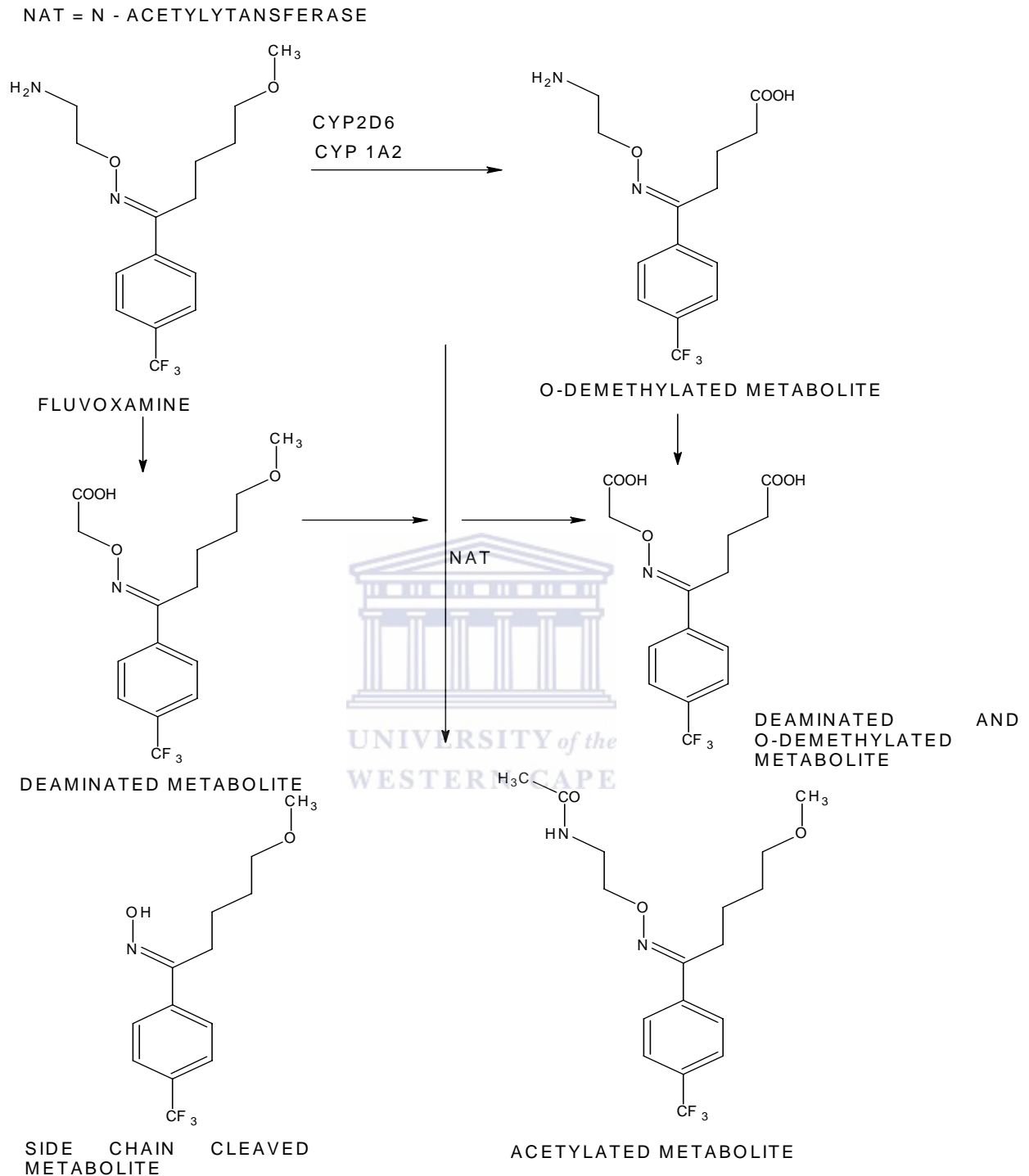
gastrointestinal effects of which nausea is the most common, but it is mild and moderate (Kovacevic *et al*, 2006; Vlase *et al*, 2005). As seen for other SSRIs, the main route for elimination of Fluvoxamine is through hepatic metabolism that includes oxidation demethylation and oxidative deamination shown in scheme 2.6. After fluvoxamine ingestion, eleven metabolites have been detected in urine, nine of which could be structurally identified. The majority of these metabolites were acids, which are likely to possess pharmacological activity. The biotransformation of fluvoxamine has been associated with the polymorphic activity of CYP 2D6 and CYP 1A2, but under the same conditions, the polymorphic isozyme CYP 2C19 was not seen to play any role.

In vivo studies have indicated fluvoxamine to inhibit CYP 2C19, CYP 3A4 and CYP 2C9. The widespread inhibitory effects of this drug is concentrated on a common inhibitory mechanism, perhaps by fluvoxamine interaction or one of its metabolites possessing a heme moiety of the cytochromes. The inhibition of several CYP isoenzymes by fluvoxamine indicates that drug-drug interactions are clinically more critical than those of fluoxetine and paroxetine. *In vitro* studies of fluvoxamine indicate that it is a potent and a selective inhibitor of neuronal serotonin reuptake and has only very weak effects when associated with norepinephrine and dopamine neuronal reuptake (Perez *et al*, 2001; Kovacevic *et al*, 2006; Vlase *et al*, 2005).

It has been discovered that fluvoxamine is often much safer than the other available SSRI medications. Investigations have shown that the chronic administration of fluvoxamine caused a downregulation to the brain norepinephrine receptors, as compared with other drugs, which are effective in the treatment of major depression disorders. The properties of fluvoxamine, which include antidepressant, anti-obsessive compulsive and anti-

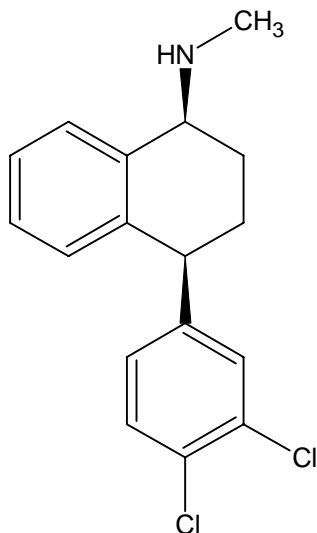
bulimic actions are assumed to be associated to its inhibition of the central nervous system neuronal uptake of serotonin. Some studies have shown fluvoxamine to have a more beneficial effect on suicidal ideation and or anxiety or somatic complaints as compared with imipramine, dothiepin and maprotiline (*Schreiber et al, 2006*).





Scheme 2.6: Metabolism of fluvoxamine by isoenzymes

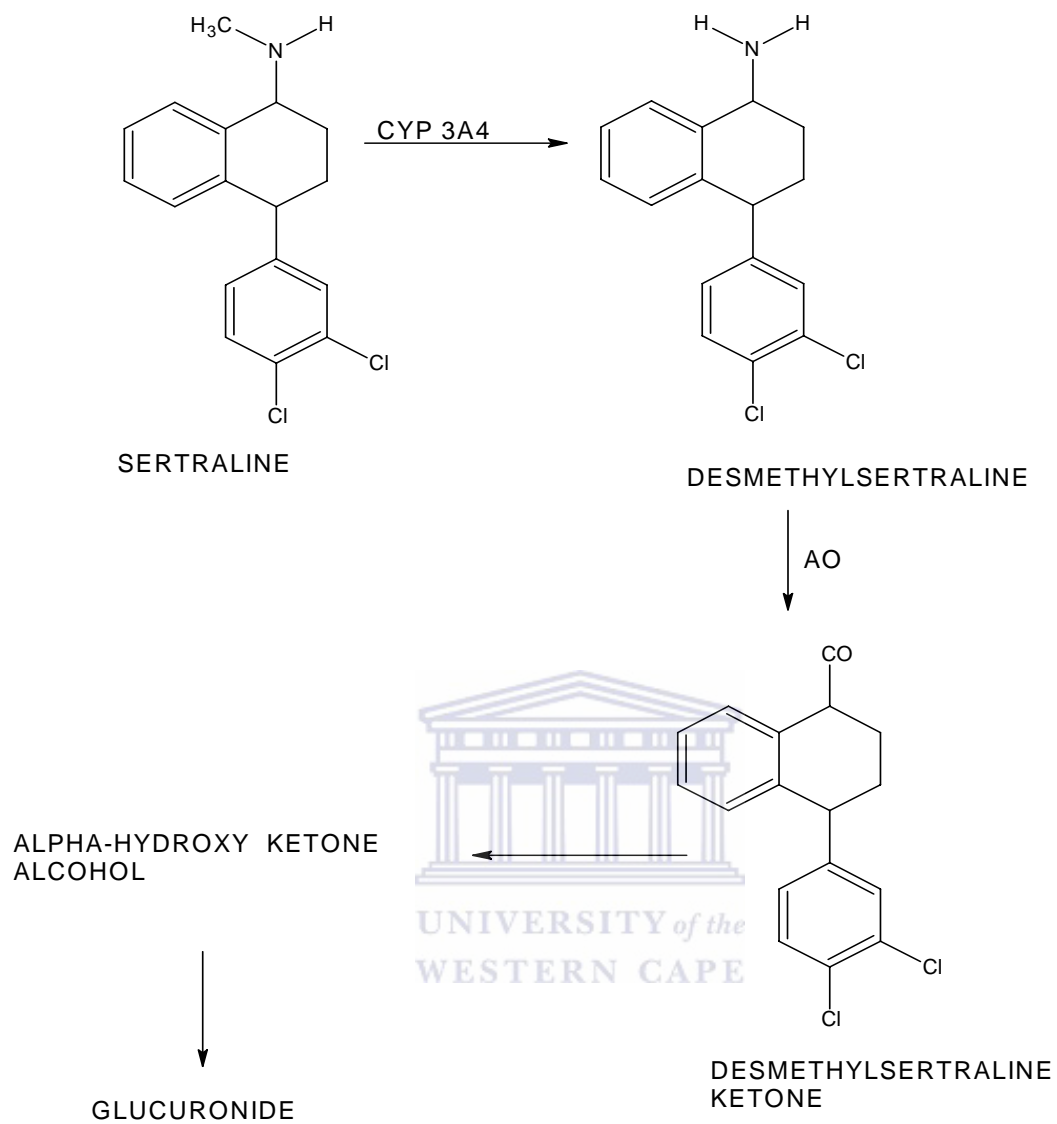
2.4.3 Sertraline:



Scheme 2.7: Structure of sertraline prior to metabolism

Sertraline (scheme 2.7) or sertraline hydrochloride is an antidepressant of the selective serotonin type, which possesses two chiral centers (*Heimke et al*, 2000). Medically, sertraline is used for the treatment of depression and anxiety but is also prescribed for the treatment of Obsessive Compulsive Disorder, post-traumatic stress disorder, premenstrual dysphoric disorder, panic disorder and bipolar disorder. Some of the adverse conditions involving sertraline include insomnia, confusion, dizziness, tremors, asthenia and decreased libido. This drug is the second most potent inhibitor of serotonin reuptake as well as the second most selective blocker of serotonin over noradrenaline uptake. It has a low affinity for neurotransmitter receptors but has an exception for α_1 -adrenoceptor blocking potential. In rats Sertraline administered chronically attenuates phencyclidine-induced locomotor hyperactivity, therefore on dopaminergic neurons, sertraline should be considered although the interaction is still obscure (*Heimke et al*, 2000, *Pedrazza et al*, 2007).

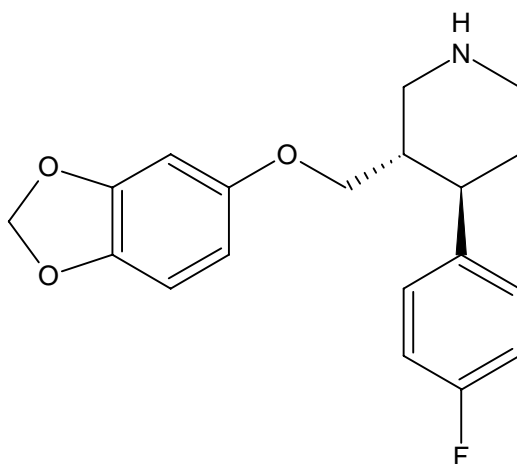
Elimination of sertraline is through hepatic metabolism illustrated in scheme 2.8 but from an oral dose 0.2% is excreted unchanged in urine, but the metabolism has been discovered to be limited. The main metabolic step is N-methylation and the N-demethylated metabolite is eliminated more slowly with a three time longer half-life than the parent drug. The plasma concentration of N-desmethylsertraline is calculated to be one to three times that of sertraline and the contribution to clinical effects can be neglected due to the fact that N-desmethylsertraline has only 5-10% of the serotonin reuptake inhibitor potency of sertraline. The N-demethylation has been discovered to be related to the activity of CYP 3A4 suggesting that this enzyme is involved. Sertraline is a substrate of CYP 3A4 suggesting that there is metabolism of this drug in the gut. This metabolism has not been examined in the gut and therefore little has been reported on other pathways which include oxidation at the side chain to a carbamic acid as well as oxidation deamination to a ketone derivative. Our study is the first to report the use of CYP 2D6 for the metabolism of sertraline where very low concentrations of this drug was analysed (*Heimke et al, 2000; Zawertailo et al, 1995*).



AO = AMINE OXIDASE

Scheme 2.8: Metabolism of sertraline by isoenzyme

2.4.4 Paroxetine:

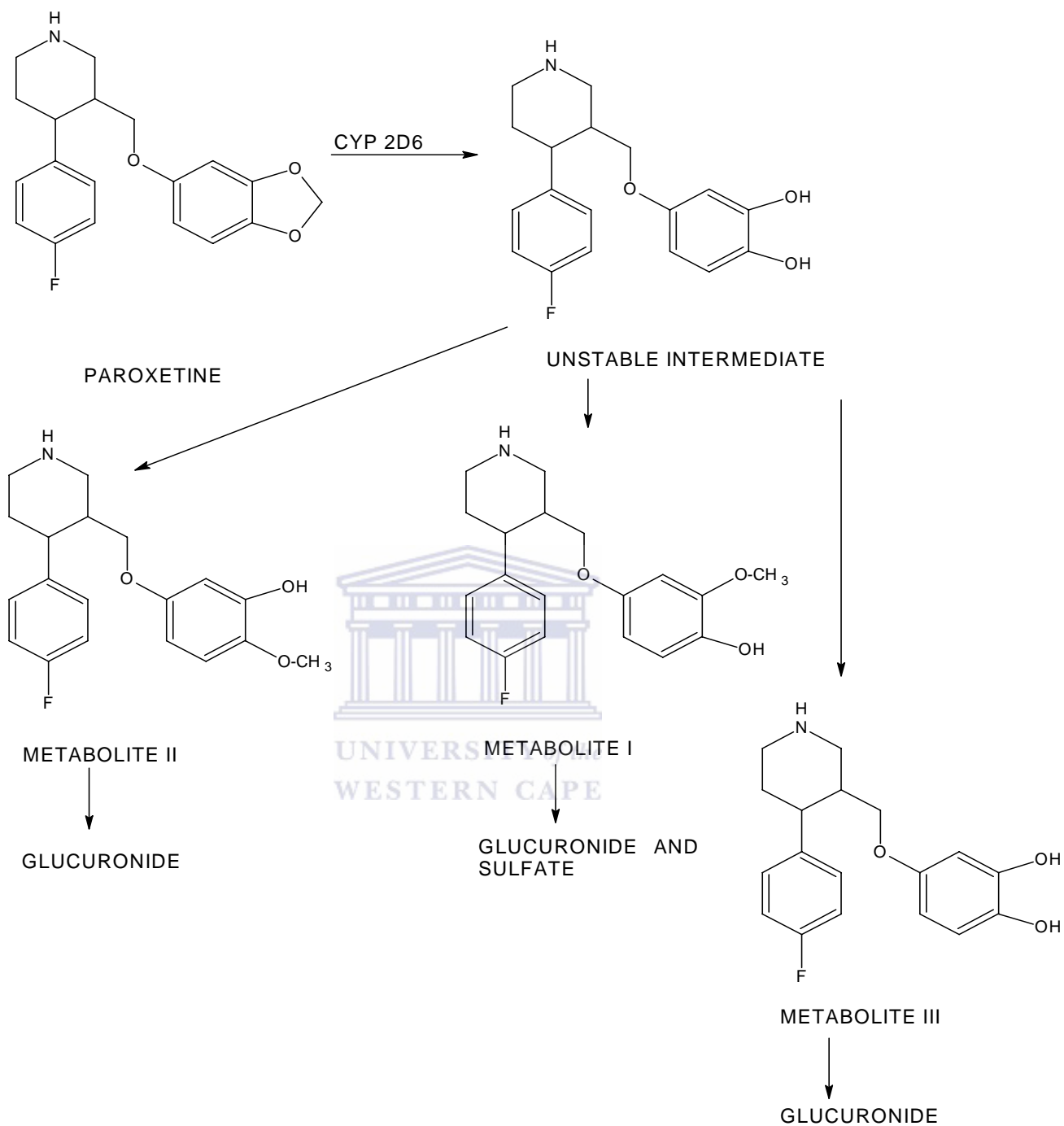


Scheme 2.9: Structure of paroxetine prior to metabolism

The pharmaceutical company GlaxoSmithKline released paroxetine in 1992 and prescribed it for depression and other related diseases. It is a phenylpiperidine derivative and is the second most prescribed antidepressant due to its most potent inhibition of the reuptake of serotonin; 5-HT, as compared to all the currently available antidepressants including other SSRIs (Najeem *et al*, 2004). It is a very weak inhibitor of norepinephrine uptake but it has been found to be more active at this site when compared to other SSRIs. In terms of selectivity, paroxetine (scheme 2.9) has a high uptake inhibition ratio of norepinephrine to serotonin of all the SSRIs (Bourin *et al*, 2001). Since paroxetine is a phenylpiperidine derivative, it is chemically unrelated to the tricyclic or tetracyclic antidepressants; therefore it has a low affinity for dopaminergic, catecholaminergic or histaminergic systems, thereby resulting in a low propensity to cause central and autonomic side effects. Paroxetine is an inhibitor of cytochrome isoenzyme P450 2D6. This drug is absorbed orally and it is able to undergo first pass metabolism that is partially saturable and its metabolites are found to be pharmacologically inactive *in vivo*.

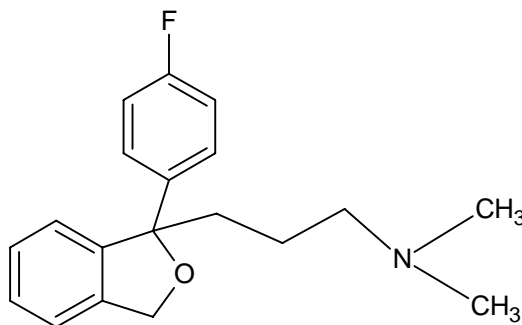
The pharmacokinetics of paroxetine in adults, the young as well as well as the elderly possessing higher plasma concentrations is found to have a wide variation. Just like all other lipophilic psychotropic drugs, the metabolism of paroxetine (scheme 2.10) takes place in the liver with the aim of forming more hydrophilic excretable compounds. This metabolism includes oxidative cleavage of the methylenedioxy bridge, thereby resulting in an unstable catechol intermediate that is further methylated in the meta position to the meta-methoxyderivative or otherwise in the para-position to the para-methoxyderivative. Both of these metabolites are further conjugated with sulfuric acid or glucuronic acid but none of them is assumed to have a contribution to the pharmacological effects of paroxetine (*Heimke et al, 2000*).





Scheme 2.10: Metabolism of paroxetine by isoenzymes

2.4.5 Citalopram:

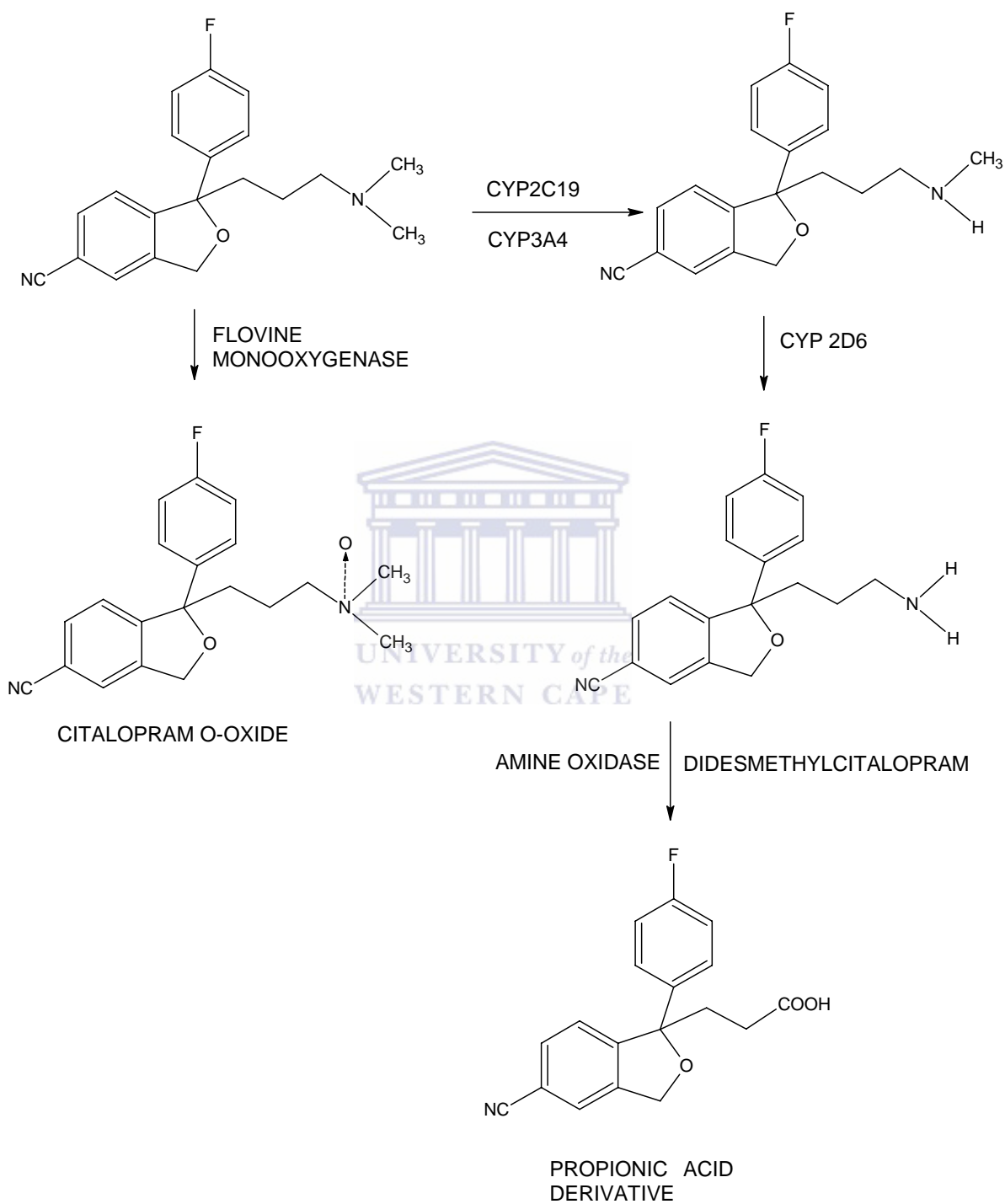


Scheme 2.11: Structure of citalopram prior to metabolism

Citalopram (CIT) (scheme 2.11) is also an antidepressant drug of the group of selective reuptake inhibitors (Rochat *et al*, 1998), also used in the treatment of depression but that associated with mood disorders. The metabolism (scheme 2.12) of CIT leads to two pharmacologically active metabolites with the main one being N-desmethycitalopram which is also further demethylated to didesmethylcitalopram. Besides the N-methylated metabolite, an N-oxide and a propionic acid derivative have also been identified. The propionic acid derivative is pharmacologically inactive therefore it does not possess any 5-HT reuptake inhibiting activity. As a racemate, CIT has its pharmacology effects almost exclusively located in its S-(+) enantiomer, but the plasma concentration of the inactive R-(-) enantiomer are higher than those of the S-(+) enantiomer. The S/R enantiomer ratio of CIT is 0.56 in patients and 0.72 for desmethylcitalopram (Rochat *et al*, 1998; Heimke *et al*, 2000).

The polymorphically expressed isoenzymes, CYP2C19 and CYP2D6, have recently been discovered to be involved in the biotransformation of CIT. The N-methylation works in conjunction with mephenytoin hydroxylase activity and in poor metabolizers of

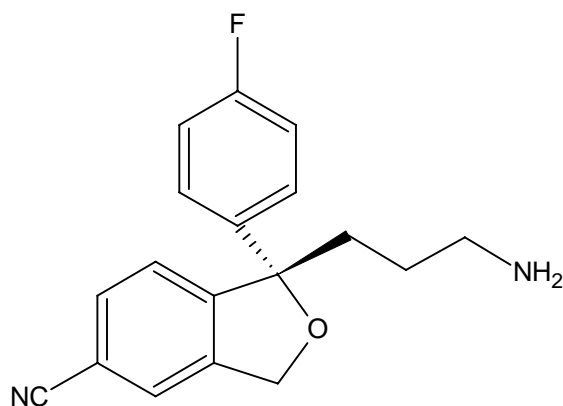
mephenytoin that lack CYP2C19 activity, the total clearance as well as N-methylation clearance being lower than in EM of CYP2C19.



Scheme 2.12: Metabolism of citalopram by isoenzymes

The S/R ratio of the CIT enantiomers have been suggested to be indicative of the activity of CYP2C19, while CYP2C19-deficient patients possessing an almost doubled CIT S/R ratio of greater than 1. However, the N-methylation of desmethylcitalopram to didesmethylcitalopram relies on CYP2D6 was detected in poor metabolizers (PM) of sparteine and the AUC's of desmethylcitalopram were about a third higher in poor metabolizers than in extensive metabolizers (EM). Poor metabolizers are a group of individuals which possess a severely impaired CYP2D6 catalytic capacity while extensive metabolizers are a group of individuals with a normal CYP2D6 catalytic function (*Hemeryck et al, 2002*). In vitro studies have however concluded CYP3A4 to be involved in N-demethylation of CIT, which has been indicated by accelerated metabolism of citalopram under treatment with carbamazepine. After the involvement of these isoenzymes on the metabolism of CIT, their activities are affected. The activity of CYP2D6 is reduced slightly after chronic treatment with CIT, which is probably due to inhibitory properties of N-desmethylcitalopram. There is no effect found on the pharmacokinetics of the substrates of CYP2C19. With other psychotropic drugs, which include TAC's, neuroleptics and tranquilizers; there are rather unlikely pharmacokinetic drug interactions. Therefore, CIT is the safest SSRI when it comes to pharmacokinetic drug interactions (*Moller et al. 2000; Heimke et al, 2000*).

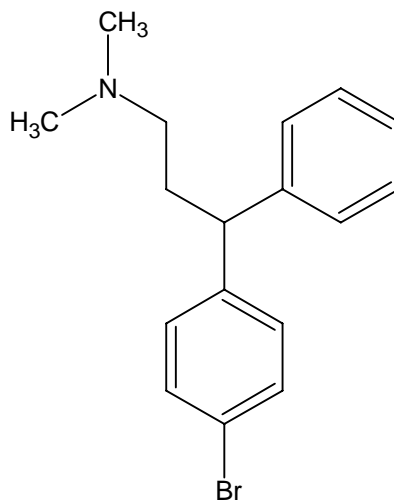
In 2003, the patent for citalopram expired, and a new SSRI drug called Escitalopram (ESC) (scheme 2.13) was produced derived from the S-enantiomer of CIT (*LoVecchro et al, 2006*).



Scheme 2.13: Structure of escitalopram prior to metabolism

This drug also functions as CIT, which is to treat depression associated with mood disorders apart from anxiety and body dysmorphic disorder (LoVecchro *et al*, 2006). ESC is presumed to be more potent towards serotonergic activity in the central nervous system (CNS), as a result of the inhibition of CNS neuron serotonin uptake. When compared to its R-enantiomer, ESC is found to be 100 times more potent when it comes to 5-HT re-uptake inhibition. ESC is metabolized by CYP3A4, CYP2C19 and CYP2D6 isozymes in the liver which are responsible for the ESC metabolism to its main metabolite, S-demethylcitalopram (S-DCIT). Generally, ESC is well tolerated by patients apart from the more frequent side effects such as nausea; while others include insomnia, dry mouth, constipation and diarrhoea.

2.4.6 Zimelidine:



Scheme 2.14: Structure of Zimelidine

Zimelidine (scheme 2.14) was the first selective serotonin reuptake inhibitor antidepressant to be produced and this was done in the early 1980's. The development of zimelidine was as a result of a search for drugs with similar structures to chlorpheniramine, which is an antihistamine with antidepressant activity. 5-Hydroxytryptamine neuronal uptake has been established to be inhibited by zimelidine as well as its active metabolite, norzimelidine, both in vitro and in vivo but having a much lesser effect on noradrenaline uptake. In a conducted research with rats, it was found that zimelidine in vivo blocked the 5-HT reuptake mechanism in the cerebral cortex, hippocampus, striatum, hypothalamus and spinal cord, thereby indicating an effect on both the ascending and descending 5-HT pathways. It was noted that ZIM failed to reduce NA turnover even high doses, but it was able to reduce 5-HT turnover in very low doses in the rat. In mice, however, the 5-HT mediated behaviours were enhanced in doses related to the inhibition of 5-HT uptake. When compared to amitriptyline and mianserin, zimelidine displayed a 5-HT receptor blocking action in vitro, but only at extremely high

doses but failed to block 5-HT mediated behaviour. When it came to histamine H₁ and H₂ receptors, zimelidine avoided any action towards them, but had a negligible impact on noradrenergic alpha 1-and alpha 2- receptors as well as on beta-receptors. Long term treatment with zimelidine did not cause any attenuation of the 5-Ht uptake blocking potency or the reduction of 5-HT turnover. Meanwhile, this treatment reduced the number of beta-receptors in the brain. On the other hand, a repeated zimelidine treatment increased a new 5-HT receptor site characterized by a low affinity and with a high number of binding sites, which resulted in a decrease in the number of high affinity 5-HT receptor binding sites.

Therefore the resultant conclusion was that ZIM has an effect on the presynaptic 5-HT reuptake mechanism but has a negligible action on noradrenergic, acetylcholine, 5-HT and histamine receptors in the brain (*Ogren et al*, 1981). This action leads to a fatal condition affecting the central and or peripheral neuropathy known as Guillain-Barre Syndrome, which caused the drug to be banned worldwide. Another factor for its banishment was based on the fact that it caused a hypersensitivity reaction that involved many organs including skin exanthema, flu-like symptoms, arthralgias and sometimes eosinophilia. Zimelidine was also found to increase suicidal ideas and or attempts among its patients but after its banning, fluoxetine and fluvoxamine overtook it, which have a reduction in this behaviour.

2.5 POLYMERS:

Polymers are being neglected for their traditional roles as electric insulators to take new roles as conductors with a wide range of applications. Researches from different fields are in a process of combining expertise to study organic solids that possess remarkable conducting properties. Organic compounds with the ability of effectively transferring charge can be divided into three main groups namely; ion radical salts charge transfer complexes, organic species and conjugated conducting polymers. In the past two decades a new class of polymers known as intrinsically conducting polymers or electro-active conjugated polymers has emerged. These polymers have gained popularity due to their interesting electrical and optical properties, which have previously been observed only in inorganic systems. The ability to produce these materials in mild conditions has enabled a range of biological compounds to be incorporated into the polymer structures. The electronic properties are then observed in this instance to stimulate and allow a direct and interactive relationship with the biochemistries of the biological components to produce analytical signals. For a polymer to be regarded as a conducting polymer there should be an overlap of molecular orbital to allow the generation of delocalized molecular wave function (Ahaja *et al*, 2007; Malholtra *et al*, 2006).

2.5.1 CONDUCTING POLYMERS:

The chemical bonding in conducting polymers produces one unpaired electron where there is a π electron per carbon atom in the backbone of the polymer. The carbon atoms are π bonded in a sp^2p_z configuration where the orbital of successive carbon atoms overlap providing delocalization of the electrons along the backbone of the polymer.

Charge mobility is exerted along the backbone of the polymer as a result of this electron delocalization introducing properties such as electrical conductivity, low energy optical transitions, low ionization potential and high electron affinity. The π bonds in conducting polymers are highly susceptible to chemical or electrochemical oxidation or reduction processes. The formations of non-linear defects such as solitons, polarons and bipolarons produced either during doping polymerization of a polymer, have made a contribution to the electrical conduction in these polymer materials. An increase in electrode modification as a result of these polymers has provided new and interesting properties, which have contributed for the wide application of conducting polymers. They have been applied in electrocatalysis, rechargeable batteries, membrane separation, optoelectronic, chromatography and solar cells (Ahaja *et al*, 2007; Malholtra *et al*, 2006).



2.5.2 SYNTHESIS OF CONDUCTING POLYMERS:

There are various available methods for the synthesis of conducting polymers, with oxidative coupling of the monomer being the most widely used technique. This technique involves the formation of a cation radical followed by another coupling to produce a dication and the repetition then leads to the polymer (Malholtra *et al*, 2006). Electropolymerization is normally carried out in a single cell compartment where a three-electrode configuration is employed subjected to an electrochemical solution consisting of a monomer and a supporting electrolyte (in some case) all dissolved in an appropriate solvent which in some cases is an acidic. The polymerization can be carried out either potentiostatically where the potential is kept constant with a variation of the current with time, or galvanostatically by keeping the current constant thereby monitoring the

electrode potential. A three-electrode system employed during the polymerization comprises of a working electrode, a counter electrode and a reference electrode. Metals such as gold, platinum, carbon, nickel, titanium and palladium are used as working electrode and function as support systems for the polymer films. Counter electrodes on the other hand supply the current required by the working electrode. A few commonly used counter electrodes include metallic foils of nickel, platinum and gold. Reference electrodes such as SCE, NCE, silver and mercurous sulfate are used in aqueous media (Ahaja *et al*, 2007).

Conductivity of the polymer is influenced by a number of factors including polaron length, the conjugation length, and the overall chain length and by the charge transfer to adjacent molecules. Research has proved that electrochemical synthesis is rapidly becoming the preferred method for polymer preparation due to the simplicity and reproducibility associated with this technique. One advantage associated with the electrochemical polymerization of conducting polymers is that their reactions can be carried out at room temperature either by varying the potential or the current and with time the thickness of the film can be monitored and controlled. Besides copolymers and graft copolymers, electrochemical synthesis can be used for the generation of free standing, homogeneous and self doped films. Conducting polymers such as polypyrrole, polythiophene, polycarbazole, polyindole and polyazulene can be synthesized using this technique.

2.5.2.1 Polypyrrole:

Polypyrrole is a conducting polymer which can be synthesized either chemically or electrochemically. Synthesizing this polymer electrochemically is advantageous since the polymer produced is better conducting and the conductivity is stabilized for a long period of time (*Lakard et al*, 2007). An applied current or voltage can control the location, morphology, thickness and chemical composition of polypyrrole. Chemical composition implies the use of a particular dopant during the synthesis. These dopants include heparin and heparin sulphate and their use is based on the fact that they have an ability to increase the conductivity of the polymer to a level of 10^3 S cm^{-1} . This polymer is one the commonly used when giving examples of the manner in which conducting polymer behave. The polymerisation of this polymer mainly occurs on platinum electrode where a wide variety of enzymes are immobilized. The mechanism of polymerisation takes place at potentials above + 600mV. There are a number of factors which affect the morphology of the film and they include the crystallographic structure of the underlying electrode, the nature of the electrolyte, the speed of the potential of deposition of the polymer known as the scan rate, the concentration of the monomer, the presence of anions and polyanions or in some instances surfactants and finally the pH of the solution.

2.5.2.2 Polyindole:

Another electroactive polymer is polyindole, which is synthesized by anionic oxidation of indole in various electrolytes. When indole is electrochemically oxidized in LiClO_4 containing acetonitrile electrolyte medium, an electrochromic polymer film with good air stability (*Pandey et al*, 1998) is produced. This polymer has a green colour in its doped

state and possesses an electrical conductivity in the range of 10^{-2} to 10^{-1} S cm⁻¹ depending on the nature of counter anion. The polymer is closely structured to polypyrrole and polyaniline but its conductivity is lower than that of both these polymer although it has a better thermal stability than them. Indole derivatives are found abundantly in a variety of natural plants and possess various physiological properties and are potentially bioactive compounds.

2.5.2.3 Polycarbozole:

Polycarbazoles are another type of conducting polymers, but they are less studied than the former mentioned polymers. They are somehow of particular interest since they exhibit photoconductivity and electrochromic properties. They are synthesized by two main procedures. The first method involves the activation of the carbon-halogen bond of 3, 6-dihalogenated monomer in the presence of a zero valent nickel complex. The dehalogenative polycondensation can be carried either chemically or electrochemically and leads to well defined polymers with 3, 6-linkages. The second route is the most commonly used and involves the electrochemical or chemical oxidation of carbazole derivatives in solution (*Fernandes et al*, 1999). The electrochemical stability of this polymer was seen to be less when compared to those of other conducting polymers. However this property can be enhanced by decreasing the poly dispersity of the material (*Tran-Van et al*, 2002).

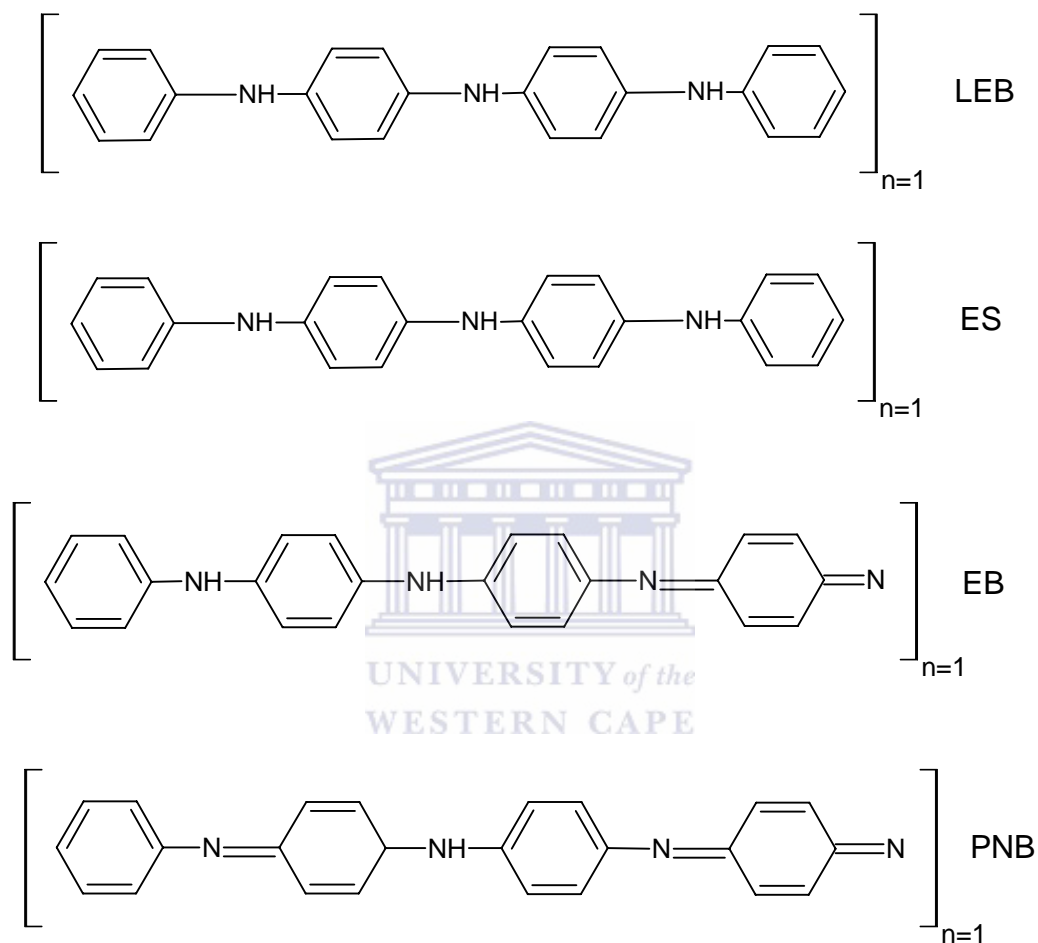
2.5.2.4 Polyaniline:

Polyaniline (PANI) is a conducting polymer of the semi-flexible rod polymer family that is electrically synthesized in the presence of an acidic medium by anionic oxidation of the aniline polymer onto an electrode surface. This attachment of PANI on the electrode surface can be done either by chemical or electrochemical means. Electrochemical polymerization is through galvanostatic, potentiostatic or potentiodynamic means, offering the potential to incorporate a wider range of dopant ions, since the reaction can be carried out in the presence of an appropriate electrolyte rather than a chemical oxidant (*Grennan et al*, 2006). This procedure allows for film property control such as morphology and thickness allowing this polymer to be the most commonly used in biosensor preparation. For the polymer to retain its conductive property in the presence of non-acid media, it is electrical neutral in the oxidized form of the polymer (*Grennan et al*, 2006; *Naudin et al*, 1998).

PANI is known for its very strong pH sensitivity existing between the half-oxidized emeraldine base (EB) and the emeraldine salt (ES) form of PANI, which is a reversible acid – base reaction. The electrochemistry of PANI is illustrated in Scheme 2.15 where the complex transformation of PANI is also shown. Therefore it is generally accepted that polyaniline has been observed to exist in three oxidation states namely: the half oxidized ES, the fully reduced leucoemeraldine (LEB) and the fully oxidized pernigraniline (PNB). ES can be obtained either by oxidation of LEB or by the protonation of EB and this form of the polymer is also electrically conducting (*Lindfors et al*, 2002).

In biosensor development, polyaniline serves as a point of attachment of bioactive compound such as enzymes, antibodies etc. as well as a means of electron transport

between the electrode and the active site of the bioactive compound (*Grennan et al*, 2006).

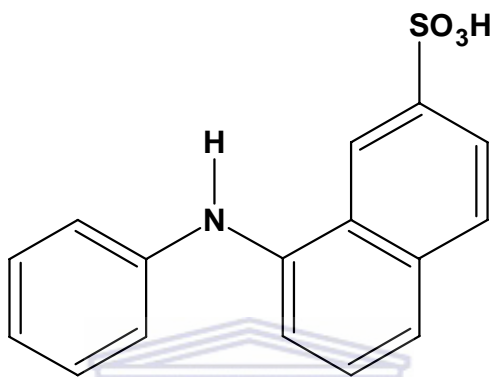


Scheme 2.15: The different forms of PANI namely; PNB, ES, LEB and EB

In this study 8-anilino-1-naphthalene sulfonic acid (ANSA) (scheme 2.16) was polymerized to produce poly (8-anilino-1-naphthaene sulfonic acid) (PANSA).

ANSA belongs to a family of substituted naphthalene's which are normally used as fluorescent probes in the study of biologically active molecule structure. These compounds are moderately soluble in water but in most cases they prefer a more

hydrophobic environment (Catena *et al*, 1989). In one study ANSA was towards the construction of biosensors where it was immobilized respectively onto different kinds of glucose oxidases, and these biosensors where used towards the detection of glucose (Scognamiglo *et al*, 2004).



Scheme 2.16: Structure of 8-anilino-1-naphthalene sulphonic acid

In our study aniline substituted naphthalene was used and it is the aniline substitute which was polymerized and the sulphuric component attached to a gold electrode. The electrochemistry of PANSA was very observed to be similar to that of PANI as seen from the work of (Mathebe *et al*, 2004) although polymerization was carried out in different acid media. This work reports the fabrication and characterization of PANSA based biosensor incorporating the enzyme CYP2D6 for the detection of SSRIs.

Since protonation does not contribute any electrons to the system for both the polymerization of aniline and 8-anilino-1-naphthalene sulfonic acid, a modification of the structure is assumed for the increased conductivity in both polymers. In some instances polymerization is done in the presence of a dopant in which two types of local distortions are involved to aid in the explanation of the emergence of charge carriers. The first is a polaron which consists of a local distortion of chain that has the capability of storing the

extra positive charge in which only a single nitrogen in the oxidized form is protonated. On the other hand, a bipolaron has a similar local distortion in which imine nitrogens are protonated. Both of these distortions are coupled to the vibrations of the chain so that they are able to move along the polymer chain (*de Oliveira et al*, 2000).



2.5.3 APPLICATIONS OF CONDUCTING POLYMERS IN

BIOSENSORS:

The increased number of governmental, academic and industrial laboratories involved in the research and assessment of the possible application of conducting polymers has shown this area to be interdisciplinary in nature. The organized molecular structures of conducting polymers on metal substrates have attracted much attention largely due to their wide application in lightweight batteries, solar cells, molecular electronic devices and sensors. These polymers seek to function as three-dimensional matrices for the immobilization of active biological components thereby preserving a long duration for their activity. This observed property of conducting polymers together with their functionality as a membrane, has promoted an investigation toward the development of sensors (*Mathebe et al, 2004*).

Redox properties of the conducting polymers especially polypyrrole and polyaniline, have been extensively studied with much emphasis on their synthesis and characterization. Polypyrrole and polyaniline are considered to be the most promising polymers for sensor development due to their ease of preparation, stability and good conductivity. The chemical structures of conducting polymers together with their facile methods of assembly make them compatible with much naturally found chemistry, thus promoting their interaction with biological molecules. This therefore has led to the application of these polymers in biosensor construction. Biosensors have found great application in various fields such as biotechnology, health care, medicine and pollution monitoring (*Malhotra et al, 2006*).

In this study the conducting polymer poly (8- anilino-1-naphthalene sulfonic acid) was used in the construction of a drug metabolism biosensor where it functioned by transporting electrons between the electrode and the active centre of the enzyme. The main objective of the study was to demonstrate electrochemical reactivities of SSRIs when in contact with the enzyme CYP2D6. The responses obtained from these studies are clearly discussed in chapter four.



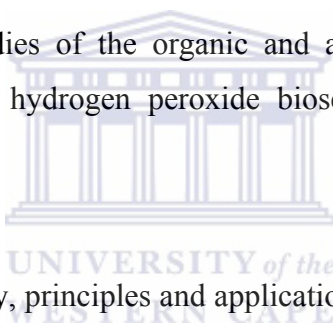
2.6 REFERENCES:

Ahuja T, Mir I. A, Kumar D: 'Biomolecular immobilization on conducting polymers for biosensing application' *Biomaterials*, 2007, 28: 791-794

Bistolas N, Wollenberger U, Jung C, Scheller F.W: 'Cytochrome P450 biosensors a review' *Biosensors and Bioelectronics*, 2005, 20: 2409-2410

Bourin M, Chue P, Guillon Y: 'Neurobiology of Anxiety and Depression' *CNS Drug Review*, 2001, 7: 25-47

Brennan S: 'Comparitive Studies of the organic and aqueous phase reactivities of a Pthathalic anhydride-modified hydrogen peroxide biosensor, Dublin City University, 1996



Brett B and O, *Electrochemistry, principles and applications*, John Wiley and Sons, 1997, 1st Edition, pg 383-389

Catena G.C, Bright F. V: 'Thermodynamic study of the effects of B-Cyclodextrin Inclusion with Anilinonaphthalenesulphonates' *Analytical Chemistry*, 1989, 61: 905-906

Chaubey A, Malhotra B.D: 'Mediated Biosensors' *Biosensors and Bioelectronics*, 2002, 17: 441-446

Conn E.E, Stumff P.K, Brueninig G: 'Outline of Biochemistry' John Wiley and Sons, 1987, 5th Edition, pg 115 -163

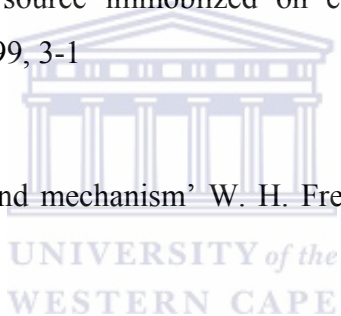
de Oliveira Z.T, dos Santos M.C: 'Relative stability of polarons and bipolarons in emeraldine oligomers: a quantum chemical study' *Solid State Communications*, 114: 49-50

Dimakis V.T, Gavalas V.G: 'Polyelectrolyte-stabilized biosensors based on macroporous carbon electrodes' *Analytica Chimica Acta*, 2002, 467: 217-223

D'Orazio P: 'Biosensors in clinical chemistry' *Clinica Chimica Acta*, 2003, 334: 41

Fernandes J.B, Kubota L.T: 'Potentiometric biosensor for L-ascorbic acid based on ascorbate oxidase of natural source immobilized on ethylene-vinylacetate membrane' *Analytica Chimica Acta*, 385, 1999, 3-1

Fersht A: 'Enzyme structure and mechanism' W. H. Freeman and Company, 1984, 2nd Edition, pg 98-107



Garcia C.A, Kubota L.T: 'New fructose biosensors utilizing a polypyrrole film and D-fructose 5-dehydrogenase immobilized by different processes' *Analytica Chimica Acta*, 1998, 374: 201-208

Grennan K, Killard A.J, Smyth M.R: 'Optimisation and characterization of biosensors based on polyaniline' *Talanta*, 2006, 68:1591-1592

Harris D, Loew G, Waskell L: 'Calculation of the electronic structure and spectra of model cytochrome P450 compound I' *Journal of Inorganic Biochemistry*, 2001, 83: 309-311

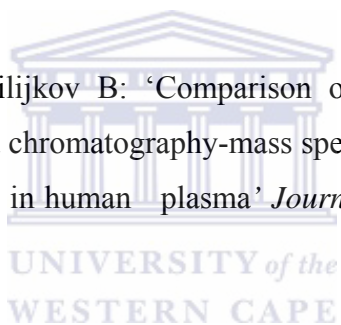
Heimke C, Hartter S: 'Pharmacokinetics of selective serotonin reuptake inhibitors' *Pharmacology and Therapeutics*, 2000, 85:20-22

Hermeryck A, Belpaire F.M: 'Selective Serotonin Reuptake Inhibitors and Cytochrome P-450 Mediated Drug-Drug Interactions: An Update' *Current Drug Metabolism*, 2003, 3: 13-17

Iwuoha E.I , Smyth M.R: 'Reactivities of organic phase: 6.Square-wave and differential pulse studies of genetically engineered cytochrome P450_{cam} (CYP101) bioelectrodes in selected solvents' *Biosensors and Bioelectronics*, 2003, 18: 237-238

Key E.R.M, Biochemistry, Collier-Macmillan Limited, London, 1966, 290-291

Kovacevic I, Pokrajac M, Milijkov B: 'Comparison of liquid chromatography with fluorescence detection to liquid chromatography-mass spectrometry for the determination of fluoxetine and norfluoxetine in human plasma' *Journal of Chromatography B*, 2006, 830, 372-373



Lakard B, Lakard S: 'Potentiometric miniaturized pH sensor based on polypyrrole films' *Sensors and Actuators B*, 2007, 122:101-102

Lindfors T, Ivaska A: 'Potentiometric and UV-vis characterisation of N-substituted Polyanilines' *Journal of Electroanalytical Chemistry*, 2002, 535: 65-66

LoVecchro F, Watts D, Winchell J, Knight J, McDoweel T: 'Outcomes after Supratherapeutic Escitapram ingestions' *Journal of Emergency Medicine*, 2006, 30:17-18

Malfara W.R, Bertucci C, Quiroz M.E.C: 'Reliable HPLC Method for Therapeutic Drug Monitoring of Frequently Prescribed Tricyclic and Nontricyclic Antidepressants' *Journal of Pharmaceutical and Biomedical Analysis*, 2007, Newly accepted manuscript

Malhotra B.D, Chaubey A: 'Prospects of conducting polymers in biosensors' *Analytica Chimica Acta*, 2006, 578:60-61

Mathebe N.G.R, Morrin A, Iwuoha E.I: 'Electrochemistry and scanning electron microscopy of polyanilin/peroxide-based biosensor' 2004, 64:115-116

McMurry F, Fay R.C: 'Chemistry' Prentice-Hall International, 1995, 2nd Edition, pg 1002-1003

Moller S.E, Larsen F, Pitsiu M, Rolan P.E: 'Effect of Citalopram on Plasma Levels of Oral Theophylline' *Clinical Therapeutics*, 2000, 22: 2-3

Murrin L.C, Sanders J.D, Bylund D.B: 'Comparison of the maturation of the adrenergic and serotonergic neurotransmitter systems in the brain: Implications for differential drug effects on juveniles and adults' *Biochemical Pharmacology*, 2007. 73: 1225-1226

Naudin E, Gouerec P, Belanger D, 'Electrochemical preparation and characterization in non-aqueous electrolyte of polyaniline electrochemically prepared from an anilinium salt' *Journal of Electroanalytical Chemistry*, 1998, 459:1

Najeem R. M: 'Amperometric biosensors for enantioanalysis' University of Pretoria edition, 2004, Chapter 4

Ogren S.O, Ross S.B, Hall H, Renyi A.L: 'The pharmacology of Zimelidine. A 5-HT selective reuptake inhibitor' *Acta Psychiatrica Supplement*, 1981, 290: 127-151

Pandey P.C, Prakash R: 'Polyindole modified potassium ion-sensor using dibenzo-18-crown-6 mediated PVC matrix membrane' *Sensors and Actuators B*, 1998, 46: 61-62

Pedrazza E.L, Senger M.R, Pedrazza L: 'Sertraline and clomipramine inhibit nucleotide catabolism in rat brain synaptosomes' *Toxicology in Vitro*, 2007, 21: 671-672

Perez E, Neto G, Kubota L: 'Bi-enzymatic amperometric biosensor for Oxalate' *Sensors and Actuators B: Chemical*, 2001, 72: 80-85

Quian L, Yang X: 'Composite film of carbon nanotubes and chitosan for preparation of amperometric hydrogen peroxide biosensor' *Talanta*, Article in press

Rochat, Kosel M, Boss G, Testa B, Gillet M, Baumann P: 'Stereoselective Biotransformation of the Selective Serotonin Reuptake Inhibitor Citalopram and Its Demethylated Metabolites by Monoamine Oxidases in Human Liver' *Biochemical Pharmacology*, 1998, 56: 15-16

Rojas-Malgarejo F., Garcia-Ruiz P.A: 'Immobilization of horseradich peroxidase on Cinnamic carbohydrate esters' *Process Biochemistry*, 2004, 39: 1455-1464

Ryne-Byrne S: 'Development of and Amperometric anti-biotin Immunosenor, *Thesis*, Dublin City University,

Schreiber S, Pick C.G: 'From selective to highly selective SSRIs: A comparison of the antinociceptive properties of fluoxetine, fluvoxamine, citalopram and escitalopram' *European Neuropsychopharmacology*, 2006: 16: 464-465

Scognamiglio V, Rossi M, D'Auria S: 'Protein-Based Biosensors for Diabetic Patients' *Journal of Fluorescence*, 2004, 14:491-492

Shumyantseva V.V, Bulko T.V, Archakov A.I: 'Electrochemical reduction of Cytochrome P450 as an approach to the construction of biosensors and bioreactors' *Journal of Inorganic Biochemistry*, 2005, 99: 1057-1058

Tran-Van F, Henri T, Cverot C: 'Synthesis and electrochemical properties of mixed ionic and electronic modified polycarbazole' *Electrochimica acta*, 2002, 47: 2927-2928

Vidal J, Esteban S: 'A comparative study of immobilization methods of a Tyrosinase enzyme on electrodes and their application to the detection of dichlorvos organophosphorus insecticides' *Talanta*, Article in press

Vlase L, Imre S, Leucuta S: 'Determination of fluoxetine and its *N*-desmethyl metabolite in human plasma by high performance liquid chromatography' *Talanta*, 2005, 66: 659-660

Worsfold P.J: 'Classification of immobilized enzymes' *Pure and Applied Chemistry*, 1995, 67: 597-600

Zawertailo L.A, Busto U, Kaplan H.L, Sellers E. M: 'Comparative abuse liability of Sertraline, alprazolam and dextroamphetamine in humans' *Journal Clinical Psychopharmacology*, 1995, 15, 22-24

CHAPTER



UNIVERSITY *of the*
WESTERN CAPE

Experimental:

3. EXPERIMENTAL:

3.1 Reagents:

Cytochrome P450-2D6 Isozyme (CYP 2D6) also known as debrisoquine hydroxylase; EC 1.14.14.1 was obtained from Sigma as a purified 200 units/mg enzyme that did not contain CYP dehydrogenase and other proteins. One unit of CYP2D6 is the amount required to convert 1 nanomole of bufuralol to hydroxybuforol per minute at pH 7.4 at 37⁰C. Other reagents used were 8-anilino-1-naphthalene sulfonic acid, ammonium hydrate salt 97% (ANSA), Sulfuric acid which are all products of Fluka. 0.1 M phosphate buffer (0.1 M KCl pH 7.4) (PBS) was prepared from Sigma-Aldrich's anhydrous disodium hydrogenorthophosphate, dihydrogenorthophosphate dihydrate and potassium chloride. The drugs used for analyses are; namely sertraline, fluoxetine, fluvoxamine, paroxetine, zimelidine, clomipramine as well as the known CYP2D6 substrate, debrisoquine sulphate were all supplied by Sigma-Aldrich's and were used as received dissolved in PBS. Analytical grade argon used to degas the cell solutions was obtained from Afrox, SA. When not used solutions were kept refrigerated at 5⁰C.

3.2 Electrochemical setup:

Electrochemical experiments were carried out with a BAS 100 W electrochemical workstation from BioAnalytical Systems (BAS, West Lafayette, IN) operated in the cyclic square wave and differential pulse voltammetric modes or constant potential amperometry. A 20 mL electrochemical cell was used in a three electrode configuration consisting of a 0.0177 cm² gold disk working electrode (BAS, West Lafayette, IN), Pt wire auxiliary electrode and Ag/AgCl reference electrode (with a 3 M NaCl salt bridge).

3.3 METHODOLOGY

3.3.1 Preparation of 8-anilino-1-naphthalene sulphonic acid on Gold

electrode:

Prior to polymerization of ANSA, the Au disk electrode was polished on aqueous slurries of 1 μm , 0.3 μM and 0.05 μM alumina and sonicated in distilled and deionised water processed with a milli-Q water purification apparatus (Millipore). The polished Au electrode was then scanned in a 0.5 M H_2SO_4 solution from -1200 mV to +1500 mV at 50 mV/s. The auxiliary Pt electrode was cleaned by the flaming method and then rinsed with deionised water.

The electropolymerization of ANSA was performed in a cell solution containing 0.01 M of the ANSA monomer in 20 mL 0.5 M H_2SO_4 solution degassed with argon for 15 min. The potential was cycled from -300 mV (initial potential, E_i) to +1100 mV (switch potential, E_λ), at a potential scan rate of 50 mV/s. An argon blanket was maintained on top of the cell solution during the polymerization process which was stopped after 5 voltammetric cycle. Poly (8-anilino-1-naphthalene sulfonic acid) PANSA was conditioned for biosensor application by rinsing out superficial acid and un-reacted monomer and then incubated in PBS. This electrode will be referred to as Au/PANSA electrode.

3.3.2 Characterization of Au/PANSA electrode in 0.5 M H₂SO₄ using Cyclic voltammetry (CV):

Characterization of the polymer film was carried out in a 20 mL 0.5 M H₂SO₄ solution which was degassed for 15 min. The potential was cycled from a E_i of -200 mV to a E_λ , of +1100mV at different scan rates: 5, 10, 15, 20, 30, 40, 60, 80, 100, 150, 200, 250, 300, 350, 400, 450 and 500 mV/s. During the characterization process, the argon gas was kept on top of the solution in order to prevent the interference by oxygen. Calculations for the surface concentration of the polymer as well as the electron transfer coefficient were estimated from the obtained results.

3.3.3 Characterization of Au/PANSA electrode in (0.1M KCl,pH 7.4) (PBS) using Cyclic Voltammetry (CV):

Characterization of the polymer in PBS was repeated with a freshly prepared Au/PANSA electrode but in this case, the characterization was carried out in the presence of 20 mL PBS solution which was also degassed for 15 min. The potential was cycled from -300 mV (initial potential, E_i) to +1100 mV (switch potential, E_λ), at different scab rates: 5, 10, 15, 20, 30, 40, 60, 80, 100, 150, 200, 250, 300, 350, 400, 450 and 500 mV/s. An argon blanket was kept on top of the solution in order to prevent interferences by oxygen. Both the surface concentration as well as the electron transfer coefficient was determined from the results.

3.4 Enzyme immobilization:

The conditioned Au/PANSA electrode was reduced potentiostatically in 5 mL PBS under argon atmosphere by applying a c potential of -500 mV until a steady state current was attained in about 10 min. 20 μ L (of 200 units/mg) concentration of solution CYP 2D6 was added to the 5 mL cell solution and the Au/PANSA film was oxidized at +650 mV for 15 min during which the polymer was doped with CYP 2D6. The resultant biosensor namely; Au/PANSA/CYP2D6 was rinsed in PBS to remove unbound enzyme and stored refrigerated at 4⁰C.

3.4.1 Characterization of Au/PANSA/CYP2D6 using CV and SWV:

Characterization of Au/PANSA/CYP2D6 bioelectrode was carried out using CV in the presence of 5 ml PBS which was degassed for 15 min. This reaction was achieved by cycling the potential from a E_i of -200 mV to a E_{λ} , of -1100 mV at different scan rates: 5, 10, 15, 20, 30, 40, 60, 80, 100, 150 and 200 mV/s. During the characterization, an argon blanket was kept on top of the solution.

Another bioelectrode was freshly prepared and used for the characterization of the polymer using SWV. To achieve the characterization, 5 mL PBS solution was used which was degassed for 15 min. The potential was scanned from a E_i of -500 mV to a E_{λ} , of -1100 mV during which an argon blanket was kept over the solution eliminating oxygen. SWV experimental conditions were: sensitivity 10 μ A/V, SWV amplitude 25 mV Step potential 4 mV and at frequencies of 5, 10 and 15 Hz.

3.5 Electrochemical measurements:

In a typical determination, the biosensor (Au/PANSA/CYP2D6), Ag/AgCl reference electrode and platinum wire were placed in the test 5 mL PBS solution and connected to the BAS 100 W electrochemical workstation. The Au/PANSA/CYP2D6 bioelectrode was used to study the reactivities of the following compounds: Fluoxetine, fluvoxamine, citalopram, sertraline, zimelidine and debrisoquine sulphate in undegassed PBS. Analyte analyses were accomplished with freshly prepared bioelectrodes in oxygenated PBS to which aliquots of the respective types of analyte solutions was added to final concentrations of 0.2 to 1.6 μM . The PBS solution was stirred after each addition of analyte in order to ensure homogeneity of the solutions prior to analyses. The same procedure was carried out for the inhibitor paroxetine.

CV experiments were carried out at a potential window of E_i of +400 mV to a E_λ , -800 mV, at a potential scan rate of 10 mV/s and at a sensitivity of 10 $\mu\text{A/V}$.

The investigation was also carried out with DPV at a potential window of +400 mV to -700 mV and scan rate of 10 mV/s. DPV experimental conditions were: sensitivity 10 $\mu\text{A/V}$, pulse amplitude 50 mV, current sampling width 17 msec and pulse width of 50 msec.

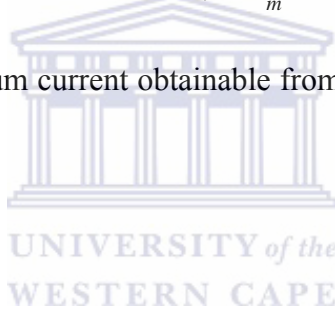
The reactivities of the biosensors towards these compounds were also studied using SWV at a potential window of +400 mV to -700 mV. SWV experimental conditions were: sensitivity 10 $\mu\text{A/V}$, SWV amplitude 25 mV, SWV frequency 15 Hz and Step potential 4 mV.

Calibration curves were plotted for all the test compounds from the DPV responses of the biosensor. The Michaelis-Menten region (hyperbolic region) of the biosensor responses

at high analyte concentrations were fitted to the electro-enzyme Michaelis-Menten kinetics in accordance with the equation:

$$I = nFAk_{cat} l[\text{CYP2D6}] S / (K_m + S) = I_{max} S / (K_m + S) \quad (1)$$

In Equation (1) I is the observed cathodic peak current, n is the number of electrons; F is Faraday constant (96,485 C/mol), while A , k_{cat} , and l are the surface area of the electrode (0.0177 cm²), turnover rate constant and the thickness of the electroactive layer, respectively. S is the substrate concentration; K_m is the apparent Michaelis-Menten constant and I_{max} is the maximum current obtainable from the sensor. I_{max} and K_m values of the sensor were evaluated.



CHAPTER



FOUR

UNIVERSITY *of the*
WESTERN CAPE

Results and Discussion:

4. RESULTS AND DISCUSSION:

4.1 Electrosynthesis of PANSAs on gold electrode:

PANSAs were grown on a 0.0071 cm² disk electrode surface in an acidic medium by the potentiodynamic oxidative polymerisation of 0.01 M ANSA in 0.5 M H₂SO₄ at 50 mV/s scanning anodically from – 300 to + 1100 mV/Ag-AgCl. Figure 4.1 shows a typical cyclic voltammogram of the polymer film on Au produced after 5 voltammetric cycles.

It can be seen that upon polymerization, PANSAs possess one redox couple with a polymerisation formal potential, E^0 , of +425 to +440 mV compared to PANI, which has three redox couples as shown by the work of (*Iwuoha et al*, 1997; *Mathebe et al*, 2004). Using the PANI CV as a reference point, the redox couple observed in the synthesis of PANSAs is attributable to the electrochemistry of *p*-benzoquinone formed in the polymerisation process.

This behaviour of PANSAs was found to be closely related to that observed in a study carried out by (*Mazeikiene et al*, 2006) in which one redox couple was also observed when aminonaphthalene sulphonates were polymerized in the presence of 0.1 M sulphuric acid. One redox couple was also observed in another study in which PANI was polymerized in the presence and absence of sodium dodecyl sulphate (*Kanungo et al*, 2002). These studies are a confirmation that aniline in 8-anilino-1-naphthalene sulphonic acid can be polymerized.

The anodic shift in the polymerization of ANSA shows that oxidation of ANSA on the polymer involves charge transportation across the polymer film. The unsymmetrical shape of the anodic peak indicates oxidation of ANSA coupled to a follow-up reaction and other physical processes which in this case are polymerization and adsorption. On the other hand the symmetry of the cathodic peak shows that the

only event here is the reduction of adsorbed polymer. There is an anodic shift in the polymerisation peak potential with the result that the $E^{\prime 0}$ values increased from +425 mV for the first polymerisation cycle to +440 mV which indicates that oxidation of ANSA on already deposited polymer involves charge transportation across the polymer film and therefore energetically more demanding, whereas the reduction of the accumulated polymer film becomes easier.

Characterizations of both PANSA and PANI in the presence of their respective polymerization acidic media show similar electrochemistry as denoted by the configuration of the peaks. Evidence of this can be seen in figure 4.2 where the characterization of PANSA shows a similar electrochemistry to that of PANI in the work done by (*Mathebe et al, 2005; Lindofors et al, 2002*).

The role of the PANSA film in the biosensor construction was to shuttle electrons between the Au disk electrode and the active site of the immobilized enzyme and it also served as a point of attachment for the enzyme CYP 2D6.

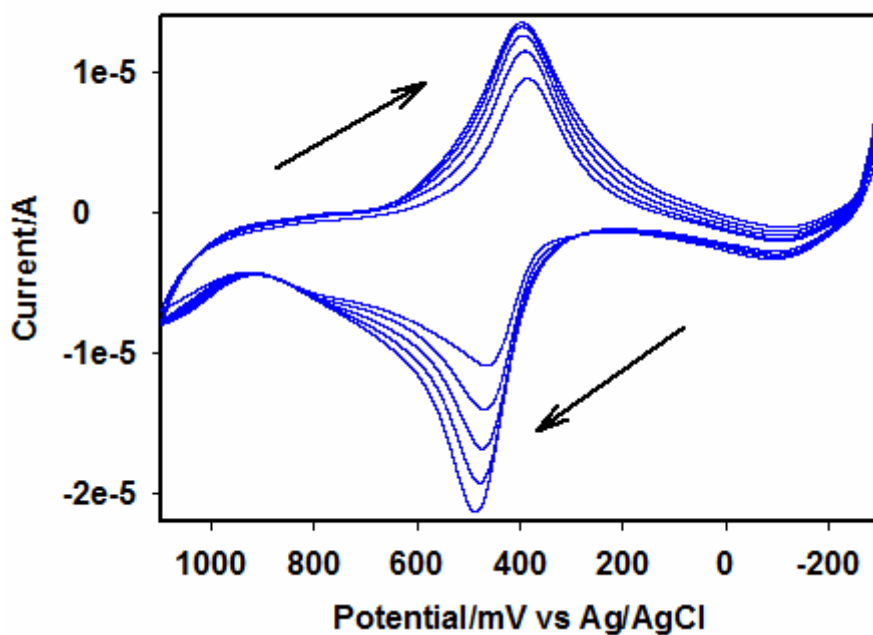


Fig. 4.1 Electrosynthesis of PANSA film on a Au electrode in 0.5 M H_2SO_4 at a potential window of -300 mV to +1100 mV and scan rate of 50 mV/s

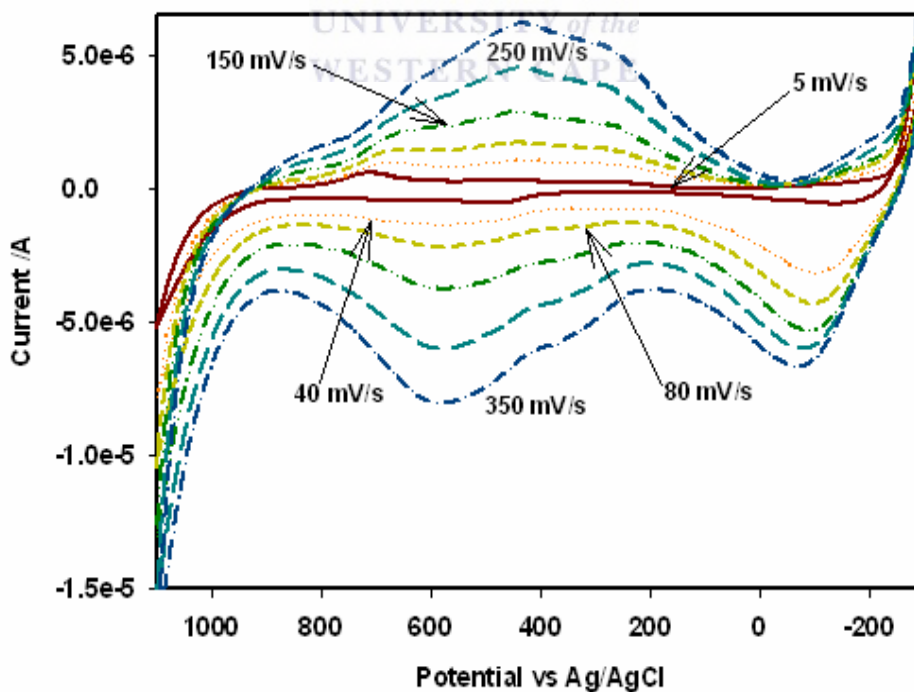


Fig. 4.2 Electrochemical characterization of the PANSA film in 0.5 M H_2SO_4 at 5, 40, 80, 150, 250 and 350 mV/s at a potential window of -300 mV to +1100 mV.

4.2 CV characterization of Au/PANSA electrode in 0.5M H₂SO₄

The characterization of the PANSA polymer film in acid medium was carried out at 5, 10, 15, 20, 25, 30, 40, 60, 80, 100, 150, 200, 250, 300, 350, 400, 450 and 500 mV/s in which two redox couples were observed. Figure 4.2 illustrates these results but only for the scan rates; 5, 40, 80, 150, 250 and 350 mV/s. The chose of these particular responses was to provide a clear illustration of the growth of the polymer. As the scan rates where increased during the study, there was less stability in the polymer. This is due to the fact that the mobility of the polymer reduced and there was difficulty in the immobilization of the enzyme. However, there was no effect on the polymer thickness.

Similar voltammograms have been reported for polyaniline (*Iwuoha et al*, 2006; *Iwuoha et al*, 1997; *Lindofors et al*, 2002; *Mazeikiene et al*, 2006) confirming that aniline in anilinonapthalene sulfonic acid can be polymerized. The redox couples A/B and C/D are attributed to intrinsic redox processes of the polymer. The redox couple A/B observed at approximately +350 mV is as a result of the transformation of aniline in ANSA from the reduced polyleucoemeraldine state to the partly oxidized polyemeraldine state. The redox couple C/D in the region approximately around +600 mV is due to the transition of polyleucoemeraldine state to the pernigraniline state, which is accompanied by oxidation of ANSA monomer. The multiscan voltammograms of the PANSA film modified Au electrode in 0.5 M H₂SO₄ solution shown in figure 4.2 indicate that the peak potentials as well as the peak currents were seen to vary as the scan rates were varied. This indicated that the polymer was electroactive and that electron diffusion was taking place along the polymer chain (*Brahim et al*, 2003). The main peaks of the polymer are illustrated in figure 4.3 and are used for further description of the polymer.

Figure 4.5 and figure 4.6 show the linear dependency of the current on the scan rate for the main redox couple C/D. This is indicative of a thin surface bound conducting electro-active polymer film undergoing a rapid reversible electron transfer reaction along the polymer backbone possibly through the conjugated benzene ring units making up the chain. $I_{p,c}$ (peak C) / $I_{p,a}$ (Peak D) which was obtained to be ~ 1.1 indicating that the polymer behaved as a stable redox species adsorbed on the electrode surface undergoing reversible electrochemistry. A similar behaviour was also observed in the work carried out by (Brahim *et al*, 2003; Mu *te al*, 1997). ΔE_p [$E_{p,a}$ (Peak 2) – $E_{p,c}$ (Peak 3)] was calculated for the polymer film grown at different scan rates but the film grown at 50 mV/s resulted in a value of ΔE_p lower than 65 mV which was also seen from the work of (Brennan *et al*, 1996; Bistolas *et al*, 2005). This suggested that the polymer grown at this scan rate exhibited a reversible and a fast electrochemistry as compared to polymer grown at other scan rates which is suggestive of a slow electron transfer rate.

The surface concentration of the polymer was estimated to be $1.0257 \times 10^{-6} \text{ mol cm}^{-2}$ (0.6 ± 0.1) using the Brown-Anson method illustrated as follows.

$$I_p = \frac{n^2 F^2 \Gamma_{\text{PANSA}}^* A v}{4RT}$$

Where n represents the number of electrons involved in the reaction, F is the Faraday constant (96,584 C/mol), Γ_{PANSA}^* is the surface concentration of the PANSA film (mol cm^{-2}), v is the scan rate (mV/s), A is the electrode area of the electrode (0.0177 cm^2), R is the universal gas constant ($8.314 \text{ J (mol K)}^{-1}$) and T is the temperature of the system (298 K). The magnitude of the peak currents was seen to increase upon increment of the scan rate suggesting that the peak currents are diffusion controlled.

D_e is the electron charge transport coefficient sometimes also known as the rate of electron charge propagation along the polymer chain. The following equation is the Randel-Sevcik method used for the estimation of this coefficient and was found to be $3.8225 \times 10^{-2} \text{ cm s}^{-1}$. For the accuracy of this calculation, there should be no variation in the potential with scan rate. Only the variation in scan rate is essential in this case. The increased value obtained in this study as compared to PANI studies in which (Mathebe *et al*, 2004) reported a value of $8.68 \times 10^{-9} \text{ cm s}^{-1}$ and (Iwuoha *et al*, 1996) reported a value of $6.46 \times 10^{-8} \text{ cm s}^{-1}$ (0.6 ± 0.1). This gives an indication of a much faster electron charge transfer.

$$I_p / \nu^{1/2} = 0.4463 (nF)^{3/2} \frac{D_e \Gamma_{\text{PANSNA}}^* A}{L (RT)^{1/2}}$$

Where L represents the polymer thickness.

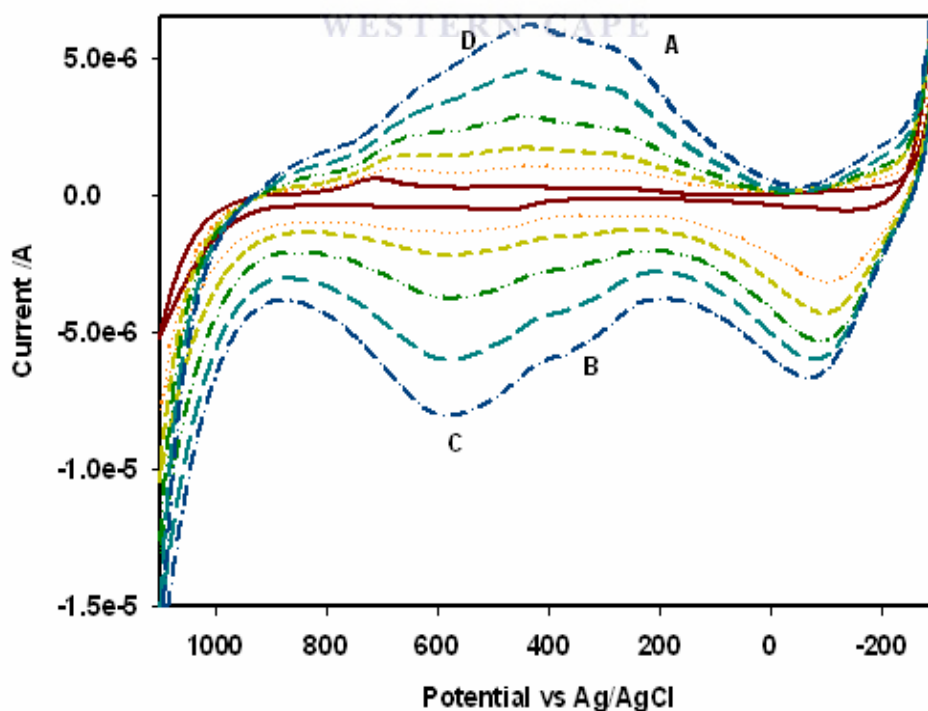


Fig. 4.3 Electrochemical characterization of the PANSA film in 0.5 M H_2SO_4 on Au electrode illustrating the main polymerization peaks.

4.3 CV characterization of Au/PANSA electrode in 0.1M Phosphate buffer (0.1M KCl,pH 7.4) (PBS):

The characterization of the PANSA film was also carried out in PBS as stipulated in section 3.4.2. The study was carried out at 5, 10, 15, 20, 25, 30, 40, 60, 80, 100, 150, 200, 250, 300, 350, 400, 450 and 500 mV/s but shown in figure 4.4 are the responses for 5, 40, 80, 150, 200 and 350 mV/s. The aim of this experiment was to confirm the conductivity and immobilization of the polymer. Figure 4.4 illustrates the CV characterization of the polymer film in PBS indicating two cathodic peaks in the reductive scan while there are no peaks observed in the oxidative scan. The peak approximately at -26 mV confirms the attachment of PANI, which was also observed in previous PANI studies carried out by (Ngece *et al*, 2004) at approximately the same region. The peak at approximately +360 mV denotes the presence of NSA in PANSA. The multiscan voltammograms of the PANSA film modified Au electrode in the PBS solution shown in figure 4.4 indicate that the peak potentials as well as the peak current varied as the scan rates were varied. This indicated that the polymer was electroactive and that electron diffusion was taking place along the polymer chain (Iwuoha *et al*, 1998; Qu *et al*, 2005). The slight shift in the peaks is indicative of the conductivity (Iwuoha *et al*, 1997) of the polymer leading to the conclusion that the polymer was effective for use in biosensor construction.

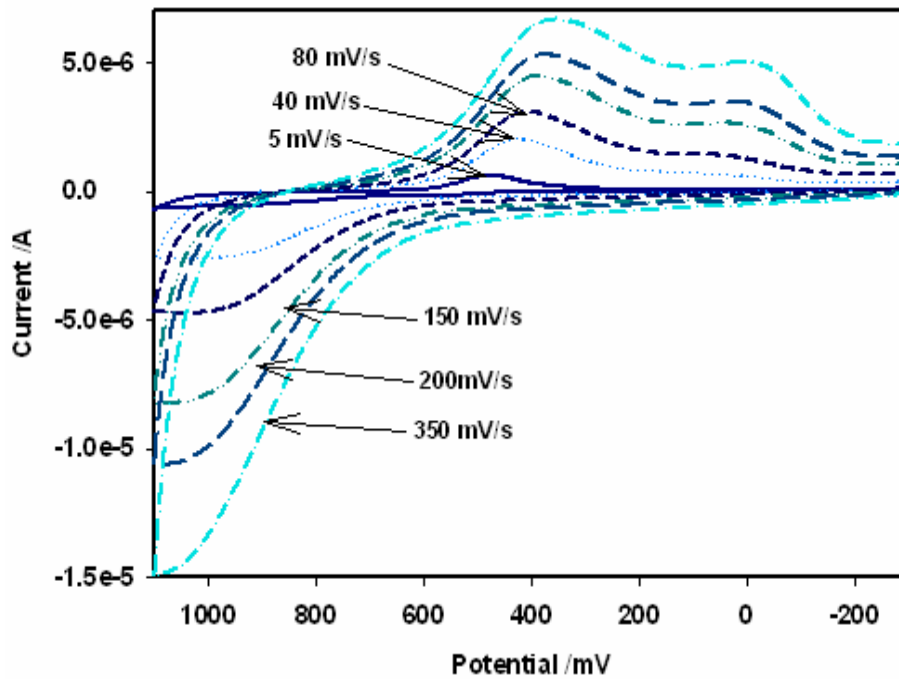


Fig 4.4 Electrochemical characterization of the PANSA film in PBS at different scan rates: 5, 40, 80, 150, 200 and 350 mV/s at a potential window of -300 mV to +1100 mV.

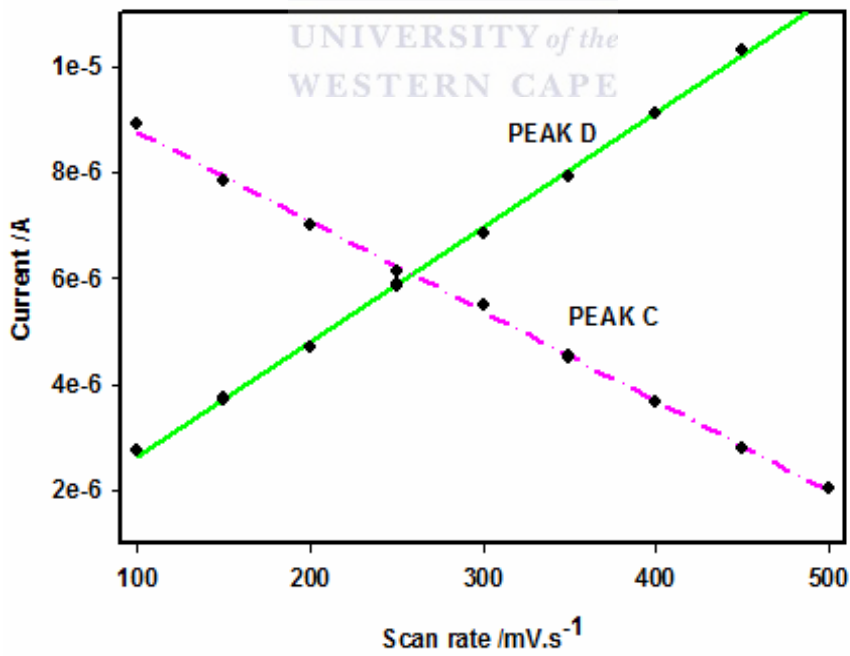


Fig. 4.5 Dependency of peak current on potential scan rate for the Au/PANSA electrode .

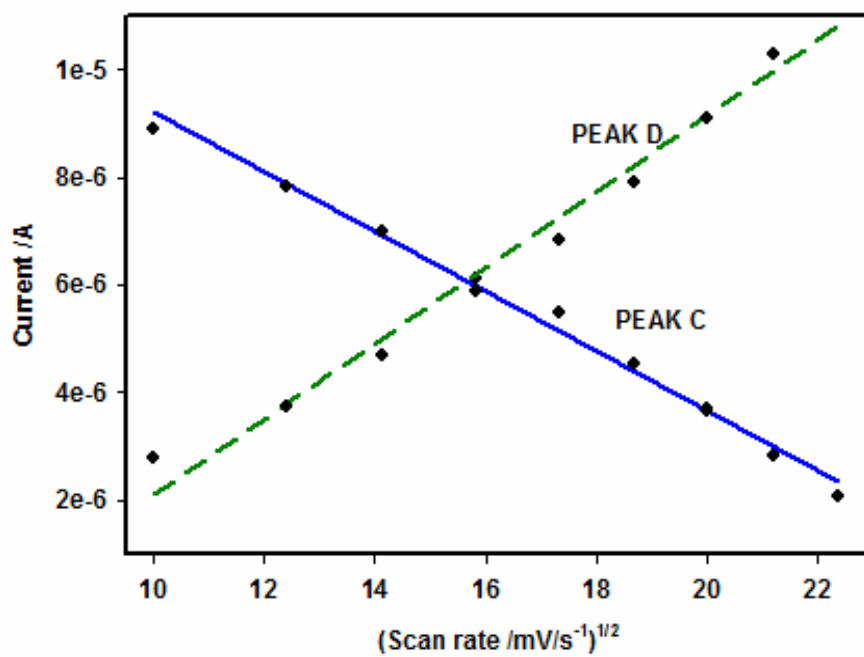
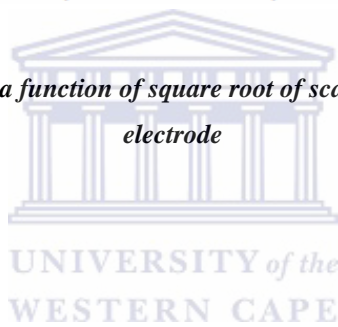


Fig.4.6 Peak currents as a function of square root of scan rate for the Au/PANSA electrode



4.4 CV and SWV characterization of Au/PANSA/CYP electrode in 0.1M

Phosphate buffer (0.1M KCl,pH 7.4)(PBS):

After enzyme immobilization, it was important to access whether the enzyme was stationed on the polymer surface or not. This assessment was achieved using CV at a potential window of -300 mV to +1000 mV at scan rates; 5, 10, 15, 20, 30, 40, 60, 80, 100, 150, 200, 250, 300, 350, 400, 450 and 500 mV/s. Figure 4.7 shows the CV voltammogram of the characterization at 5, 15, 30, 60, 100 and 150 mV/s where one redox couple was observed. As the scan rates increased, the amplitude of the peaks also increased confirming immobilization of the enzyme. On the other hand, a slight shift in both the current and the potential was observed illustrating that the polymer had not lost its conductivity and electro-activity upon enzyme immobilization (*Iwuoha et al, 1998; Qu et al, 2005*).

Characterization with SWV was achieved at the potential window of -500 mV to +900 mV carried out at different frequencies; 5, 10 and 15 Hz. The SWV voltammogram illustrated in figure 4.8 shows two peaks observed on the reductive scan; one in the region around +250 mV and the other in the region around -350 mV. The same behaviour observed for the bioelectrode in CV was also observed in SWV. Upon repeated scans the amplitude of the peaks was seen to increase confirming the immobility of the enzyme on the polymer surface. Conductivity and electroactivity were also confirmed by the slight shift observed for both the current and the potential also indicating fast charge transportation along the polymer chain. (*Iwuoha et al, 1998; Qu et al, 2005*). The D_e value of $3.788 \times 10^2 \text{ cm s}^{-1}$ obtained in this study gives evidence of a more conductive polymer when compared values reported by (*Iwuoha et al, 2004*). The surface concentration was also determined and estimated to be $6.684 \times 10^{-6} \text{ mol cm}^{-2}$ illustrating an increased value to that reported for the polymer in the absence

of the enzyme. It should be noted that both of these calculation were achieved as a result of CV responses and not SWV responses.

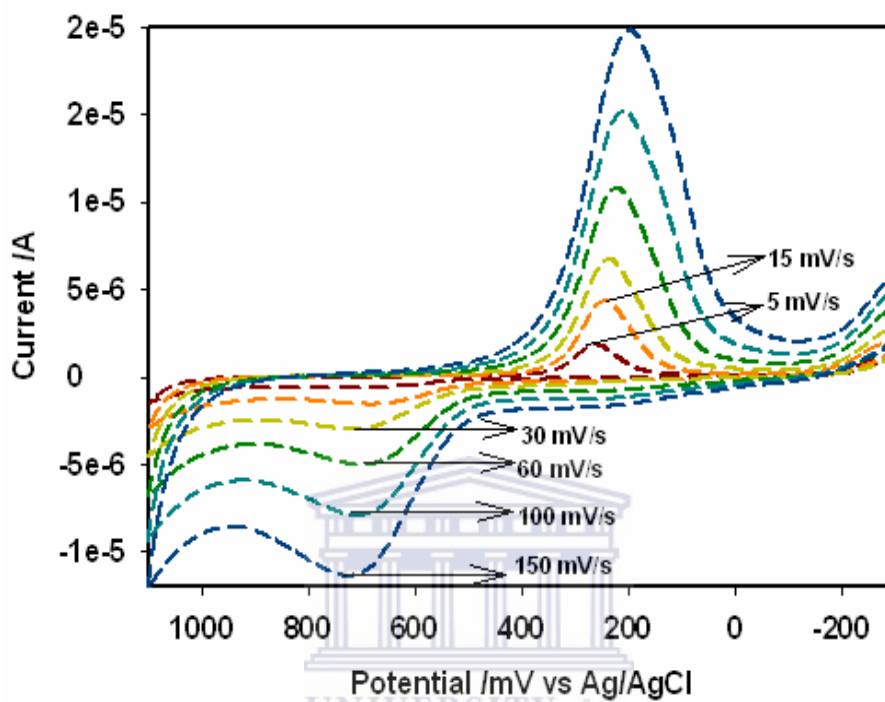


Fig. 4.7 Electrochemical characterization of the Au/PANSA/CYP in PBS at 5, 15, 30, 60, 100 and 150 mV/s at a potential window of -300 mV to +1100 mV.

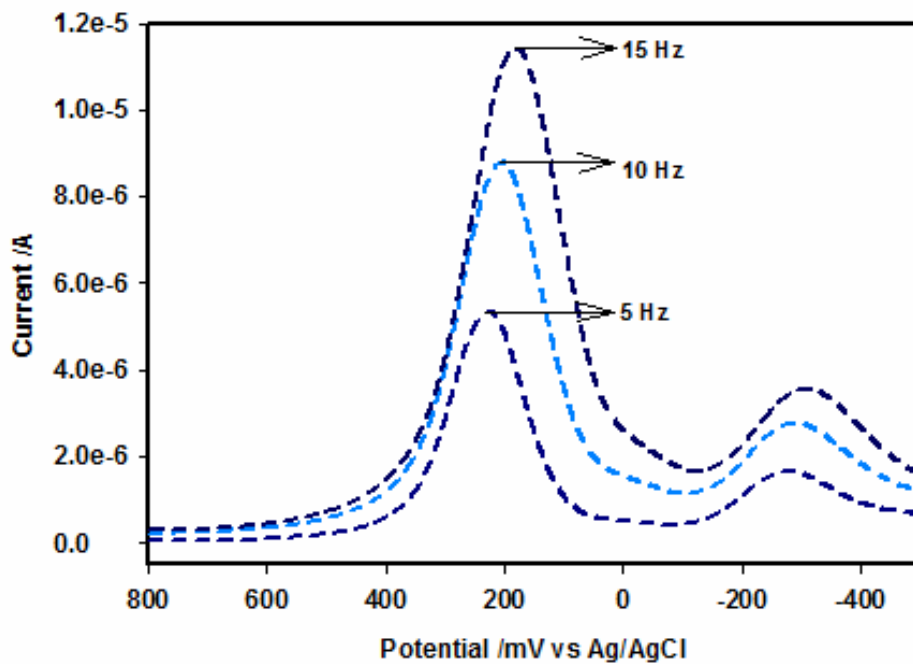
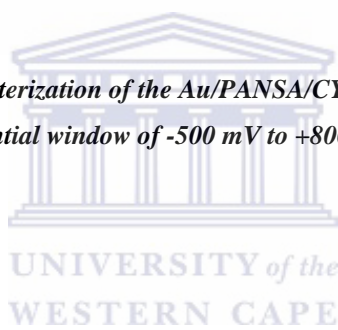


Fig. 4.8 Electrochemical characterization of the Au/PANSA/CYP in PBS at 5, 10 and 15 Hz at a potential window of -500 mV to +800 mV.



4.5 PANSA-mediated electrocatalytic reduction of substrates and SSRI drugs:

CYP2D6 is known to have the ability to metabolise debrisoquine sulfate, a known substrate of this enzyme (*Cerqueira et al, 2000*). In this work this compound was metabolized by a CYP2D6 biosensor. The responses obtained from this study were compared to those obtained when the same biosensor was used in the biotransformation of SSRIs and a tricyclic antidepressant. All the biosensor responses obtained for the substrate, the SSRIs and the tricyclic antidepressants were very similar and the conclusion that the SSRIs were substrates of CYP2D6 was finally made. In the sections below the CV, DPV and SWV result of these compounds namely; fluoxetine, fluvoxamine, zimelidine, clomipramine, sertraline, paroxetine and debrisoquine sulphate, are discussed.

A number of calculations have been made based on the data that was obtained. Among these was the determination of K_m and I_{max} in the linear range of the individual biosensor systems. These values were obtained by plotting calibration curves, which are plots of the current against analyte concentrations which in our case are the concentrations of the above mentioned compounds.. The importance of plotting the calibration curves was to also determine the sensitivity and detection limits of the respective biosensors as shown in table 4.1. The sensitivities of the biosensors were determined as the slopes of the calibration curves. The sensors are more sensitive as a result of the electrochemical immobilization of CYP2D6 as well as the presence of the electron mediator; PANSA (*Svobodova et al, 2002*).

The detection limit was also determined and the importance of doing so is to know what the lowest concentration a particular biosensor can detect, lower than the least amount of concentration which that particular biosensor was subjected too. Detection limits are dependant on the background current exhibited by the polymeric film. The

current is a function of the morphology of the polymer which depends on the polymerization conditions employed (*Grennan et al, 2006*). These values are also stipulated in table 4.1 were a clear comparison among the sensor systems can be made.



4.5.1 Electrocatalytic reduction of SSRIs using CV:

Of great interest to our study was the similarity observed in the electrochemistry of fluoxetine (figure 4.9) and sertraline (figure 4.10). These figures illustrate the voltammetric responses of the Au/PANSA/CYP2D6 biosensors in the absence and presence of fluoxetine and sertraline using CV under aerobic conditions in the presence of PBS. The voltammograms show that as the potential was scanned reductively from +500 mV to -800 mV, in which the reduction (cathodic) current steadily increased to a maximum value after which the current decreased until, the switch potential was reached. It should be noted that illustrated in the figures are the potential windows from +500 mV to -700 mV. Scanning oxidatively (anodically) did not show any anodic peak.

One prominent peak was observed in the cathodic scan when the analyte concentration was increased steadily from 0.2 μM to 1.2 μM . The first reductive cyclic voltammogram illustrated from the top shows that the solution contains 1.2 μM fluoxetine and 1.2 μM sertraline respectively. This defined cathodic peak depicts the coupling of a fast electron transfer reaction taking place at the electrode surface to a fast chemical process in which the reduced electro-active species have been used up.

During the cathodic scanning Fe^{2+} was produced as a result of the binding of the analytes to the active sites of CYP2D6 which was then used up in a fast follow-up chemical reaction, thus making it unavailable for re-oxidation during the anodic scan, which is why there is no peak in the anodic scan. The irreversible cyclic voltammograms recorded in aerobic conditions suggests that there is a binding of molecular oxygen to the Fe^{2+} heme redox centre of the enzyme (*Iwuoha et al, 2004*). As mentioned in chapter two, this process involves a second electron which is responsible for the cleavage of the di-oxygen bond leading towards the generation of

products (*Shumyanteva et al*, 2005). In the case of the biotransformation of fluoxetine by the Au/PANSA/CYP2D6 biosensor, the product generated is norfluoxetine. This metabolite was produced as a result of the abstraction of the methyl group from fluoxetine resulting in a water soluble and easy excretable compound (*Heimke et al*, 2000, *Iwuoha et al*, 1998). The same biotransformation reaction was assumed for the Au/PANSA/CYP2D6 biosensor towards sertraline in which desmethylsertraline was the resultant product also produced by the abstraction of methyl from sertraline.

The peak observed below that observed for 1.2 μM , illustrates the presence of the 1.6 μM concentrations for both sertraline and fluoxetine respectively, in which a decrease in the current was observed indicating a case of substrate-inhibition. This therefore suggests that beyond the addition of 1.2 μM for both fluoxetine and sertraline the activity of CYP2D6 had been altered due to the unavailability of the enzyme's active site for further binding of the analytes (*Conn et al*, 1987). This agrees with what has been reported by other researchers on their work on CYP2D6 (*Iwuoha et al*, 2004; *von Moltke et al*, 1997; *Margolis et al*, 2000). This is therefore confirmation that fluoxetine and sertraline are both substrate – inhibitors of CYP2D6. Therefore upon continuous cycling, the current continues to reduce.

The Au/PANSA/CYP2D6 biosensor responses in the absence and presence of clomipramine, fluvoxamine, debrisoquine sulphate and zimelidine are illustrated in figures 4.11, 4.12, 4.13 and 4.14 respectively. All the calculations involving these two compounds are also illustrated in table 4.1.

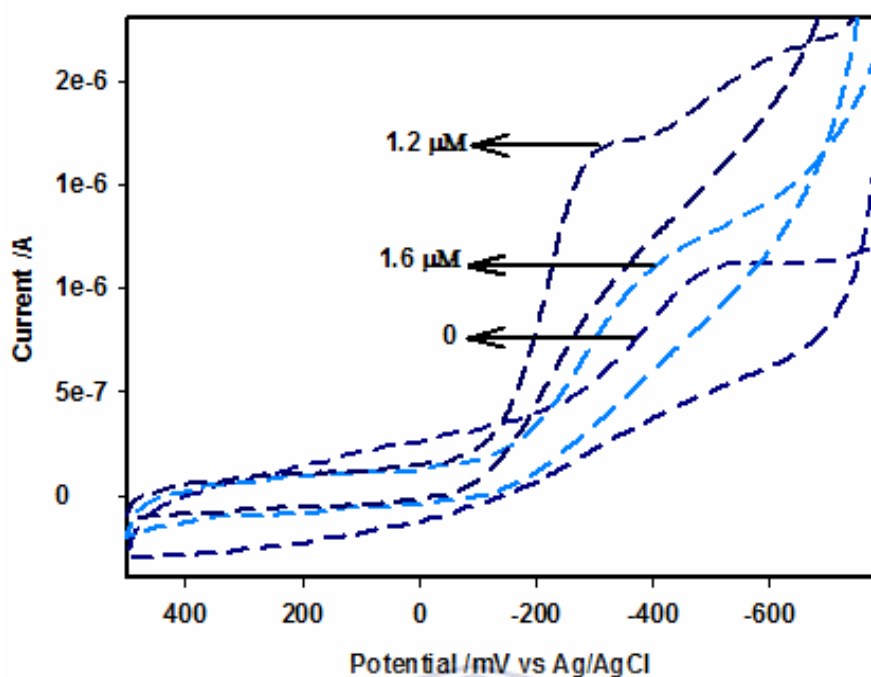


Fig. 4.9 CV of CYP2D6 biosensor in the presence of varying concentrations of fluoxetine under aerobic conditions in the potential window of +500 mV to -700 mV at a scan rate of 10 mV/s

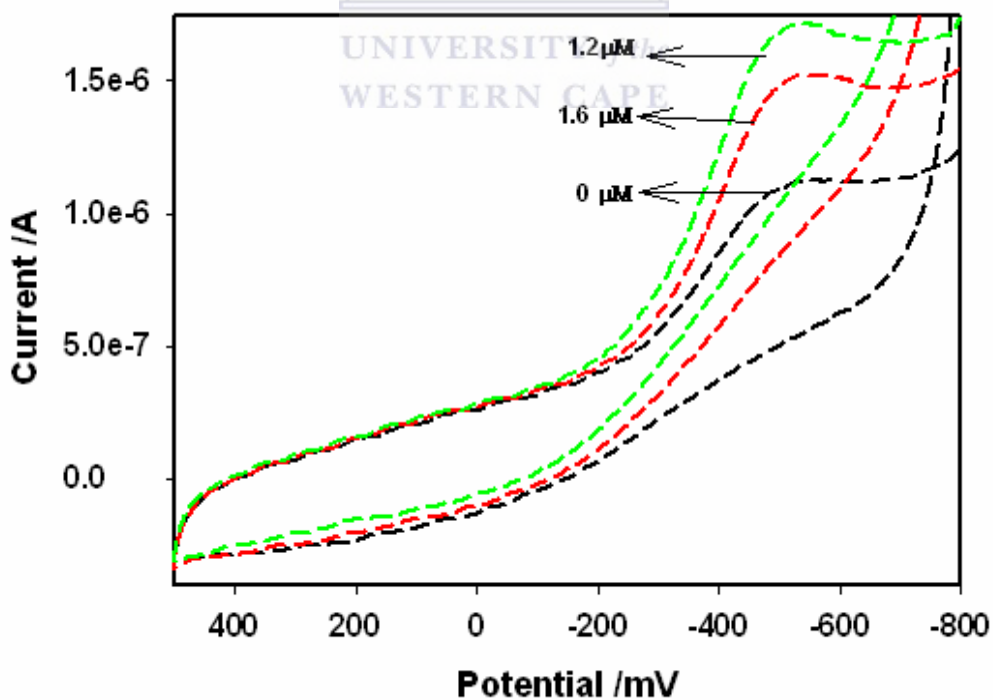


Fig. 4.10 CV of CYP2D6 biosensor in the presence of varying concentrations of sertraline under aerobic conditions in the potential window of +500 mV to -800 mV at a scan rate of 10 mV/s

The Au/PANSA/CYP2D6 biosensor responses in the absence and presence of fluvoxamine, zimelidine, clomipramine and debrisoquine sulphate were also studied using CV. Although the concentration range studied for the biosensor responses was from 0.2 to 1.6 μM , only the responses for 0.2 and 0.4 μM are shown. The voltammograms in each case show that as the potential was scanned from +500 mV to -800 mV the cathodic current steadily increased to a maximum value after which it decreased until, the switch potential was reached. This behaviour was observed for all the above mentioned compounds. During the cathodic scanning the heme redox centre; Fe^{2+} was produced from the interaction of the respective analytes with the heme redox centre; Fe^{3+} and later used up in a fast follow-up chemical reaction, thus making it unavailable for re-oxidation during the anodic scan. This is said to be a change from the low spin form of the enzyme to the high spin form which has a high affinity for oxygen. The irreversible cyclic voltammograms recorded for each analyte in aerobic conditions suggests that there is a binding of oxygen to the Fe^{2+} heme redox centre of the enzyme (*Wilson et al*, 2004). For all of these compounds one prominent peak was observed in the cathodic scan when the analyte concentration was increased steadily from 0.2 μM to 1.6 μM . A cathodic peak in the region around -300 mV was observed for fluvoxamine and in the region around - 400 mV a cathodic peak was also observed for zimelidine. For clomipramine and debrisoquine sulphate, the peaks were observed for both compounds in the region approximately +450 mV. As mentioned before, it is the second electron which assists in the release of products even though the products do not necessary follow the same reaction pathway. Debrisoquine sulphate is hydroxylated to 4-hydroxydebrisoquine by the Au/PANSA/CYP2D6 biosensor to produce an excretable compound while

clomipramine is demethylated to desmethylclomipramine. These findings are all as a result of their respective interaction with CYP2D6 (*Heimke et al*, 2000).

It was also found that the biotransformation of zimelidine and fluvoxamine respectively by the Au/PANSA/CYP2D6 biosensor also produced water soluble compounds. In the case of zimelidine, desmethylzimelidine was produced as a result of the abstraction of methyl while in the case of fluvoxamine, an o-demethylated metabolite was produced. This metabolite was also produced as a result of the abstraction of methyl but at the very same time, an oxygen atom from the surrounding reaction solution was added, producing it into a carboxylic acid (*Heimke et al*, 2000).

Finally, from the voltammograms it is evident that the biosensor responses obtained for the analytes are closely related to that of the biosensor responses of the known substrate of CYP2D6, namely debrisoquine sulphate. This therefore suggests that these analytes /SSRIs and the tricyclic antidepressants: clomipramine are substrates of CYP2D6. This is deduced from the fact that the cathodic peaks observed for all these biosensors occur at very similar potentials. To further substantiate these findings, DPV and SWV analyses were also carried out.

The calibration curve of fluoxetine is shown in figures 4.15 where it follows Michaelis-Menten kinetics in which K_m and I_{max} were determined and their values are shown in table 4.1. Figure 4.15 also shows the linear range of the fluoxetine biosensor in which was established in the region from 0 to 1.0 μM (with $r = 0.968$). All calculations for the biosensor are all stipulated in table 4.1. Calibration curves for zimelidine and fluvoxamine are shown in figure 4.16 and 17 respectively. A linear relationship in the case of zimelidine was observed in the range from 0 to 1.4 μM (with $r = 0.981$) were K_m , I_{max} , sensitivity and the detection limit of the biosensor

were estimated. The linear range for fluvoxamine was established in the region from 0 to 1.0 μM (with $r = 0.919$) where the same calculations were determined.

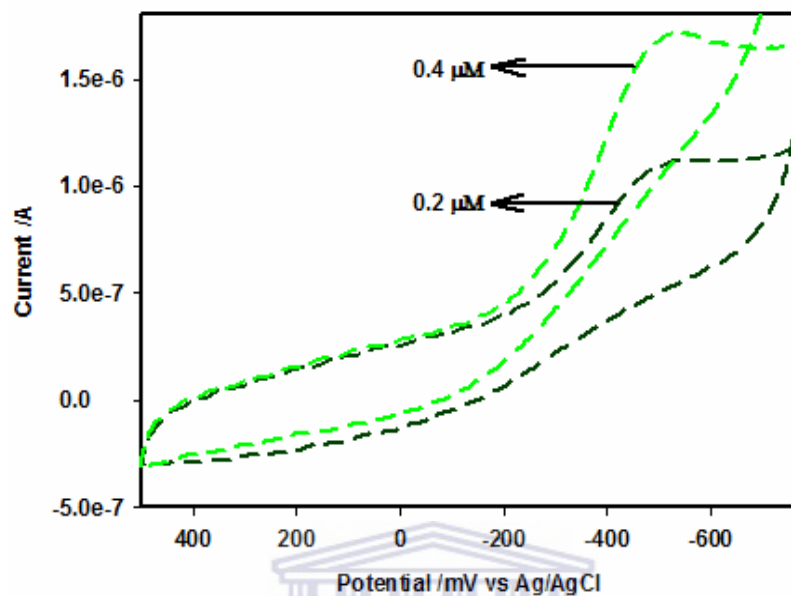


Fig. 4.11 CV of CYP2D6 biosensor in the presence of varying concentrations of clomipramine under aerobic conditions in the potential window of +500mV to -700 mV at a scan rate of 10 mV/s

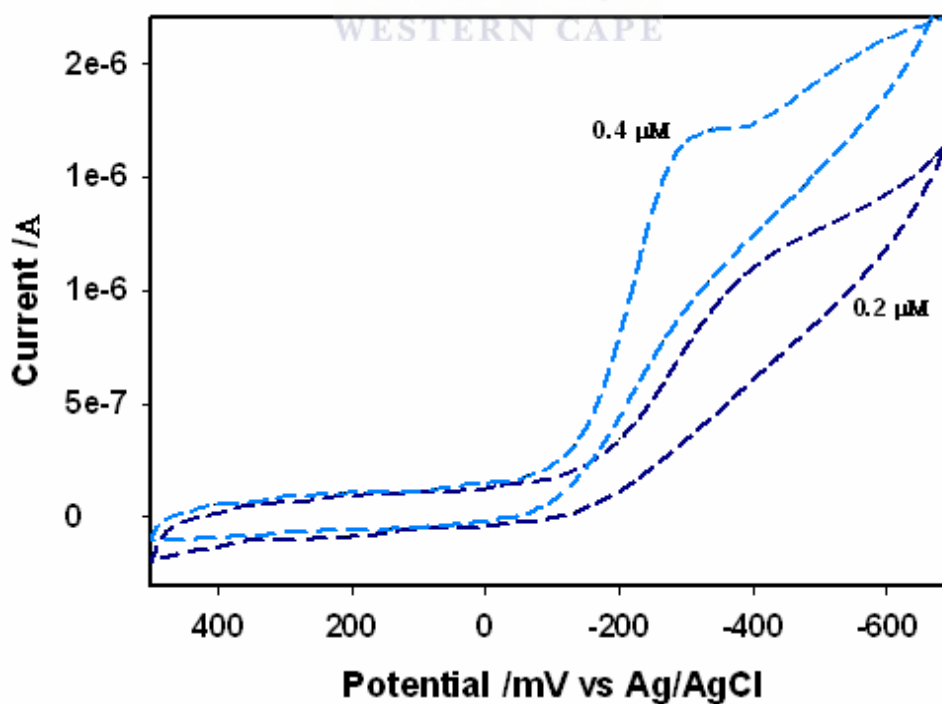


Fig. 4.12 CV of CYP2D6 biosensor in the presence of varying concentrations of fluvoxamine under aerobic conditions in the potential window of +500mV to -700 mV at a scan rate of 10 mV/s

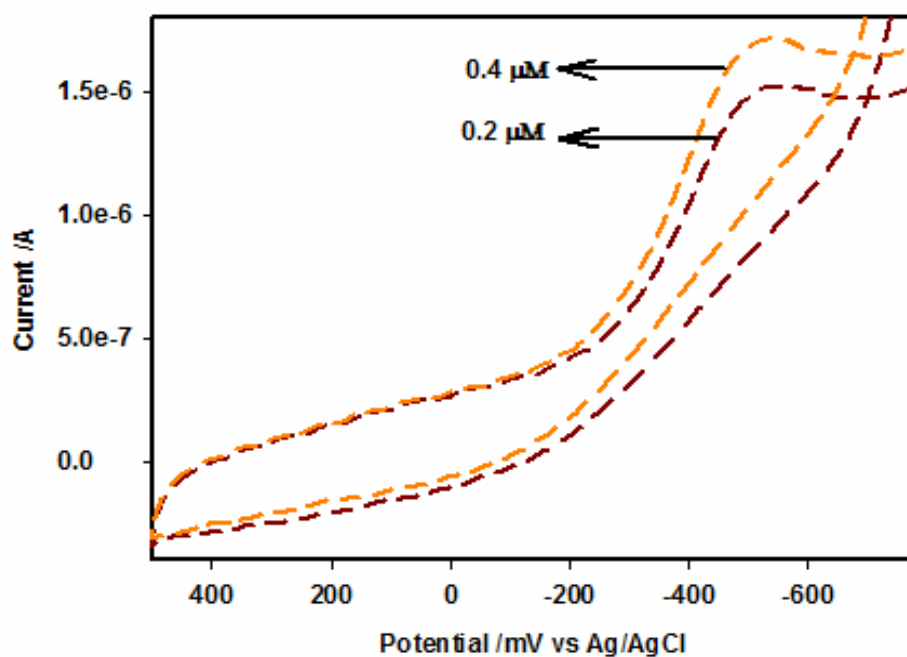


Fig. 4.13 CV of CYP2D6 biosensor in the presence of varying concentrations of debrisoquine sulphate under aerobic conditions in the potential window of +500mV to -700 mV at a scan rate of 10 mV/s

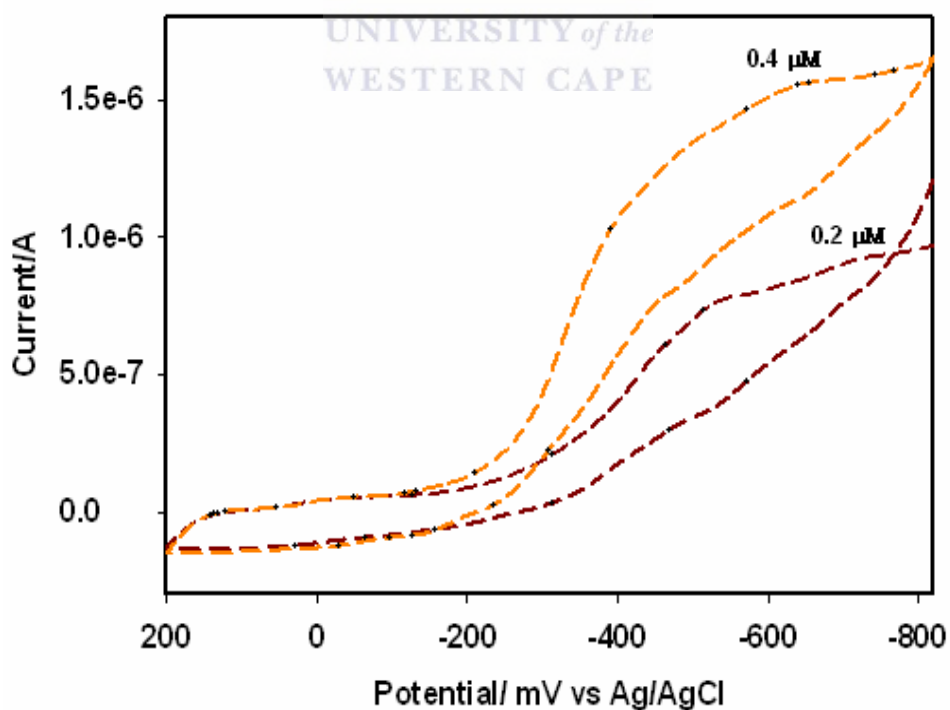


Fig. 4.14 CV of CYP2D6 biosensor in the presence of varying concentrations of zimelidine under aerobic conditions in the potential window of + 500 mV to -800 mV at a scan rate of 10 mV/s

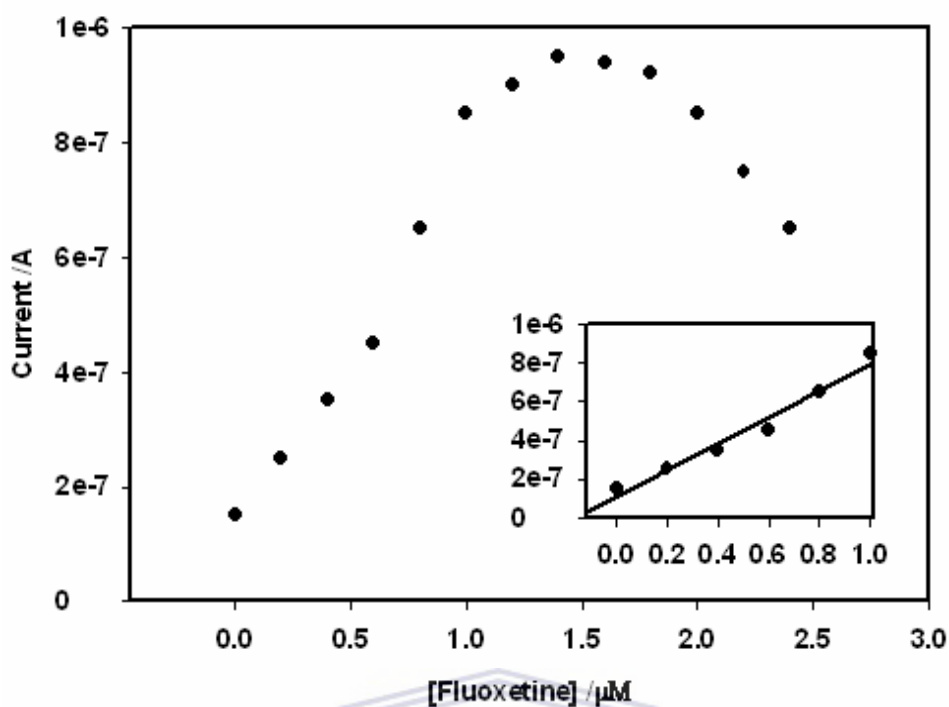


Fig 4.15 Calibration curve of fluoxetine biosensor illustrating the linear range of the biosensor with a detection limit of $0.9 \mu\text{M}$ and $r^2 = 0.968$

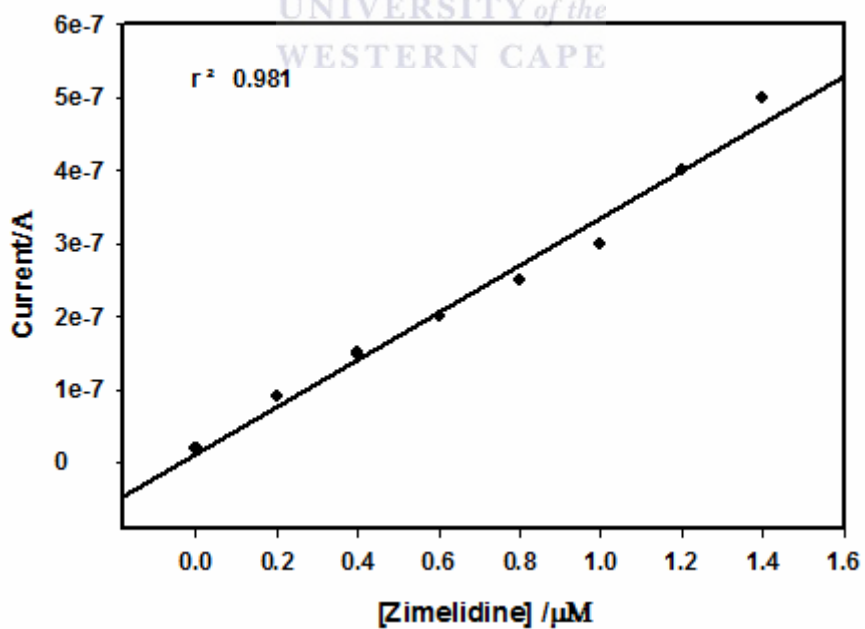


Fig. 4.16 Calibration curve for zimelidine biosensor with a sensitivity of 3.220×10^{-1} and a detection limit of $0.03 \mu\text{M}$

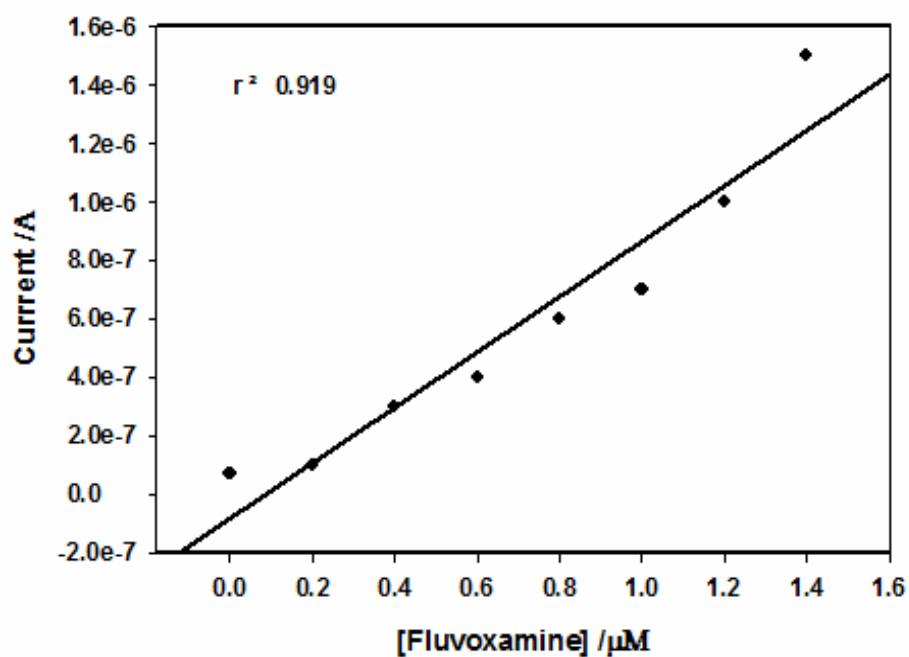
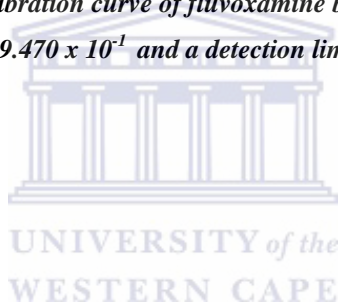


Fig. 4.17 Calibration curve of fluvoxamine biosensor with a sensitivity of 9.470×10^{-1} and a detection limit of $0.15 \mu\text{M}$.



4.5.2 Electrocatalytic reduction of SSRIs using DPV:

DPV was also carried out to study the reactivities of the Au/PANSA/CYP biosensor towards the biotransformation of SSRI. The biosensor responses in the absence and presence of these analytes can be illustrated in figure 4.18 for zimelidine, figure 4.19 for clomipramine, figure 4.20 for debrisoquine sulphate, figure 4.21 for fluvoxamine, figure 4.22 for sertraline and figure 4.23 for fluoxetine; all carried out in aerobic conditions. The DPV was performed in a reductive mode by scanning the potential from +400 mV to -700 mV however for visual purposes; the figures either show the potential window from +200 mV to -500 mV, +300 mV to -500 mV or from +200 mV to -600 mV. The cathodic current steadily increased to a maximum value after which the current was seen as decreasing. One prominent DPV peak was observed in the cathodic scan when the concentration of each of the analytes was respectively increased steadily from a concentration of 0.2 μM to 1.6 μM . However in some of the figures below, this concentration range is not shown in full but shown either from 0.2 μM to 1 μM or from 0.2 μM to 0.8 μM . For zimelidine the cathodic peak was observed in the region approximately +250 mV, for clomipramine the cathodic peak was observed in the region approximately around +270 mV, for fluvoxamine the cathodic peak was observed in the region approximately around +200 mV, for debrisoquine sulfate this peak was observed in the region approximately around +290 mV and finally for sertraline and fluoxetine the peak was observed in the region approximately around +250 mV.

After each addition of the respective analytes, an increase in current was observed which was also accompanied by a slight shift in potential implying a reduction in the redox potential. Presumably, the cathodic biosensor responses, illustrated as the cathodic peaks; are due to the coupling of the $\text{Fe}^{3+} \leftrightarrow \text{Fe}^{2+}$ electron transfer reaction as

well as the electro-catalytic reactions involved in the binding of oxygen to Fe^{2+} (Shumyanteva *et al*, 2005). According to (Iwuoha *et al*, 2004), this electro-catalytic reaction is fast; however in our case this reaction was achieved at 10 mV/s. As mentioned before, this study also produced the water soluble metabolites as discussed previously as a result of the mono-oxygenation reaction in which the di-oxygen bond is broken by the second electron as shown in scheme 2.2. In this section we can again observe the similarity in the electrochemical behaviour of the analytes as compared to that of debrisoquine sulphate. The DPV studies have also confirmed the similarities which exist between the electrochemistry of sertraline and fluoxetine as shown by figures 4.22 and 4.23 respectively. It should also be noted that although the DPV studies were carried out in the potential window from +400 mV to -700 mV, shown in the figures is the potential window from -100 mV to -400 mV. For both the sertraline and fluoxetine studies, an increase in the current was observed upon the addition of the respective analytes between the concentration ranges of 0.2 μM to 1 μM . Beyond this range, the current decreased illustrating a case of analyte/SSRI inhibition which was also observed by the work done by (Iwuoha *et al*, 2004; von Moltke *et al*, 1997; Margolis *et al*, 2000). CYP2D6 demethylated these compounds to desertraline and nor-fluoxetine. It could therefore be concluded that both of these SSRIs are substrate-inhibitors of CYP2D6. Another finding of this study was the similarity in the electrochemistry of debrisoquine sulphate to that of the SSRIs and the tricyclic antidepressant; clomipramine. The experiment with debrisoquine sulphate was carried out in order to demonstrate that the CYP2D6 biosensor actually works which was proved to be true. This is based on the almost common cathodic peak potential observed for the electrochemistry of the known CYP2D6 substrate relative to those obtained for the SSRIs and clomipramine. From this we could then deduce that the

SSRIs as well as clomipramine are substrates of CYP2D6 due to the presumption that the reactivity of the Au/PANSA/CYP2D6 bioelectrode towards debrisoquine sulphate is the same as them. As shown in scheme 2.2, the metabolisms of the analytes are essentially oxygenation reactions, where the first electron is used to reduce the ferri heme of CYP2D6 to the ferro heme.

The calibration curves for the other SSRIs are shown in the other sections, but in this section only the calibration curve for debrisoquine sulphate is shown in figure 4.24 where the sensitivity, detection limit, K_m and I_{max} were estimated. Their values are clearly stipulated in table 4.1.

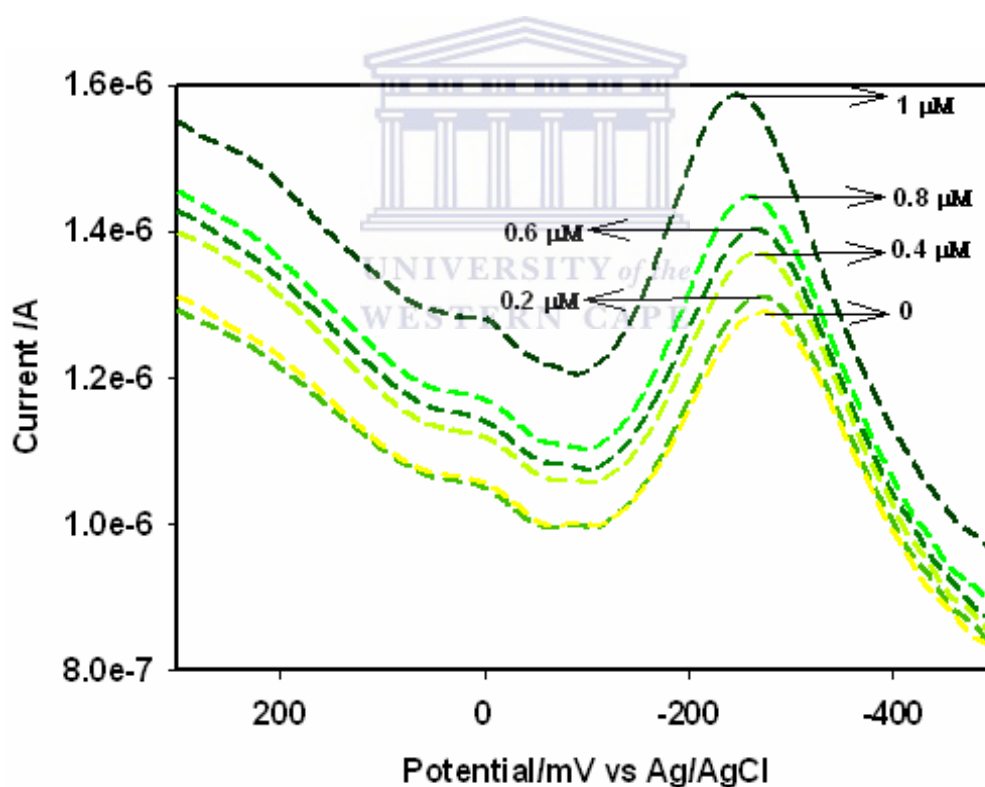


Fig. 4.18 DPV of CYP2D6 biosensor in the presence of varying concentrations of zimelidine under aerobic conditions in the potential window of +300 mV to -500 mV at a scan rate of 10 mV/s

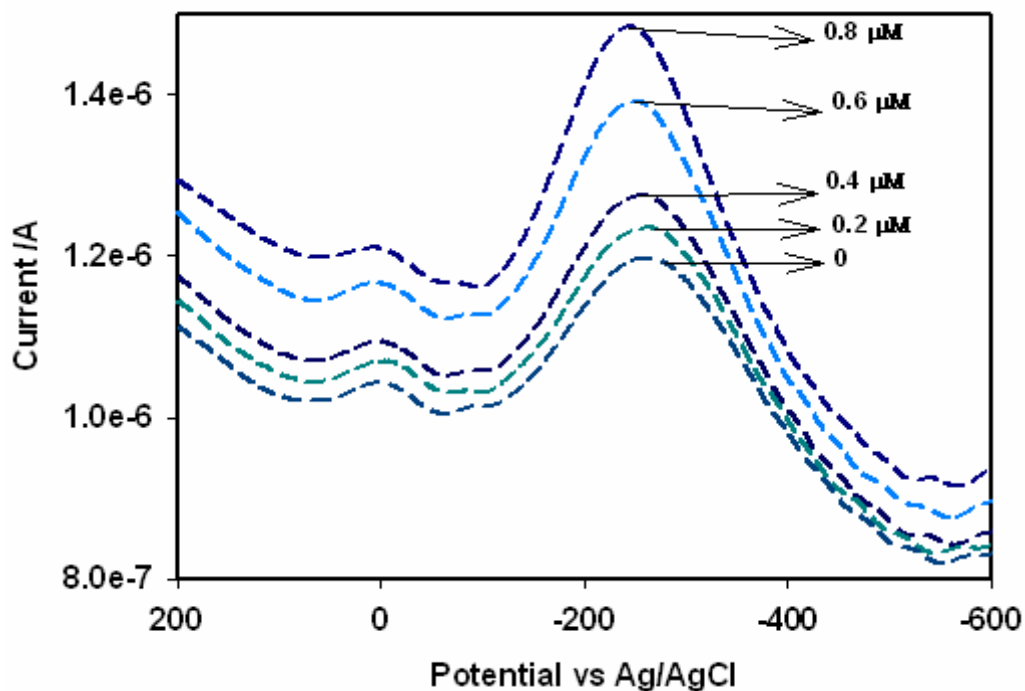


Fig. 4.19 DPV of CYP2D6 biosensor in the presence of varying concentrations of clomipramine under aerobic conditions in the potential window of +200 mV to -600 mV at a scan rate of 10 mV/s

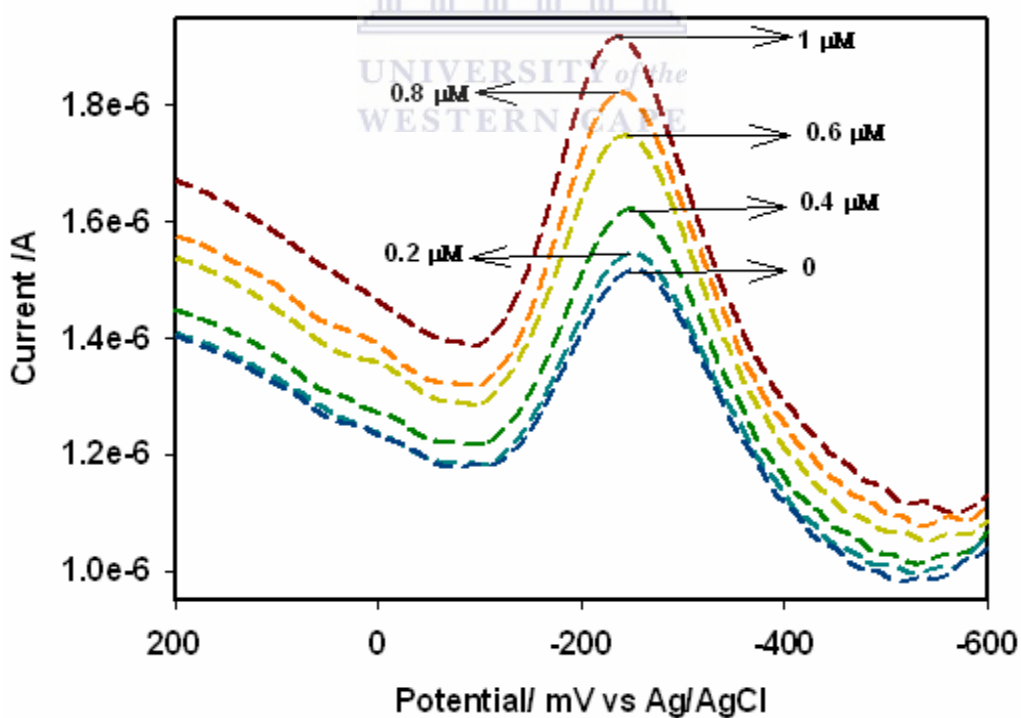


Fig. 4.20 DPV of CYP2D6 biosensor in the presence of varying concentrations of debrisoquine sulphate under aerobic conditions in the potential window of +200 mV to -600 mV at a scan rate of 10 mV/s

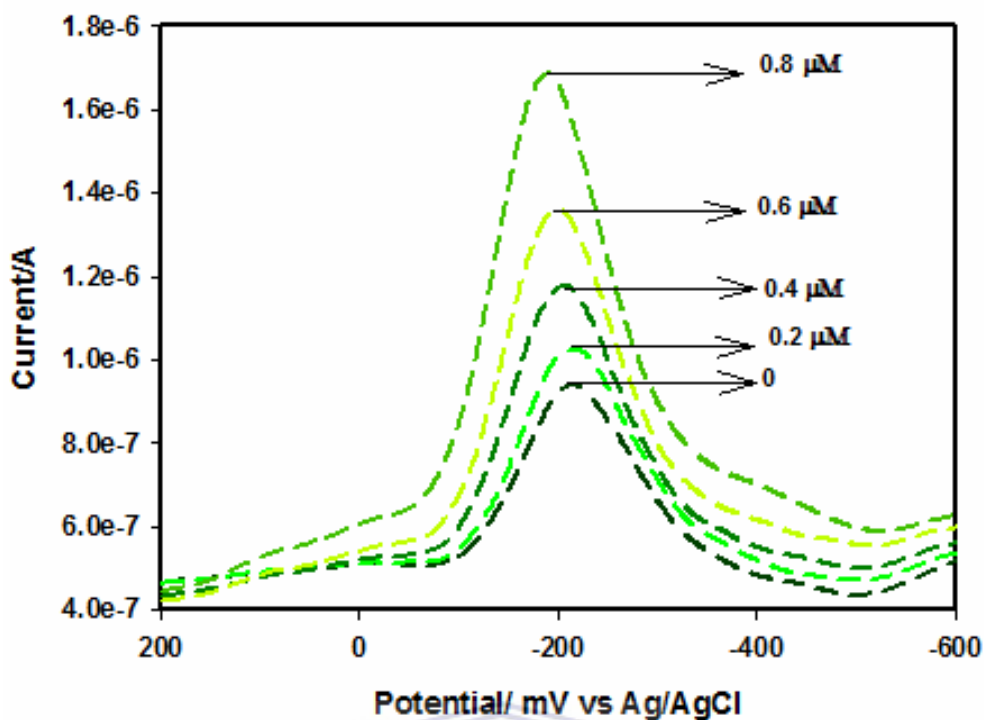


Fig.4.21 DPV of CYP2D6 biosensor in the presence of varying concentrations of fluvoxamine under aerobic conditions in the potential window of +200 mV to -600 mV at a scan rate of 10 mV/s

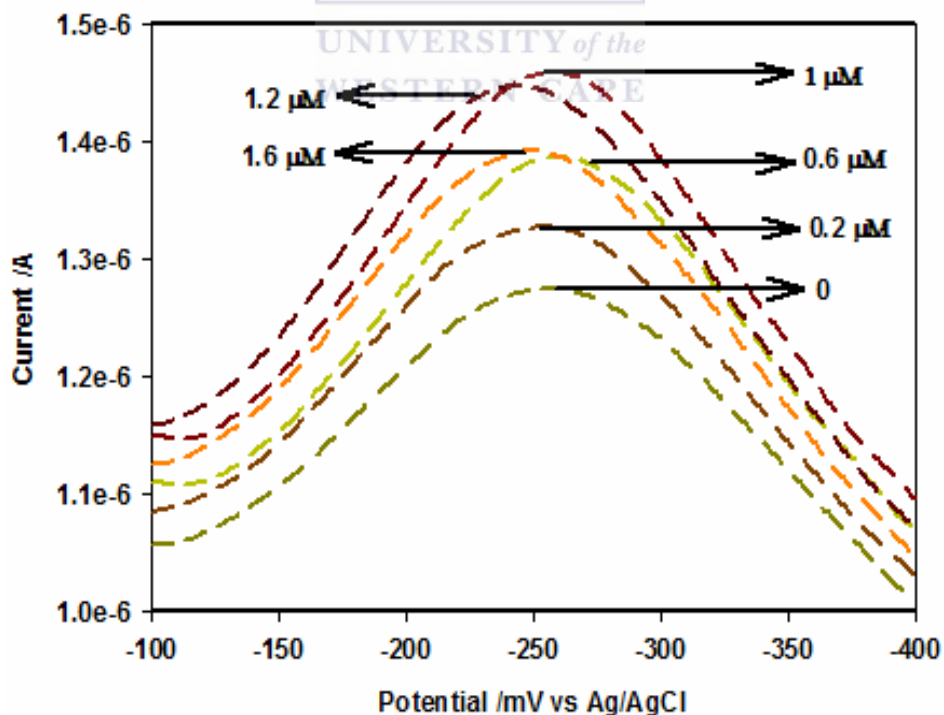


Fig.4.22 DPV of CYP2D6 biosensor in the presence of varying concentrations of sertraline under aerobic conditions in the potential window of -100 mV to -400 mV at a scan rate of 10 mV/s

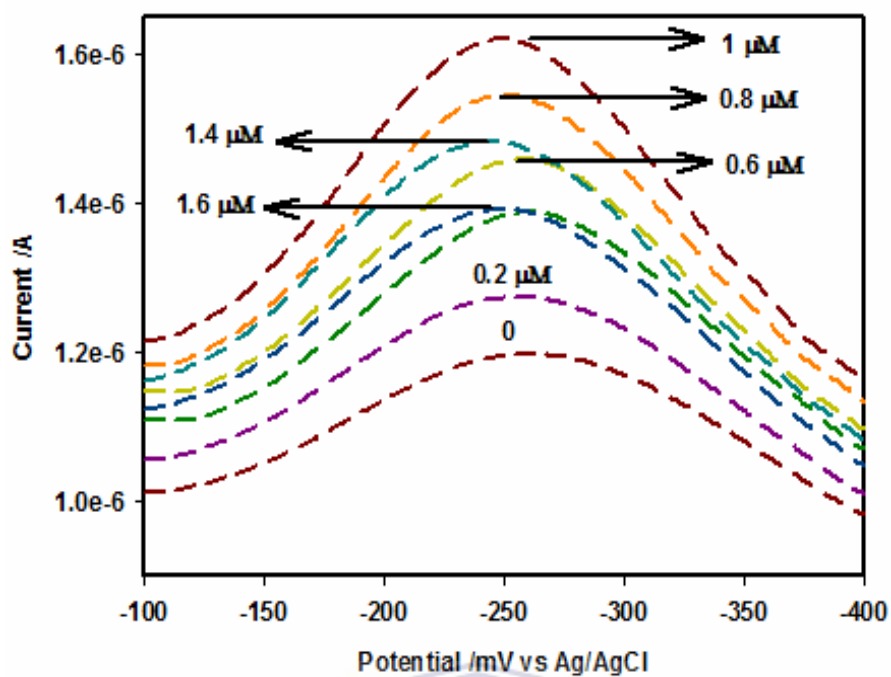


Fig.4.23 DPV of CYP2D6 biosensor in the presence of varying concentrations of fluoxetine under aerobic conditions in the potential window of -100 mV to -400 mV at a scan rate of 10 mV/s

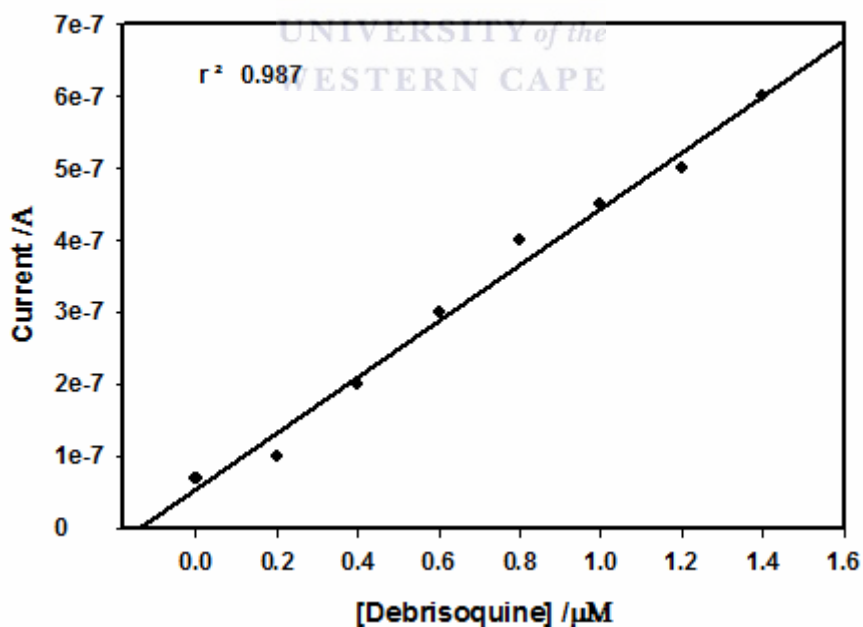


Fig. 4.24 Calibration curve of debrisoquine sulphate biosensor with a sensitivity of 3.904×10^{-1} and detection limit of $0.02 \mu\text{M}$.

4.5.3 Electrocatalytic reduction of SSRIs using SWV:

The reactivities of the Au/PANSA/CYP2D6 biosensor towards the analytes/SSRIs were further studied using SWV in the absence and presence of the respective analytes. The use of this technique also provided confirmation for the electrochemical similarity existing between fluoxetine and sertraline respectively shown as figures 4.25 and 4.26. Also shown are the SWV responses for fluvoxamine zimelidine debrisoquine sulphate and clomipramine illustrated respectively in figure 4.27, 4.28 4.29 and 4.30, in the absence and presence of these compounds under aerobic conditions. The voltammograms show that as the potential was scanned from +500 mV to -700 mV, the current steadily increased to a maximum value after which the current decreased. Illustrated in the provided figures are the potential windows from +100 mV to -600 mV, 0 to -600 mV or 0 to -500 mV.

For sertraline one prominent peak in the region approximately around -200 mV was observed in the cathodic scan when the analyte concentration was increased steadily from 0.2 μM to 1.2 μM where the current was seen to increase after each addition. In vitro and in vivo depression studies by (Kobayashi *et al*, 1999) indicate sertraline to be a possible inhibitor of CYP2D6. Addition of sertraline beyond 1.2 μM , showed a decrease in the peak currents suggesting saturation of the enzyme or possibly inhibition of the enzyme (Mandrioli *et al*, 2006). (Mandrioli *et al*, 2006, Heimke *et al*, 2000) suggested sertraline to be an inhibitor of CYP2D6 functioning by binding to the substrate binding sites of CYP2D6. Our study has proven otherwise, where at very low concentrations of sertraline reductive catalysis was observed and saturation or inhibition occurring at high concentrations. A similar behaviour to that of sertraline was also observed for fluoxetine where an increase in the current was observed when the analyte concentration was increased steadily from 0.2 μM to 1.0 μM . A prominent

peak in the region approximately around +200 mV was observed in the cathodic peak during the addition of fluoxetine. Fluoxetine addition beyond this concentration range resulted in a decrease in the current also illustrating a case of substrate-inhibition (Iwuoha *et al*, 2004; von Moltke *et al*, 1997; Margolis *et al*, 2000).

One prominent peak was observed in the region approximately around -300mV for fluvoxamine, in the region approximately around -305 mV for debrisoquine sulphate and in the region approximately around -315 mV for clomipramine. This was observed in the cathodic scans when the analyte concentrations were increased steadily from 0.2 μM to 1.6 μM respectively for these compounds. The peaks observed for the respective biosensors towards the analytes are a result of the transformation of Fe^{3+} to Fe^{2+} (Shumyanteva *et al*, 2005) when the analytes react with the active site of the enzyme in the Fe^{3+} state. The produced high spin state of the enzyme was then able to bind molecular oxygen. Again, these biotransformations have led to the production of water soluble and easy excretable metabolites (Iwuoha *et al*, 1998) as stated previously. The resultant products were successfully produced when the second electron breaks the di-oxygen bond.

Finally with the SWV results we could confidently say that indeed the SSRIs including the tricyclic antidepressant used in our study are substrates of CYP2D6 as confirmed by the similarities of the electrochemical behaviour of them relative to that of debrisoquine sulphate as observed by the location of their cathodic peaks.

Figure 4.31 illustrates the calibration curve of sertraline which followed Michaelis-Menten kinetics. The linear relationship was obtained in the range from 0 to 1.2 μM (with $r = 0.985$). The calibration curve of clomipramine is shown in figure 4.32 (with $r = 0.980$). K_m , I_{max} , sensitivities and the detection limits were estimated and are stipulated in table 4.1.

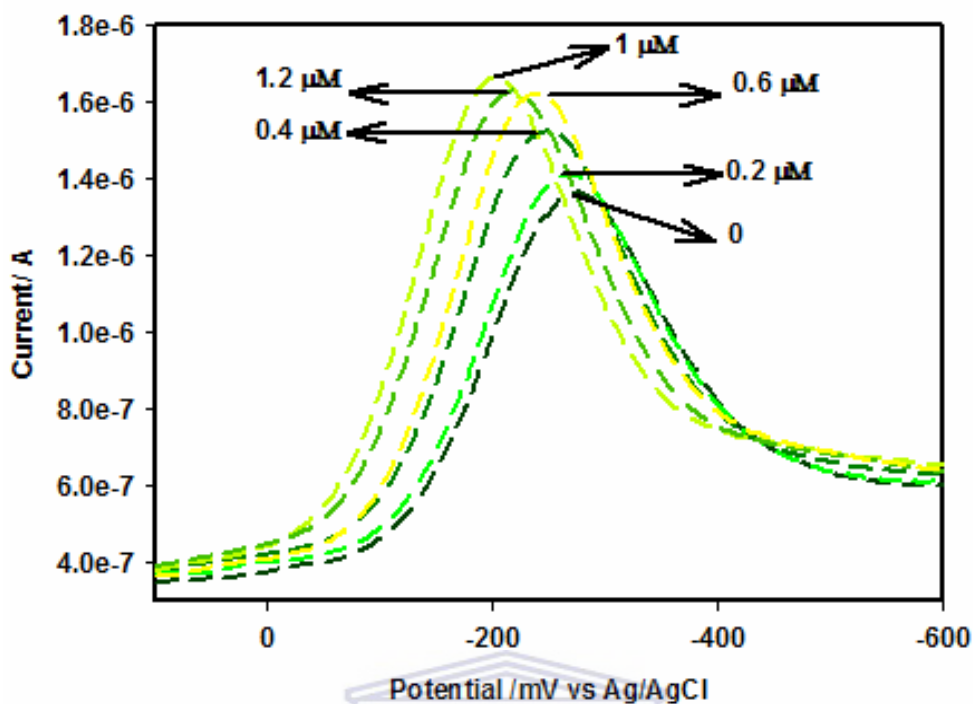


Fig. 4.25 SWV of CYP2D6 biosensor in the presence of varying concentrations of fluoxetine under aerobic at a potential window of +100 mV to -600 mV at a frequency of 10 Hz

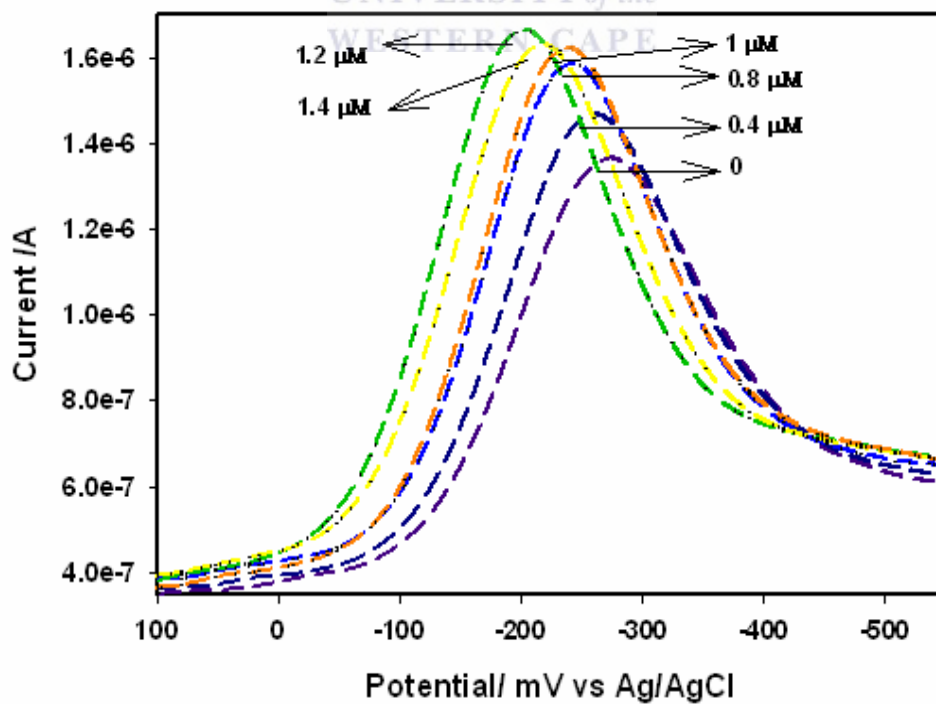


Fig. 4.26 SWV of CYP2D6 biosensor in the presence of varying concentrations of sertraline under aerobic conditions at a potential window of +100 mV to -600 mV at a frequency of 10 Hz

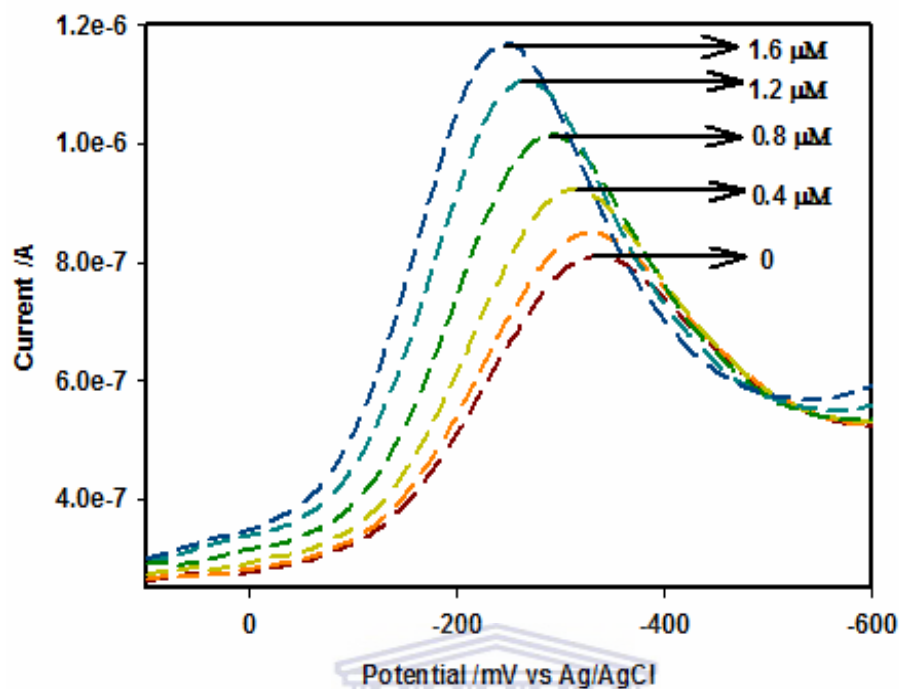


Fig. 4.27 SWV of CYP2D6 biosensor in the presence of varying concentrations of fluvoxamine under aerobic conditions at a potential window of +100 mV to -600 mV at a frequency of 10 Hz

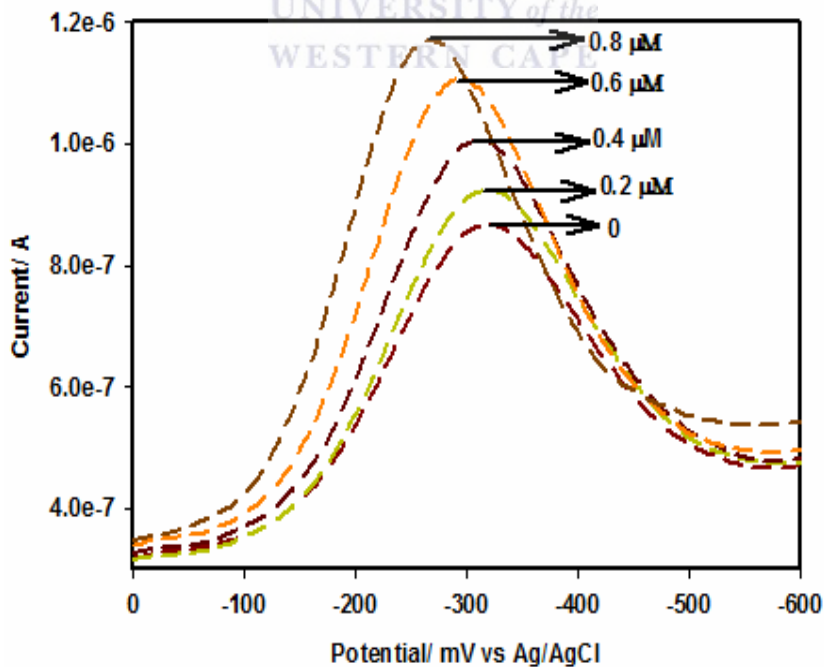


Fig. 4.28 SWV of CYP2D6 biosensor in the presence of varying concentrations of zimelidine under aerobic conditions at a potential window of 0 mV to -600 mV at a frequency of 10 Hz

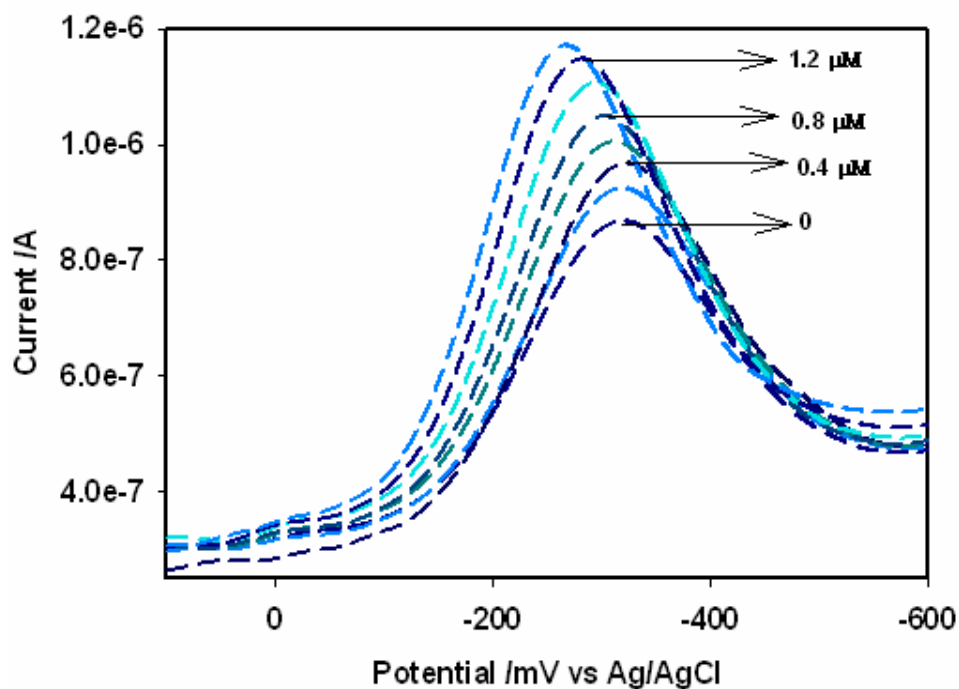


Fig. 4.29 SWV of CYP2D6 biosensor in the presence of varying concentrations of debrisoquine sulphate under aerobic conditions at a potential window of +100 mV to -600 mV at a frequency of 10 Hz

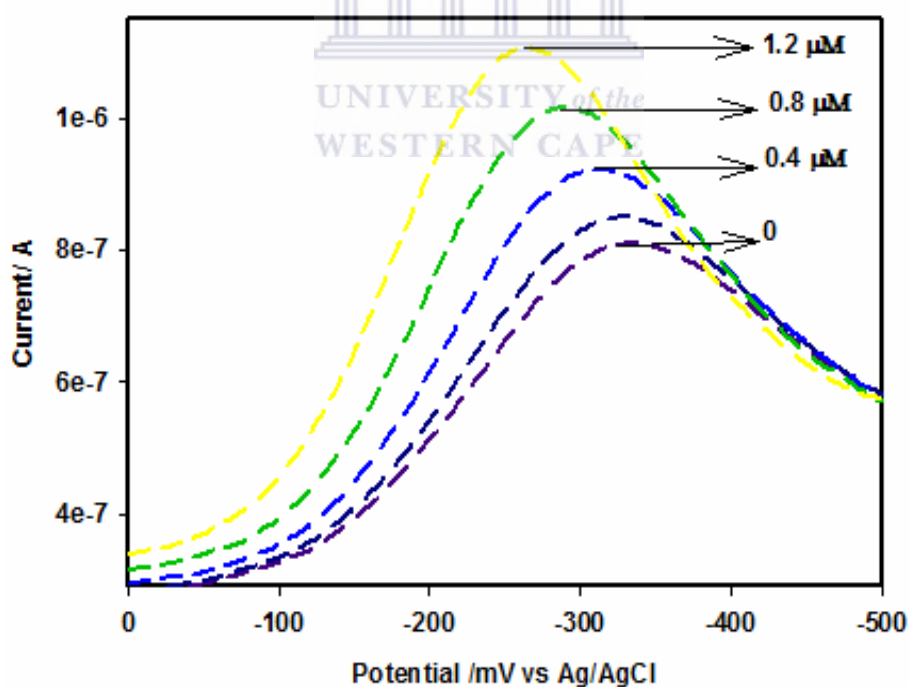


Fig. 4.30 SWV of CYP2D6 biosensor in the presence of varying concentrations of clomipramine under aerobic conditions at a potential window of 0 mV to -500 mV at a frequency of 10 Hz

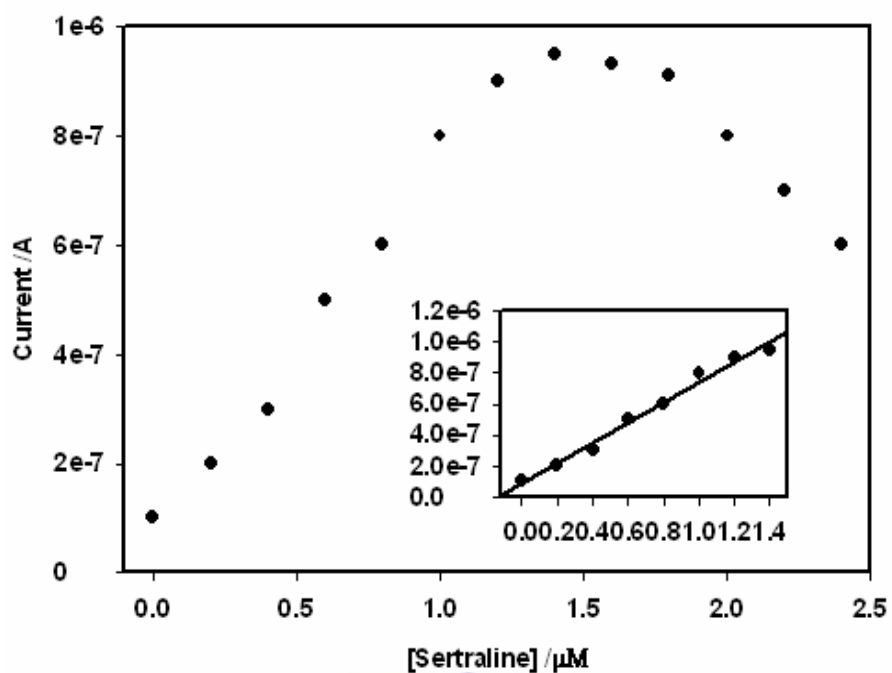


Fig 4.31 Calibration curve of sertraline biosensor illustrating the linear range of the biosensor with a detection limit of $0.13 \mu\text{M}$ and $r^2 = 0.985$

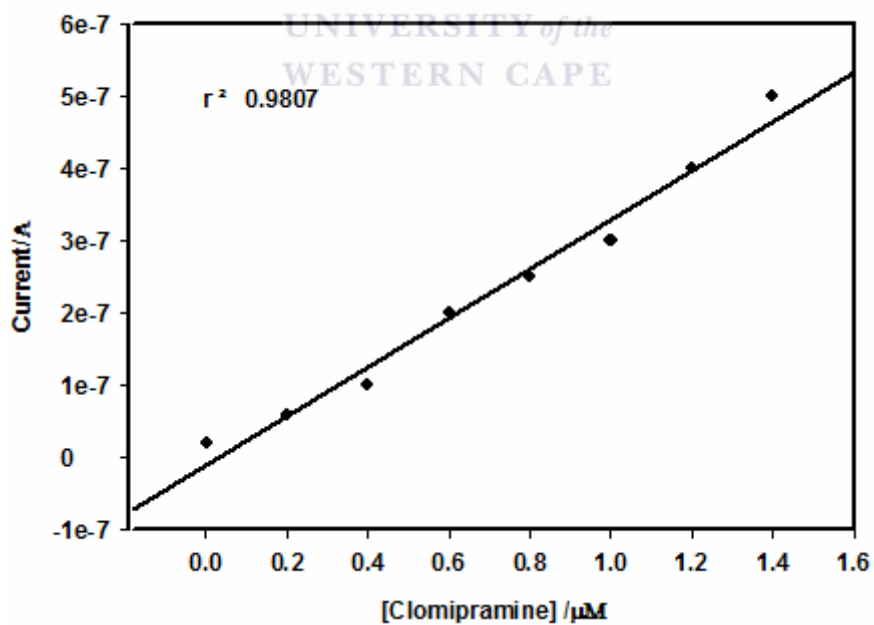


Fig 4.32 Calibration curve of clomipramine biosensor illustrating the linear range of the biosensor with a detection limit of $0.05 \mu\text{M}$.

4.6 Inhibition of CYP2D6 by Paroxetine:

The DPV of paroxetine was performed in a reductive mode by scanning the potential from +400 mV to -700 mV (shown is the potential window from +300 mV to -700 mV) during which the cathodic current steadily increased to a maximum value after which it then decreased. Figure 4.33 shows the DPV voltammetric responses of CYP2D6 to PBS in the absence and presence of paroxetine. From the voltammogram we can see that after the first addition of paroxetine, there was a decrease in the current illustrating enzyme inhibition. This behaviour of the biosensor confirms that our biosensor contains CYP2D6. The same behaviour was observed when the biosensor responses were studied using SWV (figure 4.34) and CV (figure 4.35).

Upon subsequent additions, the current continued to decrease accompanied by a slight shift in the potential after each addition. This is a case of uncompetitive inhibition in which the inhibitor paroxetine has changed the shape of the enzyme. The active site of the enzyme has also changed in such a way that the substrate can no longer bind (*Fersht et al, 1984; Conn et al, 1987*). This interaction can be clearly observed in figure 4.36 where both fluvoxamine; a known substrate of CYP2D6 was reacted with paroxetine in the same cell solution. Figure 4.36 (a) shows an increase in the current upon the addition of the substrate but immediately when the inhibitor is introduced into the system, the current started to decay. When the inhibitor was first introduced into the reaction solution, as shown in figure 4.36 (b); a particular current was observed which was seen to decrease upon the addition of the substrate; fluvoxamine. The reason for this is the fact that upon the addition of paroxetine, the activity of the enzyme is immediately eliminated due to the possible formation of covalent bonds between the inhibitor and the active site of the enzyme, observed as the immediate decrease in current. From figure 4.36 (b) we can see that even increasing the

concentration of the substrate fluvoxamine does not overcome the inhibition (*Conn et al, 1987; Subehan et al, 2006*).

Inhibition does not mean that biotransformation of paroxetine by CYP2D6 did not occur. The product of this reaction was an unstable catechol intermediate which was as a result of the oxidative cleavage of paroxetine by CYP2D6. This intermediate is in most cases further methylated in the meta-position to the meta-methoxyderivative or in the para-position to the para-methoxyderivative (*Heimke et al, 2000*).

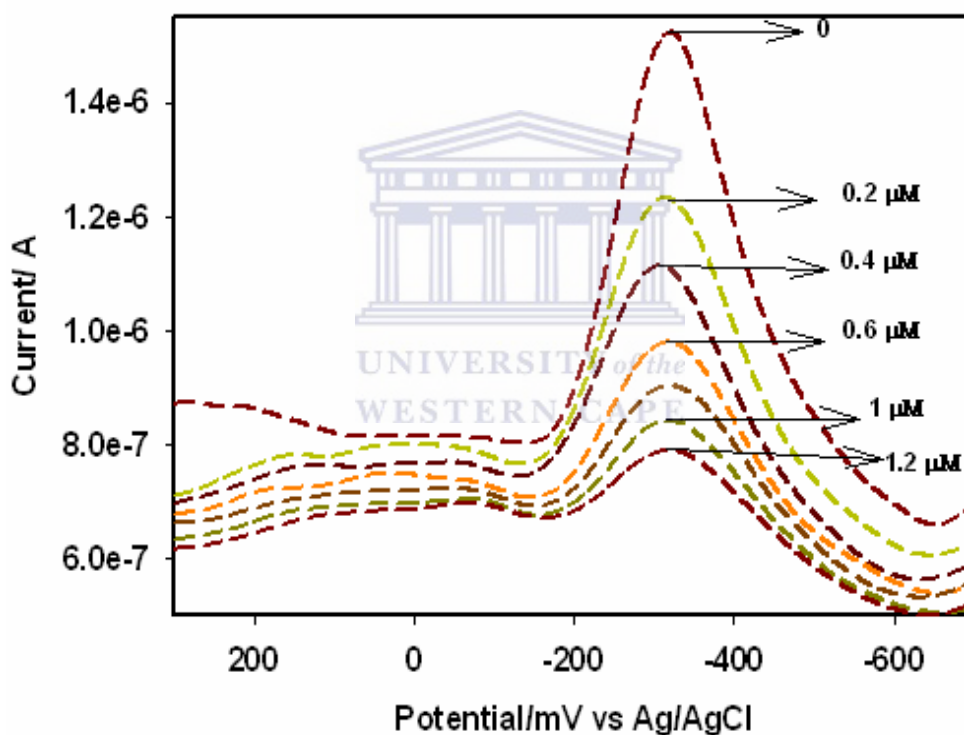


Fig. 4.33 DPV of CYP2D6 biosensor in the presence of varying concentrations of paroxetine under aerobic at a potential window of +300 mV to -700 mV at a scan rate of 10mV/s.

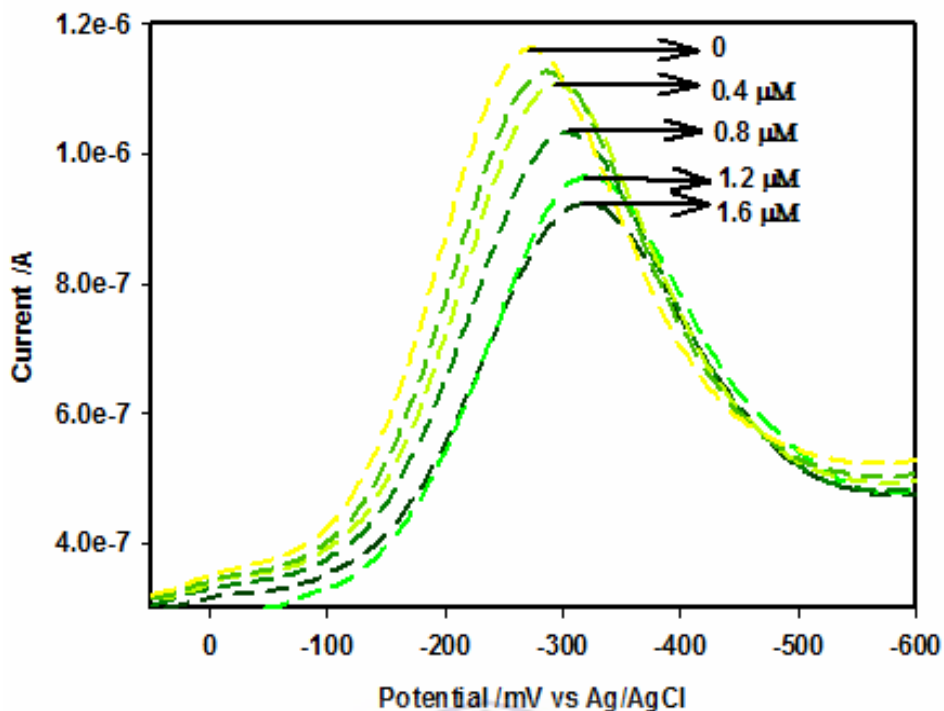


Fig. 4.34 SWV of CYP2D6 biosensor in the presence of varying concentrations of paroxetine under aerobic conditions at a potential window of +100 mV to -600 mV at a scan rate of 10mV/s.

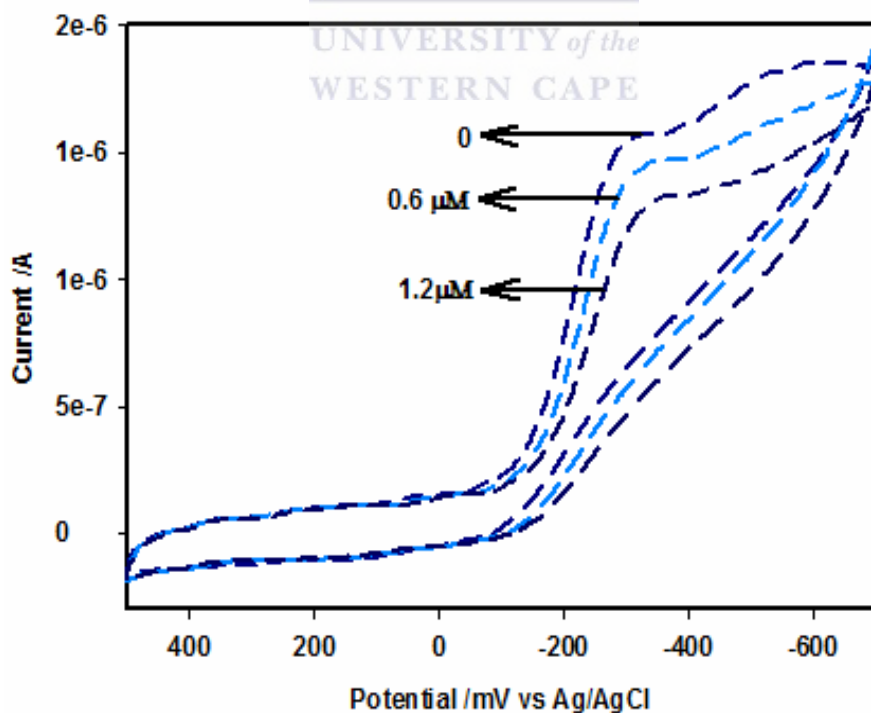


Fig. 4.35 CV of CYP2D6 biosensor in the presence of varying concentrations of paroxetine under aerobic conditions at a potential window of + 500 mV to -700 mV at a scan rate of 10 mV/s

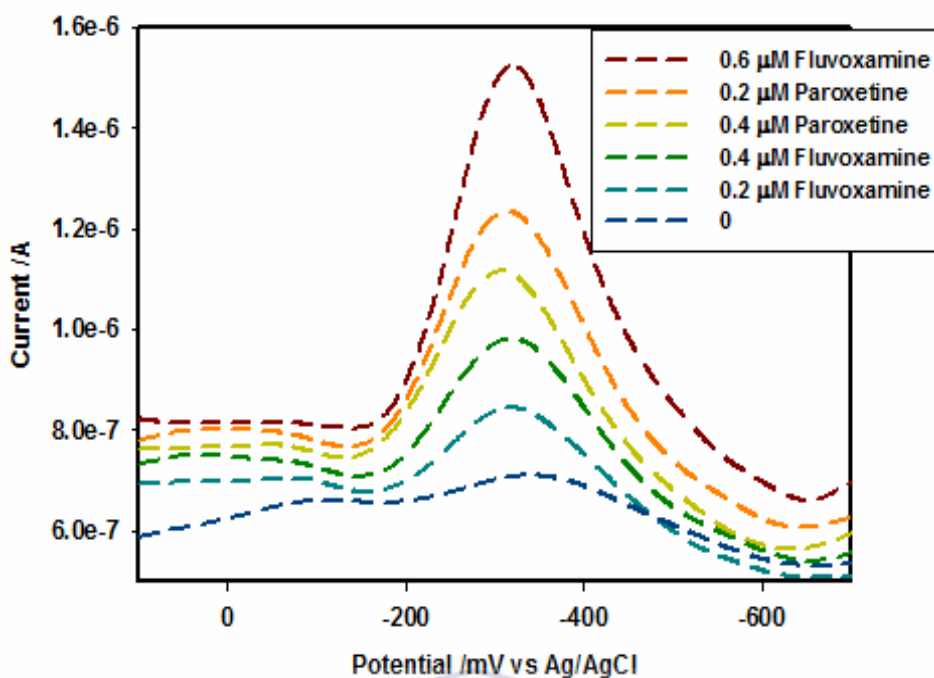


Fig. 4.36 (a) CV of CYP2D6 biosensor in the presence of varying concentrations of paroxetine and fluvoxamine under aerobic conditions at a potential window of + 100 mV to -700 mV at a scan rate of 10 mV/s

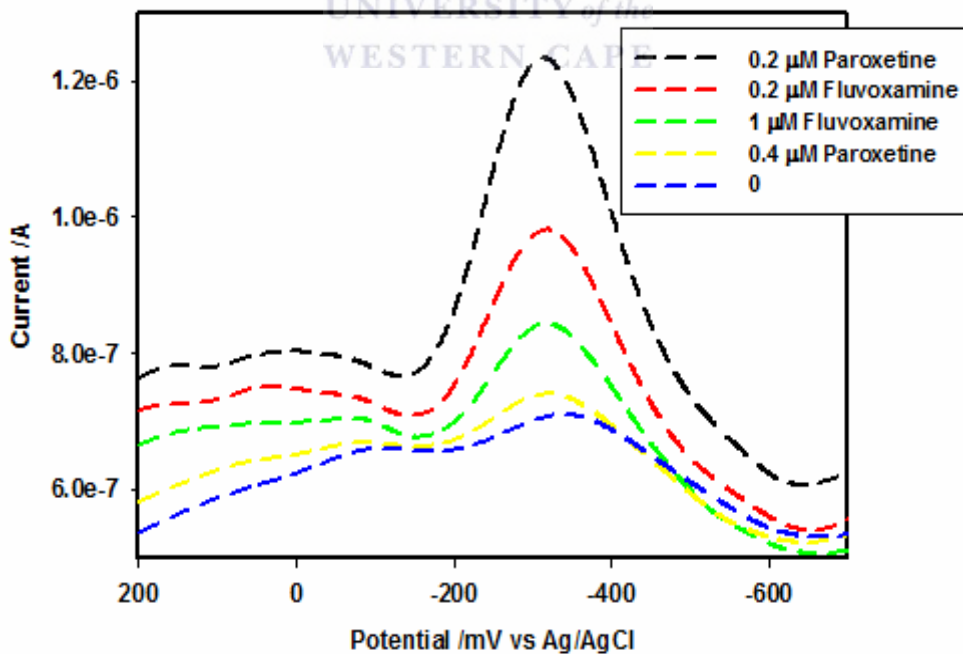


Fig. 4.36 (b) DPV of CYP2D6 biosensor in the presence of varying concentrations of paroxetine and fluvoxamine under aerobic conditions at a potential window of + 100 mV to -700 mV at a scan rate of 10 mV/s

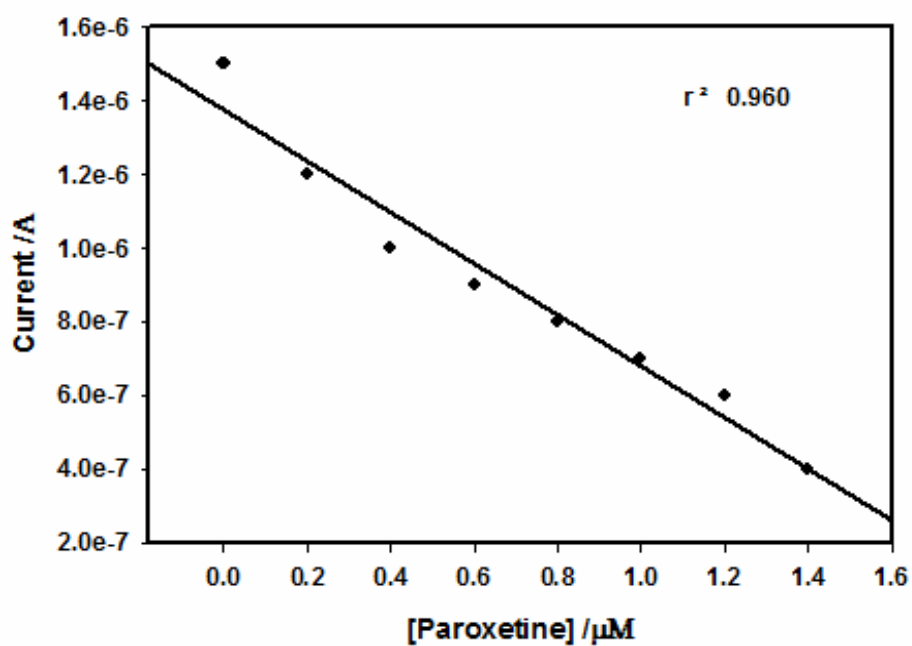
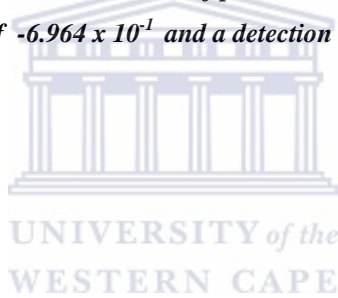


Fig 4.37 Calibration curve of paroxetine biosensor with a sensitivity of -6.964×10^{-1} and a detection limit of $-0.085 \mu\text{M}$.



4.7 Steady State Amperometry:

The biosensor response time was evaluated from steady state amperometry experiments performed at -315 mV. In the experiment, the Au/PANSA/CYP2D6 biosensor was used as the working electrode in an air saturated PBS cell solution which was stirred at 500 rpm. Response time can be described as the time necessary to reach 95% of the steady-state current level. The biosensor was polarised at -315 mV and the background (capacitive) current was allowed to decay to a constant value which occurred after about 107 s. Observed from the amperometry results was an increase in the current when the respective analytes were added until steady-state was reached after some time (*Svobodova et al, 2002*). We can see that the response times are in the order of seconds varying from 20 to 25 s showing that the sensor responses can be achieved in real time even if the time required for the background current to decay is included. This time is much shorter when compared to the hours required for immunoassay. These responses are quite similar to response time values carried out by the work of (*Iwuoha et al, 2002*) where values ~20 s were obtained in the case of experiments carried out with modified electrodes, which is the same method employed in this particular study. Table 4.1 illustrates the response times of the different drug materials. The response times of a few analysed drugs are illustrated in figure 4.38 for fluoxetine and fluvoxamine and figure 4.39 for sertraline and debrisoquine sulphate.

From the results stipulated in table 4.1 we can see that there is a variation in the detection limits for the respective biosensors. The detection limits of fluvoxamine, sertraline and clomipramine are higher than those observed for the other sensor systems. For the other biosensors this is probably as a result of the less homogenous distribution of the enzyme molecules on the sensor surface, thus restricting access of

the analytes to the active site of CYP2D6 (Svobodova *et al*, 2002). This is especially true for the fluoxetine biosensor whose intra-hepatic concentration is reported in the range from 2 to 7 $\mu\text{mol /L}$ (Iwuoha *et al*, 2004). The detection limit of the two SSRIs and the tricyclic antidepressant are in the same concentration range which gives us the confirmation that these compounds are substrates of CYP2D6.

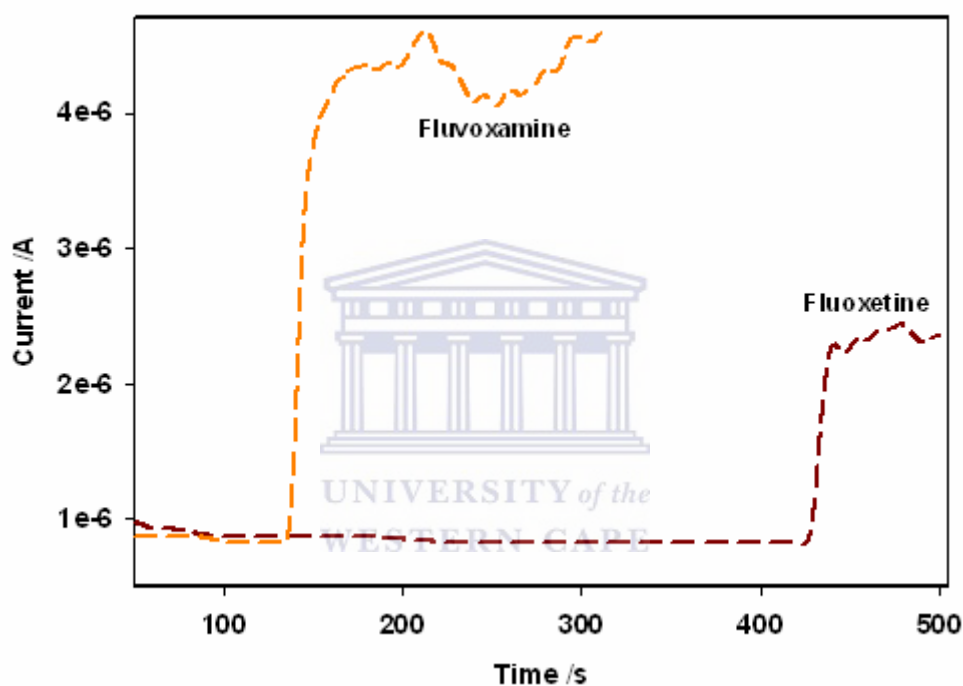


Fig.4.38 Response times of fluvoxamine and fluoxetine.

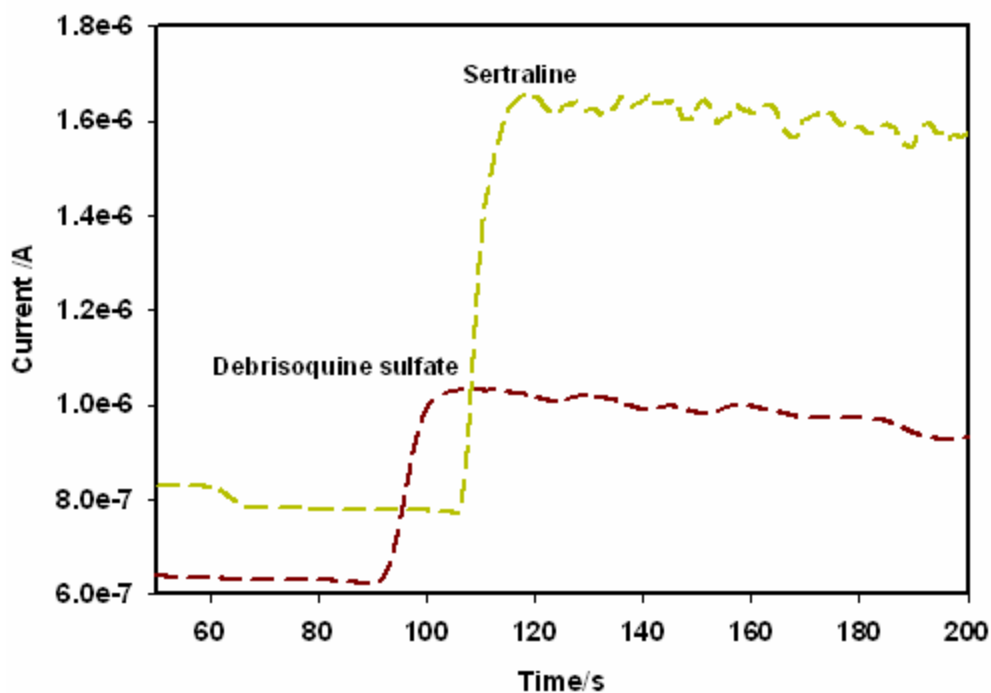


Fig.4.39 Response times of sertraline and debrisoquine sulphate.

Table 4.1: Compounds and their respective biosensor analyses:

COMPOUND	I_{max}	K_m	Detection Limit	Sensitivity	Response Times
FLUOXETINE	9.103×10^{-7} A	$0.9 \mu\text{M}$	$0.94 \mu\text{M}$	6.327×10^{-1}	20 s
FLUVOXAMINE	1.55×10^{-7} A	$0.79 \mu\text{M}$	$0.15 \mu\text{M}$	9.470×10^{-1}	22 s
ZIMELIDINE	5.123×10^{-7} A	$0.81 \mu\text{M}$	$0.03 \mu\text{M}$	3.220×10^{-1}	21 s
SERTRALINE	6.011×10^{-7} A	$0.75 \mu\text{M}$	$0.13 \mu\text{M}$	3.021×10^{-1}	25 s
CLOMIPRAMINE	5.121×10^{-7} A	$0.82 \mu\text{M}$	$0.05 \mu\text{M}$	3.398×10^{-1}	19 s
DEBRISOQUINE SULFATE	1.121×10^{-7} A	$0.81 \mu\text{M}$	$0.02 \mu\text{M}$	3.904×10^{-1}	23 s
PAROXETINE	1.100×10^{-8} A	$0.5 \mu\text{M}$	$-0.085 \mu\text{M}$	-6.964×10^{-1}	20 s

4.8 Conclusion:

PANSA-on-gold electrode modified with CYP2D6 is suitable for application in drug biotransformation biosensors as observed from the output of this study. PANSA served as a point of attachment for the enzyme as well as an efficient electron mediator between the redox centre of CYP2D6 and the electrode surface. The results obtained are confirmation that the Au/PANSA/CYP2D6 biosensors were successful in the reductive catalysis of the various SSRIs into respective water soluble and easy excretable metabolites. The catalytic current responses were amperometrically monitored by cyclic, differential pulse and square wave voltammetric techniques where an increase in current was observed for the substrates and the reverse for the inhibitor. Another interesting aspect of this work is the similarity existing between the electrochemistry of debrisoquine sulfate and that of the used SSRIs resulting in a conclusion that the SSRIs are CYP2D6 substrates. Prior studies of sertraline have indicted sertraline to be a possible inhibitor of CYP2D6, our study has indicated that at very low sertraline concentration, this compound behaves as a substrate of CYP2D6 as illustrated by an increase in current upon addition of sertraline aliquots up to the saturation/inhibition cross-over concentration determined by the amount of CYP2D6 in the biosensor. This behaviour of sertraline was found to be very similar to that observed for fluoxetine. On the other hand, the inhibitory effects of paroxetine were also explored and an irreversible inhibition was observed since there was no current change even in the presence of a substrate. From the calibration curves, linear responses were established in which the sensitivities as well as the detection limits were estimated. Michaelis-Menten kinetics was used to determine the values of K_m and I_{max} of the various biosensor systems. The apparent Michaelis-Menten constants were found to be higher than the peak plasma concentration (C_{max}) value of 0.55

μM , thereby making the sensor systems suitable for the determination of the respective analytes in serum.

4.9 Acknowledgements:

Thank you to National Research Foundation of South Africa and Cannon Collins Trust of South Africa for financial support.



5. REFERENCES:

Bistolas N, Wollenberger U, Jung C, Scheller F.W: 'Cytochrome P450 biosensors a review' *Biosensors and Bioelectronics*, 2005, 20: 2409

Brahim S, Guiseppi-Elie A: 'Chemical and Biological Sensors Based on Electrochemical Detection Using Conducting Electroactive Polymers' *Michim Acta*, 2003, 143: 133

Brennan S: 'Comparitive Studies of the organic and aqueous phase reactivities of a Pthathalic anhydride-modified hydrogen peroxide biosensor' *Ph.D Thesis*, 1996, Dublin City University

Cerqueira P.M, Mateus F. H, Evandro Jose' Cesarino E.J: 'Enantioselectivity of debrisoquine 4-hydroxylation in Brazilian Caucasian hypertensive patients phenotyped as extensive metabolizers' *Journal of Chromatography B*, 72000, 749: 153

Conn E.E, Stumff P.K, Brueninig G: 'Outline of Biochemistry' John Wiley and Sons, 1987, 5th Edition, 115 -163

Fersht A: 'Enzyme structure and mechanism' W. H. Freeman and Company, 1985, 2nd Edition, pg 98-107

Grennan K, Killard A. J, Symth R. S: 'Optimisation and characterization of biosensors based on polyaniline' *Talanta*, 2006, 68:1593

Heimke C, Hartter S: 'Pharmacokinetics of selective serotonin reuptake inhibitors' *Pharmacology and Therapeutics*, 2000, 85:20-22

Iwuoha E. I, Williams A. R: 'Novel Transfer Mediators for Amperometric Bioelectrodes: Introduction of Methylsuarate and Phenylsuarate' *Electroanalysis*, 2002, 14:1181-1182

Iwuoha E. I, Mavundla S. E, Somerset V.S: 'Electrochemical and Spectroscopic Properties of Fly Ash-Polyaniline Matrix Nanorod Composites' *Microchim Acta*, 2006, 155:456

Iwuoha E. I, Howel M, Wilson A: 'Cytochrome P450_{2D6} (CYP2D6) Bioelectrode for Fluoxetine' *Analytical Letters*, 2004, 37:5: 933-939

Iwuoha E. I, Joseph S: 'Drug metabolism biosensors: electrochemical reactivities of cytochrome P450_{cam} immobilized in synthetic vesicular systems' *Journal of Pharmaceutical and Biomedical Analysis*, 1998,17: 1101-1110

Iwuoha E.I, de Villaverde D.S, Smyth M.R: 'Reactivities of organic phase biosensors.2. The amperometric behaviour of horseradish peroxidase immobilised on a platinum electrode modified with an electrosynthetic polyaniline film' *Biosensors and Bioelectronics*, 1997, 12:8, 753-754

Kanungo M, Kumar A, Contractor A.Q: 'Studies on electropolymerization of aniline in the presence of sodium dodecyl sulphate and its application in sensing urea' *Journal of Electroanalytical Chemistry*, 2002, 528: 51

Kobayashi K: 'Sertraline N-Demethylation Is Catalyzed by Multiple Isoforms of Human Cytochrome P-450 In Vitro' Laboratory of Biomedical Pharmacology and Toxicity, Chiba University, 1999, 27:763-764

Lindfors T, Ivaska A: 'Potentiometric and UV-vis characterisation of N-substituted polyanilines' *Journal of Electroanalytical Chemistry*, 2002, 535: 69-71

Mandrioli R, Ferarri S: 'HPLC analysis of the second-generation antidepressant sertraline and its main metabolite N-desmethylsertraline in human plasma' *Journal of Chromatography B*, 2006, 836: 116

Mathebe N.G.R, Morrin A, Iwuoha E.I: 'Electrochemistry and scanning electron microscopy of polyaniline/proroxide-based biosensor' *Talanta*, 2004, 64:116-119

Mathebe N.G.R: 'Fabrication and kinetic modelling of Cytochrome P450 2D6 amperometric biosensors for serotonin reuptake inhibitors' *M.Sc Thesis*, 2005, Western Cape University

Margolis J.M, O'Donnell P.J, Obach R.S: '(R)-, (S)-, and racemic fluoxetine N-demethylation by cytochrome P450 enzymes' *Drug Metabolism and Disposition*, 2000, 28: 1187-1191

Mazeikiene R, Niaura G, Malinauskas A: 'Raman spectroelectrochemical study of self-doped copolymers of aniline and selected aminonaphthalenesulfonates' *Electrochimica Acta*, 2006, 51:1919-1920

Mu S, Cheng C, Wang J: 'The kinetic behaviour for the electrochemical polymerization of aniline in aqueous solution'. *Synthetic Metals*, 1997, 88: 249-254

Ngece R.F: 'Development of an electroanalytical sensor system for the determination of phenols', *Honour Thesis*, 2004, University of the Western Cape

Qu F, Yang M, Jiang J, Yu R: 'Amperometric biosensor for choline based on layer-by-layer assembled functionalized carbon nanotube and polyaniline multilayer film' *Analytical Biochemistry*, 2005, 344: 110-111

Rusling J.S, Lvov J.F, Friedberg Y.M: 'An amperometric biosensor with human CYP3A4 as a novel drug screening tool' *Biochemical Pharmacology*, 2003, 65:1817-1826

Shumyantseva V.V, Bulko T.V, Archakov A.I: 'Electrochemical reduction of Cytochrome P450 as an approach to the construction of biosensors and bioreactors' *Journal of Inorganic Biochemistry*, 2005, 99: 1057

Subehan, Usia T, Kadota S: 'Mechanism based inhibition of CYP3A4 and CYP2D6 by Indonesian medicinal plants' *Journal of Ethnopharmacology*, 2006

Svobodova L, Snejdarkova M, Hianik T: 'Properties of glucose biosensors based on dendrimers layers.Effect of enzyme immobilization' *Analytical Bioanalytical Chemistry*, 2002, 373:737-738

von Moltke L.L, Greenbalt D.J, Duan S.X, R.I Shader: 'Human cytochromes mediating N-demethylation of fluoxetine in vitro'. *Psychopharmacology*, 1997, 132: 402-407

